

國立臺灣大學生命科學院植物科學研究所

碩士論文

Graduate Institute of Plant Biology

College of Life Science

National Taiwan University

Master Thesis


文心蘭 ascorbate peroxidase 對阿拉伯芥在中高溫生長下

對於開花機制的調控功能

Molecular function of *Oncidium* ascorbate peroxidase on

thermal-induced flowering process in

Arabidopsis thaliana



黃柏睿

Bo-Ruei Huang

指導教授：葉開溫 博士

Advisor: Kai-Wun Yeh, Ph.D.

中華民國 100 年 7 月

July, 2011

Table of the Content

Chinese Abstract.....	8
English Abstract	9
1. Introduction	11
1.1 <i>Oncidium Grower ramsey</i>	12
1.2 <i>The Current Work on Oncidium Phase Transition</i>	13
1.3 <i>Regulatory Pathways of Flowering</i>	16
1.3.1 <i>Research of Flowering Time in the Pre-molecular Biology Era</i>	16
1.3.2 <i>Regulation of Flowering by Day Length</i>	17
1.3.3 <i>Gibberellic Acid Pathway: A Hormonal-Controlled Flowering</i>	18
1.3.4 <i>Autonomous Pathway of Flowering</i>	19
1.3.5 <i>Effect of Ambient Temperature on flowering</i>	20
1.3.5.1 <i>Effect of Vernalization on Flowering</i>	20
1.3.5.2 <i>Thermal-induced flowering</i>	21
1.4 <i>Ascorbate: An Emerging Field in the Regulation of Flowering Time</i>	22
1.4.1 <i>Physiological Functions of Ascorbate</i>	22
1.4.2 <i>Ascorbate: A Negative Regulator of the Phase Transition in Planta</i>	23
1.5 <i>The Bridge between Ascorbate and Flowering</i>	25
1.5.1 <i>The Issue of Ascorbate Peroxidase</i>	25
1.5.2 <i>Hierarchy of Hydrogen Peroxide, Ascorbate and Ascorbate Peroxidase in</i> <i>Flowering process</i>	26
1.6 <i>Goals of This Thesis</i>	27
2. Results.....	28
2.1 <i>Characterization of Transgenic Arabidopsis Overexpressing Oncidium</i> <i>Ascorbate Peroxidase</i>	28
2.1.1 <i>Generation of Transgenic Arabidopsis Overexpressing Oncidium Ascorbate</i> <i>Peroxidase</i>	28
2.1.2 <i>Morphological Characterization of OgAPXOX Transgenic Plants</i>	29
2.1.3 <i>Effects of Oncidium Ascorbate Peroxidase on Ascorbate Homeostasis and</i> <i>H₂O₂ Level under Different Environmental Condition in Arabidopsis</i>	29

2.1.4 <i>Effect of Oncidium Ascorbate Peroxidase on Flowering Time under Different Environmental Condition in Arabidopsis</i>	31
2.2 Genetic Network of Ascorbate Peroxidase Involving in Thermal-induced Flowering Process	34
2.2.1 <i>Decreased Expression Level of FLM in OgAPXOX Plants Suggests the Role of AsA in Regulating Thermal-induced Flowering</i>	34
2.2.2 <i>Transcriptional Profiling of OgAPXOX Arabidopsis under Elevated Growth Temperature</i>	35
2.2.3 <i>Functional Categories of Expression Clusters in Accordance with Genotypes and Growth Temperature Condition</i>	45
2.2.4 <i>Transcription Profiling Revealed That Genes Encoding MYB and AP2 TFs Expressed with Higher/ Lower in OgAPXOX Plants under Elevated Growth Temperature</i>	46
2.2.5 <i>Genes Involving in Circadian Rhythm and Starch Synthesis Were Significantly Altered in APXOX Plant under Elevated Growth Temperature</i>	48
2.2.6 <i>Quantification of Expression Level of Candidate Genes by Real-time PCR</i>	49
2.2.7 <i>Expression Profiling of Candidate Genes in AsA Deficient or Accumulated Mutants</i>	51
3. Discussion	52
4. Prospective	59
5. Materials and Methods	61
5.1 <i>Plant Materials and Growth Conditions</i>	61
5.2 <i>RNA Extraction, Microarray and qPCR</i>	62
5.3 <i>Ascorbate Peroxidase Activity Analysis</i>	63
5.4 <i>Ascorbate Measurement</i>	65
5.5 <i>Hydrogen Peroxide Measurement</i>	68
5.6 <i>Hydrogen Peroxide Staining</i>	71
5.7 <i>Quantitative Analysis of Protein Concentration</i>	72
5.8 <i>RNA Extraction</i>	73
5.9 <i>RT PCR for Gene Expression (One-step RT PCR)</i>	77

5.10 Construction of Functional Plasmid for Overexpressing the Interested Genes
in Arabidopsis 78

5.11 Agrobacterium Infiltration (Host: Arabidopsis thaliana Col.) 85

References 88



List of Tables

Table 1. GO analysis of cluster 1.....	95
Table 2. GO analysis of cluster 2.....	98
Table 3. GO analysis of cluster 3.....	100
Table 4. GO analysis of cluster 4.....	101
Table 5. GO analysis of cluster 5.....	102
Table 6. GO analysis of cluster 6.....	105
Table 7. GO analysis of cluster 7.....	107
Table 8. GO analysis of cluster 8.....	110
Table 9. GO analysis of cluster 9.....	112
Table 10. GO analysis of cluster 10.....	114
Table 11. Transcriptional profiling of <i>MYB</i> or <i>MYB-like</i> transcription factors.....	116
Table 12. Transcriptional profiling of <i>AP2-like</i> transcription factors.....	118
Table 13. Transcriptional profiling of circadian genes.....	120
Table 14. Transcriptional profiling of <i>QQS</i>	121

List of Figures

Figure 1. The enzymatic activity and expression level of APX in several independent lines.....	122
Figure 2. The foliar phenotype and H ₂ O ₂ content in transgenic and control plants growing under long-day photoperiod and 22°C condition.....	123
Figure 3. The chlorophyll content of control and transgenic plants.....	124
Figure 4. The AsA level in transgenic and control plants growing under 22°C condition and long-day photoperiod. AsA content in 4 leaves of transgenic and control plants growing under 22°C condition and long-day photoperiod.....	125
Figure 5. The H ₂ O ₂ content in transgenic and control plants growing under long-day photoperiod and 22°C condition.....	126
Figure 6. The AsA level in transgenic and control plants growing under 22°C condition and short-day photoperiod.....	127
Figure 7. The H ₂ O ₂ content in transgenic and control plants growing under 22°C condition and short-day photoperiod.....	128
Figure 8. H ₂ O ₂ level in wild type and <i>OgAPXOX</i> transgenic <i>Arabidopsis</i> after elevating growth temperature to 30°C.....	129
Figure 9. AsA content in transgenic plants <i>OgAPXOX</i> after heat treatment.....	130
Figure 10. The AsA redox ratio in transgenic plants <i>OgAPXOX</i> after elevating growth temperature to 30°C.....	131
Figure 11. The higher growth temperature brought about drastic decrease of AsA level in wild type and transgenic plants.....	132
Figure 12. The number of rosette leaves at the time of flowering in <i>OgAPXOX</i> and control plants.....	133
Figure 13. The phenotype of transgenic <i>Arabidopsis</i> and control plants growing under	

short-day photoperiod and 22°C condition.....	134
Figure 14. The flowering time of transgenic <i>Arabidopsis</i> and control plants growing under 22°C condition and short-day photoperiod.	135
Figure 15. The phenotype of transgenic <i>Arabidopsis</i> and control plants growing under 30°C condition and long-day photoperiod.	136
Figure 16. The percentage of rosette leave number when flowering in transgenic <i>Arabidopsis</i> and control plants growing under 30°C condition and long-day photoperiod.	137
Figure 17. <i>OgAPXOX</i> transgenic plants exhibited the shorter length of inflorescence stem.	138
Figure 18. The phenotype of transgenic <i>Arabidopsis</i> and control plants growing under 30°C condition and short-day photoperiod.....	139
Figure 19. The percentage of rosette leave number when flowering in <i>OgAPXOX</i> and control plants growing under 30°C condition and short-day photoperiod.	140
Figure 20. Relative expression levels of thermal sensitivity gene <i>FLOWERING LOCUS M (FLM)</i> in wild type and transgenic plants under elevated growth temperature.	141
Figure 21. Clustering analysis of 860 transcripts which displayed up- or down-regulated 2 fold levels between each samples with CK under LD-22°C at 0 day.	143
Figure 22. Functional categories of expression clusters in accordance with genotypes and growth temperature condition.	144
Figure 23. Relative expression levels of <i>AP2</i> transcription factors in wild type and transgenic plants under elevated growth temperature.	145
Figure 24. Relative expression levels of circadian genes in wild type and transgenic plants under elevated growth temperature.....	146

Figure 25. Relative expression levels of <i>AtMYB70</i> and <i>QQS</i> in wild type and transgenic plants under elevated growth temperature.....	147
Figure 26. Relative expression levels of <i>qua-quine starch (QQS)</i> in three independent lines.....	148
Figure 27. Relative expression levels of <i>AP2</i> transcription factors in <i>vtc1</i> or <i>OgPMEOX</i> mutants.	149
Figure 28. Relative expression levels of circadian genes in <i>vtc1</i> or <i>OgPMEOX</i> mutants.	150
Figure 29. Relative expression levels of <i>AtMYB70</i> and <i>QQS</i> in <i>vtc1</i> or <i>OgPMEOX</i> mutants	151
Figure 30. Proposal model of genetic network for activated APX in modulating flowering process.....	152

List of Appendixes

Appendix 1. The oligonucleotides used for RT-PCR and qRT-PCR.....	153
Appendix 2. Schematic representation of ascorbate homeostasis in pseudobulb cell of <i>Oncidium</i> orchid in three developmental stages.....	154
Appendix 3. Ascorbate oxidation and regeneration from monodehydroascorbate and dehydroascorbate.....	155
Appendix 4. Abbreviation.....	156

中文摘要

南西文心蘭 (*Oncidium Gower ramsey*) 是亞洲的重要經濟花卉。前人研究指出，維他命 C 對於開花調節扮演著負調節的角色，然而，文心蘭生長在日/夜溫度 30/25°C 較生長於 25/20°C 環境中，明顯有較高的開花比例。因為較高的生長溫度可以有效地誘導維他命 C 過氧化氫酶 (*OgAPX*) 的基因表現量與提高其活性，進而使大量的維他命 C (ascorbate) 被消耗掉。為了解維他命 C 在熱誘導開花中所扮演的角色，我們在阿拉伯芥中大量表現 *OgAPX*。結果發現，轉殖植物 (*OgAPXOE*) 在 22°C 的生長環境下，其形態上與野生型 (control) 並無顯著差異。然而提高其生長溫度至 30°C 時，發現其較野生型有提早開花與較少的葉綠素累積。利用 microarray 分析受熱與維他命 C 共同影響的基因，發現這些基因主要種類為：氧化還原酶 (oxidoreductase)、老化、防禦、訊號傳遞以及轉錄因子。進一步利用 real-time PCR 檢測下述之基因表現量，包括 *AtMYB70*、*At3g30720*、參與 circadian rhythms 以及含有 *AP2-domain* 等基因。結果顯示，這些基因在較高的生長溫度中的表現量確實較高/較低。而這些基因於 *vtc1* (維他命 C 含量僅有野生型 30% 的突變株) 也有類似的較高表現量，而在 *OgPMEOX* 轉植株 (大量累積維他命 C 的轉植株) 當中卻有較低的表現量，這些證據顯示這類基因表現確實是受到內生性維他命 C 的含量所調控。綜合所有結果，我們推論維他命 C 參與在熱誘導開花過程可誘發較上游的開花相關基因之表現，上述基因皆屬於目前所有已知開花調控機制的較上游調控因子，此外，我們亦推論：在熱誘導開花中，醣類 (sugar/energy) 亦可能具有調節開花機制之功能。

Abstract

Oncidium Gower ramsey is an economically important cutting flower in orchid industry. Mild increase of growth temperature is effective to promote *Oncidium* flowering, in example of elevating day/night temperature from 25°C/20°C to 30°C /25°C. Our previous studies have revealed that higher growth temperature also induced the expression of *ASCORBATE PEROXIDASE* (*OgAPX*) and resulted in the deprivation of ascorbate (AsA) level. In order to decipher the underlying role of AsA under thermal-regulated flowering, *OgAPX* was overexpressed in *Arabidopsis*. There was no significant change on morphology between transgenic and control plants when growing under 22°C. The *OgAPXOE* transgenic plants exhibited precocious flowering and reduction of chlorophyll content compared with control when growing at 30°C condition. Microarray analyses of transgenic and control plants growing at 22°C condition displayed differential expression patterns of genes to plants growing at 30°C in categories in oxidoreductase, senescence, defense, signal transduction and transcription factors. *AtMYB70*, *AP2*, circadian genes and *At3g30720*, which displayed up/down-regulated expression pattern under elevated growth temperature condition were further validated by quantitative RT-PCR. Moreover, their expression levels were

associated with the endogenous AsA level and displayed up-regulation level in ascorbate-deficient mutant, *vtc1*, but down-regulated level in ascorbate-accumulated transgenic plants, *OgPMEOX*. Noteworthy, attenuated expression level of At3g30720 encoding qua-quine starch (QQS) which acting on starch biosynthesis, provides a regulatory function of AsA state on the cross-talk of thermal- and energy-regulated flowering. Taken together, our results bring about a genetic network of flowering mechanism orchestrated by the elevated growth temperature.



1. Introduction

Oncidium Gower ramsey in Taiwan is a high-value flower with a net value of nearly US\$7.35 million annually. In 2008, *Oncidium* cut-flowers made up 41.7% of the market for cut-flowers in Taiwan. One of the most important strategies to keep Taiwan as the leading producer of *Oncidium* in the world is to control *Oncidium* flowering time to meet market demand. However, *Oncidium* flowering time is controlled by the environmental factors that have intrigued and puzzled phytologists, and the control is different from flowering controls of *Phalaenopsis*, *Dendrobium* and other Orchidaceae species (Lopez and Runkle, 2005). Studies from *Arabidopsis* have revealed four flowering time regulatory pathways, including photoperiod pathway, gibberellin pathway, the autonomous pathway, and the vernalization pathway (Mouradov et al., 2002). In the last decades, it has been paid attention to the strong effect of ambient growth temperature on flowering because of the acute changes in global climate (Long and Ort, 2010). The thermal-induced flowering would reduce the net yield attributing to the much shorter vegetative growth for accumulating photosynthesis product. The detail mechanism of thermal-induced flowering is still unclear, but increased ROS under elevated growth temperature in plant was perceived as a determinant molecule to trigger

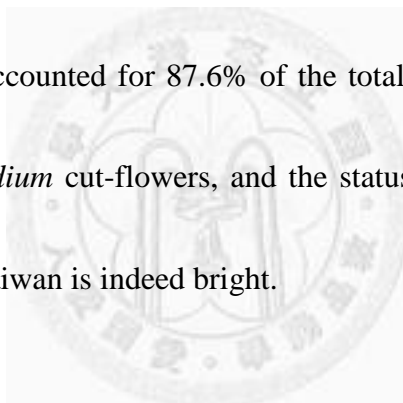
flowering (Balasubramanian et al., 2006; Chin et al., unpublished). Ascorbate (AsA) is an important antioxidant for ROS scavenge, and has been well-identified as a repressor in flowering process (Shen et al., 2009). This study declares in-depth discussions on orchestration of AsA level and ambient temperature on the flowering process.

1.1 Oncidium Gower ramsey

People have been fascinated by the beauty and mystery of orchids for a very long history in Western and Eastern cultures. Orchid varieties have become one of the largest in floriculture throughout the world. Propagation of orchids became possible because of the breakthrough in tissue culture techniques and promotes large-scale cultivation of cuts or potted plants in Taiwan, Netherlands, Germany, Thailand, and United States. Today, orchid cut-flowers of *Oncidium* and potted plants of *Phalaenopsis* had contributed substantially to the economy in Taiwan.

Oncidium “Gower ramsey” is a hybrid orchid produced by crossing two species of the same genus: *Oncidium Goldiana* × *Oncidium Guiana gold*. Its name was derived from the Greek word ‘onkos’, meaning “swelling”. Diverse color in *Oncidium* lips likes a dancing girl known “Dancing Lady” orchids. *Oncidium* has an enlarged bulb structure

at the base of their leaves, termed a pseudobulb. The genus *Oncidium* (*Oncidium* spp.) is a thin-leaf, sympodial orchid which was native to tropical and subtropical America's epiphytic orchids, including Florida, Mexico, Central America, West Indies, Brazil, Peru, Bolivia and Taiwan. *Oncidium* was mostly planted in Nantou and Pingtung. The marketable potential for *Oncidium* Gower ramsey is its long inflorescence for cut-flowers. The export of *Oncidium* cut-flowers into Japan had been increasing steadily from 2002 to 2007. Base on the Japanese flower auction sale figure for 2007, *Oncidium* cut-flowers from Taiwan accounted for 87.6% of the total market share. Japan is now the major market for *Oncidium* cut-flowers, and the status and future development of the *Oncidium* industry in Taiwan is indeed bright.



1.2 Current Work on Oncidium Phase Transition

The pseudobulb of *Oncidium* is hetroblastic (single internode) type and numerous studies revealed that carbohydrates and minerals transported from leaves into developing pseudobulb organ (Yong and Hew, 1995). Tan and coworkers (2005) reported that peroxidase, sodium/dicarboxylate cotransporter, and mannose-binding lectin were highly expressed during bolting by subtracting *Rsa*I-digested cDNAs of leaf

from those of pseudobulb (Tan et al., 2005). Moreover, fluctuate expression levels of genes relating to mannan, pectin, and starch and sucrose biosynthesis inferred a differential requirement of carbohydrate for vegetative and reproductive growth (Wang et al., 2008).

Pectin and mannan were two important resources for AsA biosynthesis (Wang et al., 2008), and the higher AsA was also present in the pseudobulb of *Oncidium* at vegetative stage (Shen et al., 2009). Moreover, *Oncidium* sprayed with AsA, displayed delayed flowering time compared with plants sprayed with water. The endogenous AsA in longer vegetative (LV) *Oncidium* variety was obviously higher than wild type and showed dramatic reduction on flowering (Shen and Yeh, 2010). Apparently, these results disclose the criterion of the AsA level on *Oncidium* flowering and pointed out possible regulation mechanism of phase transition triggered by redox signals information concerning the changing environmental conditions (Shen et al., 2009).

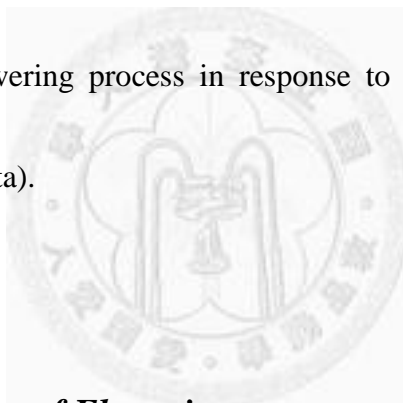
In Appendix 2, the proposed model hypothesizes the control of the phase transition by AsA homeostasis at different growth stages in *Oncidium* (Shen and Yeh, 2010).

The sucrose transported from epiphytic leaves to the pseudobulb, which was

preferentially converted to precursors of mannan and pectin. Copious pectin was demethylated by pectin methylesterase (PME) during cell wall enlargement process in young pseudobulbs. Concomitant with the degradation of pectin, methanol was generated. During detoxified process, the methanol converted to H_2O_2 and formaldehyde by alcohol oxidase. Furthermore, H_2O_2 could trigger the expression of AsA biosynthetic genes including of Smirnoff-Wheeler pathway and prevent the excess of ROS level. At bolting period, the pectin and mannan decreased gradually and converted to starch. While a presumable increase of calcium conjugation with cell wall could result in rigid cell wall which prevented from cell elongation by digest pectin. Less pectin content would result in a decrease of byproduct from the demethylation of pectin, including of methanol and H_2O_2 . It also affected the AsA biosynthesis cascades. Noteworthy, higher OgAPX activity was also present in *Oncidium* during bolting. It is possible that it not only scavenges ROS but also reduces the AsA redox ratio and presumably brought about the bolting (Shen et al., 2009). Moreover, the increase of starch was further generated and utilized in the pseudobulb to provide energy for floral development in comparison with deprivation of pectin and AsA (Shen and Yeh, 2010).

Noteworthy, Chin et al indicated the higher activity of APX was apparent in

Oncidium, while growing under elevated growth temperature condition, such as 30°C/25°C (day/night temperature) and exhibited the higher bolting percentage (95%) comparing to bolting percentage either at 25°C/20°C (50%) or 20°C /15°C (35%) (Chin et al., unpublished data). Thermal-induced flowering has been validated in *Arabidopsis* (Shen et al., 2009), and Chin et al disclosed the presumable role of AsA state on the thermal-induced phase transition of *Oncidium* (Chin et al., unpublished). Therefore, APX, an important enzyme on fluctuating AsA redox ratio, has been perceived as a critical determinant in flowering process in response to versatile environment event (Chin et al., unpublished data).



1.3 Regulatory Pathways of Flowering

1.3.1 Research of Flowering Time in the Pre-molecular Biology Era

The control of flowering time is an important topic, and plants can be further classified as long-day plants and short-day plants according to their photoperiod responses. The essential distinction between long-day and short-day plants is that flowering in long-day plants is promoted only when the day length exceeds a certain duration, called the critical day length, in every 24-hour cycle; whereas promotion of

flowering in short-day plants requires a day length that is less than the critical day length. Mouradov provided extensive discussions of flowering pathway and identified to the photoperiod, gibberellin, vernalization, and autonomous and pathways attributing to numerous forward and reverse genetic evidences (Mouradov et al., 2002).

1.3.2 Regulation of Flowering by Day Length

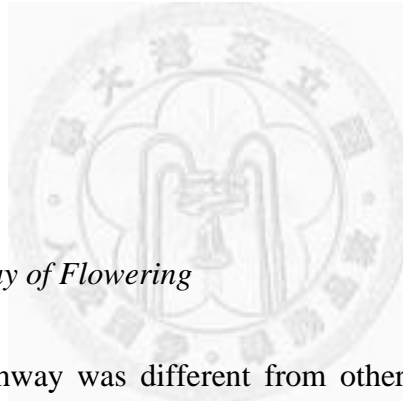
Circadian rhythms have a period length of 24 h. Plants are sensitive to light only at certain times of the day-night cycles. The *CO* was perceived a determinant gene in response to different photoperiod affecting flowering. It encodes a putative zinc finger transcription factor, and its expression was controlled by circadian clock protein, such as GIGANTEA (GI), FLAVIN-BINDING, KELCH REPEAT, F-BOX 1 (FKF1), and CYCLING DOF FACTOR1 (CDF1). The FKF-GI complexes repress CDF1 and bring about *CO* gene expression. However, stability of CO protein also depends on the photoreceptor-debilitating proteasome. The decrease of CO protein by PHYB would be repressed when plant present more CRYs and PHYA protein under long-day photoperiod. Moreover, COP1 was perceived as a negative regulator of *CO*, and CRY protein also inhibit the transport of the E3 ubiquitin ligase-COP1 complex into the

nucleus. Apparently, photoreceptor could prevent the excess ubiquitination of the CO protein under LD condition. The accumulation of CO protein triggers a systemic flower-induced signal in the leaves and further promotes the expression level of *FLOWERING LOCUS T (FT)* transcription. FT, acting as a long distance signal transducer “florigen”, moves through the phloem from the leaves to the apex. FT interacts with the meristem-specific *bZIP* transcription factor FD and conveys the flowering information from leaves to the shoot apical meristem. Subsequently, the integrator genes, such as *SUPPRESSOR OF OVEREXPRESSION OF CONSTANS 1 (SOC1)* and *LEAFY (LFY)*, would be turned on and further promote flowering. It shows that the blossoming under differential photoperiod is tightly controlled by the series signaling cascades (Srikanth and Schmid, 2011).

1.3.3 Gibberellic Acid Pathway: A Hormonal-Controlled Flowering

Gibberellin affects the flowering of short-day plant and was perceived by *GIBBERELIC INSENSITIVE DWARF 1 (GID)*, which induced the ubiquitination of DELLA proteins and brought about the degradation by 26S proteasome. In previous studies, exogenous application of GA could increase expression level of *LFY* in

short-day photoperiod (Blazquez et al., 1998). Interestingly, the R2R3 type *MYB* transcription factors had been implicated in GA signaling (Gocal et al., 2001; Millar and Gubler, 2005; Millar et al., 2010). *MYB33* was induced by GAs in *Arabidopsis* apex, but *MYB33* and its paralogs, *MYB65* and *MYB101*, would be down-regulated by *miR159*. Interestingly, *miR159* was also shown to be down-regulated by the DELLA proteins. Taken together, GA mediates *miR159* by repressing DELLA proteins and results in promoting *MYBs* to trigger *LFY* in the meristem (Gocal et al., 2001; Millar and Gubler, 2005; Millar et al., 2010).



1.3.4 *Autonomous Pathway of Flowering*

The autonomous pathway was different from other environmental factors with internal signals for regulating flowering (Koornneef et al., 1998). FCA/FY interaction was required for autoregulation of *FCA* expression and carried out the binding of the proximal polyadenylation site of *FLC* transcript resulting in the down-regulation of *FLC* (Ausin et al., 2004). Another *FLC* repressor, *FLD*, was shown to prevent hyperacetylation of *FLC* locus. *FPA* would express throughout the whole life of plant, in particular in newly formed tissues and meristems. *FPA* and *FCA* were shown to act

in a partially redundant function to control RNA-mediated chromatin silencing of *FLC* (Schomburg et al., 2001). All of above evidences showed that genes in the autonomous pathway normally repress the floral repressor *FLC* by regulating chromatin remodelling and affect RNA processing.

1.3.5 Effect of Ambient Temperature on flowering

1.3.5.1 Effect of Vernalization on Flowering

The exposure to prolonged periods of cold, winter temperatures is an important signal to ensure plants flower in the next spring. This process was called vernalization. Analysis of the genetic differences between rapid cycling and winter-annual varieties of *Arabidopsis thaliana* revealed that *FRIGIDA (FRI)* mediated vernalization via *FLC* for winter-annual life history (Johanson et al., 2000) *FRI* protein interacted with the cap binding complex (CBC) and further up-regulated *FLC* shown to block the transcriptional activation of *SOC1*. Genetic screen of flowering time mutants affected by temperature exhibited *VERNALIZATION 1 (VRN1)*, *VERNALIZATION 2 (VRN2)* and *VERNALIZATION 3 (VRN3)* were the up-stream hierarchy to repress *FLC* (Bond et al., 2009) at the end of vernalization. *VIN3* established the initial silence of *FLC*, and

VRN1 and VRN2 maintained the epigenetic repression of *FLC*, even after the temperatures became warmer.

1.3.5.2 Thermal-induced flowering

Besides the vernalization, elevated growth temperature had a marked effect on flowering. Two *Arabidopsis* ecotypes, *Landsberg erecta* (*Ler*) and *Columbia* (*Col*), displayed the early flowering when growing at temperature condition from 23°C transiting to 27 °C under short-day photoperiod. Balasubramanian (2006) pointed out that the MADS box transcription factor *FLOWERING LOCUS M* (*FLM*), a *FLOWERING LOCUS C* (*FLC*) paralogue was a determinant repressor in the thermal-induced flowering. Under mild increase in growth temperature, of the active form of *FLM* transcript would reduced and further retrieve the expression level of *FT* and resulted in more early flowering in two ecotypes under short-day photoperiod. Interestingly, the up-regulation of *FT* in the thermal-induced flowering required the attendance of phytohormone gibberellin rather than *CO*, which is a flowering activator controlled by photoperiod (Balasubramanian et al., 2006). The flowering-time repressor *SHORT VEGETATIVE PHASE* (*SVP*) (Hartmann et al., 2000) was also identified well

as the determinant repressor in temperature-responsive flowering by down-regulating *FT* (Kardailsky et al., 1999; Kobayashi et al., 1999). SVP protein preferentially binds on vCARG III element of *FT* promoter and repressed its expression, and brought about the delayed flowering (Lee et al., 2007).

1.4 Ascorbate: An Emerging Factor in the Regulation of Flowering Time

1.4.1 Physiological Functions of Ascorbate

AsA is primary antioxidant molecule in plants and is considered the most abundant vitamin on earth (De Tullio and Arrigoni, 2004). The function of AsA has been validated on plant growth (Pignocchi and Foyer, 2003), programmed cell death (de Pinto et al., 2006), pathogen responses (Barth et al., 2004), hormone responses, senescence, as well as protection against environmental stresses including ozone (Conklin and Barth, 2004), UV radiation (Gao and Zhang, 2008), high temperatures (Larkindale et al., 2005) and high light intensity (Muller-Moule et al., 2004). Current evidences exhibited that not only AsA level but also its redox ratio affected versatile physiological processes, including stomatal movement (Chen and Gallie, 2004) and flowering time (Kotchoni et al., 2009). Ascorbate oxidase (AO) (EC 1.10.3.3) was an

apoplastic enzyme in plants that catalyzes the oxidation of AsA with oxygen to monodehydroascorbate (MDHA). Transgenic tobacco plants over-expressing the *AO* antisense displayed severely delayed flowering and higher AsA redox ratio. (Yamamoto et al., 2005).

1.4.2 Ascorbate: A Negative Regulator of the Phase Transition in Planta

The concentration of AsA could reach to millimolar in plants (Smirnoff, 2000). The AsA level in AsA-deficient mutant, *VITAMIN C DEFECTIVE 1 (VTC1)*, contains 30% of wild type AsA content and displayed early flowering time under both LD and SD photoperiod (Conklin et al., 1997). *VTC1* encoded a GDP- D -mannose pyrophosphorylase (GMP), which is an enzyme in the Smirnoff–Wheeler pathway for AsA biosynthesis in plants (Conklin et al., 1999). Smirnoff-Wheeler pathway had been proposed the major route in plants for AsA biosynthesis. The alternative pathways, such as the galacturonate (GalUA) pathway (Agius et al., 2003), the gulose pathway (Wolucka and Van Montagu, 2003) and the *myo*-inositol pathway (Lorence et al., 2004) also participated in AsA biosynthesis. L-galactono-1,4-lactone:ferricytochrome c oxidoreductase (GALDH; EC 1.3.2.3) required a redox-sensitive thiol for optimal

production of AsA , which is an ultimate step enzyme for AsA biosynthesis (Leferink et al., 2009).In addition, Shen et al is validated the important role of gene in galacturonate pathway on phase transition from vegetative to reproductive stage in *Oncidium* (Shen et al., 2009). It means that regulation of any AsA biosynthesis affecting final AsA level would brought about the change of flowering time in *Arabidopsis* and *Oncidium*.

Numerous studies (Kotchoni et al., 2009) addresses that *vtc1* mutant displayed early flowering phenotype. However, *vtc1* exhibiting delayed flowering under short-day photoperiod condition could be attributed to lower AsA limiting GA20-oxidase activity for GA biosynthesis (Kotchoni et al., 2009). Furthermore, *Arabidopsis* feeded with AsA precursor, L-galactono- γ -lactone, resulted in delayed *LFY* expression and late flowering (Attolico and De Tullio, 2006). *Oncidium* applying with AsA also resulted in retardation of inflorescence stalk growth and *OgLEAFY* expression. In *OgPMEOX* transgenic plants, observed very high concentrations of AsA had a negative impacted on flowering time. An increase in the number of rosette leaves was also observed.(Shen et al., 2009).

In summary, the role of AsA on regulating flowering could be an orchestration of ROS/antioxidant homeostasis and well-characterized flowering pathways.

1.5 The Bridge between Ascorbate and Flowering

1.5.1 The Issue of Ascorbate Peroxidase

Plants have evolved versatile strategies against the fluctuate environments including favorable and inappropriate events. AsA is a major constituent of the intracellular redox buffer in *planta*. Ascorbate peroxidase (APX; EC 1.11.1.11) is a major scavenging enzyme to convert H₂O₂ to H₂O by utilizing AsA as its specific electron donor. Various evidences indicated that APX played a key role in *Arabidopsis* in response to abiotic stresses.(Pnueli et al., 2003; Davletova et al., 2005; Miller et al., 2007; Koussevitzky et al., 2008). Knockout-*apx1* plant displayed H₂O₂ accumulation and protein oxidation under light stress, but have favor growth potential than control plants under hyperosmotic or salinity condition (REF). Soybean mutant lacking *APX1* also proved more tolerance against chilling. Oppositely, reduced expression of *tylAPX* in *Arabidopsis* would result in the increase of tolerance against both osmotic and salt stresses. Moreover, *apx1/tylapx double* mutant exhibited an increased sensitivity to sorbitol treatment (Miller et al., 2010). Noteworthy, *apx1* mutant presented the delay flowering and discloses its function on AsA redox ratio affecting flowering.

1.5.2 Hierarchy of Hydrogen Peroxide, Ascorbate and Ascorbate Peroxidase in Flowering process

In higher plants, reactive oxygen species (ROS) would be generated from versatile metabolism during growth or undergoing numerous stresses. Endogenous H₂O₂ were mainly produced from vigor cells or organs which exhibit active oxidation, such as electron transport chains (ETC) in chloroplasts and mitochondria, or photorespiration in peroxisomes (Noctor and Foyer, 1998; Dat et al., 2000). Plant cells prevent excess H₂O₂ via APX functioning on scavenging H₂O₂ by using AsA. Therefore, H₂O₂ trigger a metabolic cascade to reduce AsA level and presumably further affects phase transition. Increasing H₂O₂ levels were detected before flowering in morning glory, wheat and *Arabidopsis* (Hirai et al., 1995; Badiani et al., 1996). Higher redox ratio was detected in vegetative growth pseudobulb, and markedly decreased during bolting period of *Oncidium* (Shen et al., 2009). Moreover, Chin et al validated thermal-induced flowering in *Oncidium*. *Oncidium* growing under elevated growth temperature 30°C/25°C (day/night temperature) displayed higher bolting percentage (95%) accompanying with the higher APX activity (Chin's unpublished data). A drastic decrease of AsA level and redox were also present in pseudobulb of *Oncidium* under

elevated growth temperature condition. The high expression level and activity of APX during phase transition under elevated temperature condition figures out a considerable interlinking between flowering and stress response.

1.6 Goals of This Thesis

AsA level and its redox ratio were recognized as a determinant on regulating phase transition of *Oncidium*. Moreover, growth temperature is a critical factor affecting the AsA status of *Oncidium* growing under green house or field. The complete and detailed genetic network is still unclear even in model species, *Arabidopsis* or rice. In this thesis, we create *Arabidopsis* overexpressing *OgAPX* of *Oncidium* to investigate the role of AsA status in controlling flowering under different photoperiod and temperature condition. We propose a genetic network to address the function of AsA and temperature on flowering mechanism by analyzing the transcriptional profiling.

2. Results

2.1 Characterization of Transgenic *Arabidopsis*

Overexpressing *Oncidium Ascorbate Peroxidase*

2.1.1 Generation of Transgenic *Arabidopsis* Overexpressing *Oncidium Ascorbate Peroxidase*

In order to dissect the role of *Oncidium* ascorbate peroxidase (*OgAPX*) on flowering process, *OgAPX* was overexpressed in *Arabidopsis* plant (hereafter denoted as *OgAPXOX*) under the control of the cauliflower mosaic virus 35S promoter. We selected three homozygous lines (*OgAPXOX line-2, 4, and 7*) for further analysis. Expression level of the *OgAPX* in transgenic lines was examined by Northern blotting (Fig. 1B). The transcript of *OgAPX* could only be detected in the transgenic plants. Total protein extracted from leaves for analyzing the APX activity in transgenic lines and control plants. All transgenic lines displayed higher APX activity compared with wild type and brought about the reduce of H₂O₂ (Fig. 1A, 5). (11.28, 8.37, 8.72 and 4.59 μ mole H₂O₂/g F.W. in line-2,-4 and -7, respectively) These results showed that *OgAPX* was functioned in *Arabidopsis*.

2.1.2 Morphological Characterization of OgAPXOX Transgenic Plants

Plants growing at 22°C under long-day photoperiod or short-day photoperiod were hereafter denoted LD-22°C and SD-22°C. To prevent the alteration of timing on phase transition attributing to elevated growth temperature affecting vegetative growth, plants would further change their growth temperature when consisting of 6 leaves and hereafter denoted LD-30°C and SD-30°C, respectively. Transgenic plants growing under LD-22°C exhibited significantly morphological differences compared with the control plants (Fig. 2A). The foliar blade of *OgAPXOX* displayed sharp and flat shape compared with control plants. Moreover, the transgenic plants exhibited decreasing chlorophyll level and brought about the chlorotic rosette leaves compared with wild type (Fig. 3). The whole chlorophyll levels in wild type were 0.14 mg per g F.W., and transgenic plants were 0.07, 0.06 and 0.02 mg per g F.W. in line-2, 4 and 7, respectively.

2.1.3 Effects of Oncidium Ascorbate Peroxidase on Ascorbate Homeostasis and H₂O₂ Level under Different Environmental Condition in Arabidopsis

Reactive oxygen species (ROS) are produced through active cellular metabolism, and plant cells provide with versatile antioxidants and scavenging enzymes to prevent excessive levels under normal growth condition. In Fig. 1, transgenic plants displayed increasing APX activity and resulted in decrease of H₂O₂. Although the significant decline of H₂O₂ concentrations was present in transgenic plants under LD-22°C (11.28, 8.37, 8.72 and 4.59 μmole H₂O₂/g F.W. in line-2, -4 and -7, respectively), the endogenous AsA levels in *OgAPXOX* slightly decreased compared with wild type (3.52, 2.57, 3.09 and 3.02 μmole AsA/g F.W. in line-2,-4 and -7, respectively) (Fig. 4, 5). Histological staining of leaves with 3, 3'-diaminobenzidine illustrating the location and intensity of H₂O₂ also presented less H₂O₂ in transgenic plants (Fig. 2B).

In Fig. 6, 7, the H₂O₂ and AsA level in transgenic and control plants had shown the similar pattern under SD-22°C

Furthermore, H₂O₂ level in wild type increased more significantly (36.9 μmole H₂O₂/g F.W.) after 4 days under LD-30°C compared with *OgAPXOX* transgenic plants displaying mild increased pattern (20.79, 18.81 and 20.28 μmole H₂O₂/g F.W. in line-2,-4 and -7, respectively) (Fig. 8). The higher growth temperature brought about drastic decrease of AsA level and redox ratio in transgenic plants growing under LD and

SD (Fig.9, 10 and 11). The redox ratio of AsA in each plants before LD-30°C and after 4 days under LD-30°C changed from 10.86 to 9.74 (wild type), 10.28 to 7.36 (lin-2), 8.49 to 1.29 (line-4), and 6.60 to 2.73 (line-7) respectively. It reveals that utilization of AsA by APX would be reinforced swiftly under elevated growth temperature for scavenging excess H₂O₂ and brought about more severe decline of AsA level and redox ratio in transgenic plants compared with wild type.

2.1.4 Effect of Oncidium Ascorbate Peroxidase on Flowering Time under Different Environmental Condition in Arabidopsis

Higher bolting was present in *Oncidium* growing under elevated growth temperature condition accompanying facilitated activity of APX and deprivation of AsA (Chen et al., unpublished data). Recent evidences also reveal that a modest increase of ambient growth temperature is equally efficient in regulating flowering of *Arabidopsis* (Blanchard and Runkle, 2006; Lee et al., 2008). In order to understand whether APX involving in thermal-induced flowering, the flowering time of *OgAPXOX* transgenic plants were monitored under different photoperiod and temperature condition . The flowering time of each plant was determined according to the number of rosettes leaves

when flowering initiation. Under LD-22°C condition, the number of rosette leaves when flowering was 12 in wild type plants, and 10 in line-2,-4 and -7, respectively (Fig. 12). The timing of flowering between wild type and transgenic plants did not present significant difference when growing under LD or SD-22°C and speculated that only or even active APX would not fulfil the flowering (Fig. 12, 13, 14). Furthermore, three independent lines would be cultivated under LD/SD-30°C from LD/SD -22°C when consisting of six leaves to monitor the effect of heat on flowering. Transgenic plants displayed facilitated flowering significantly when plants were grown under LD-30°C (Fig.15, 16). Wild type and transgenic plant would not flower before consisting of 8 leaves when growing at 22°C, but there were 90 % of *OgAPXOX* plants flowered before less than or equal to 8 leaves compared with 40% of wild type. This result indicates that APX could consolidate the thermal-induced flowering. The transgenic plants exhibited not only accelerated flowering but also enervated growth potential, such as severe chlorosis, stunted inflorescence and smaller leaf blade under LD (Fig. 15, 17). Average length of inflorescence in each transgenic line was shorter than 10 cm ($n > 70$) compared with 15cm in control plants under LD. Transgenic plants displayed facilitated flowering significantly when plants were grown under SD-30°C (Fig. 18, 19).

Accordingly, accelerated flowering in *OgAPXOX* transgenic plants could be attributed to the swift ROS-scavenging system bringing about drastic decrease of AsA and redox ratio under elevated growth temperature.



2.2 Genetic Network of Ascorbate Peroxidase Involving in Thermal-induced Flowering Process

2.2.1 Decreased Expression Level of FLM in *OgAPXOX* Plants Suggests the Role of AsA in Regulating Thermal-induced Flowering

Previous studies showed that AsA was a repressor on flowering in *Arabidopsis* and *Oncidium* (Attolico and De Tullio, 2006; Shen et al., 2009). The AsA level fluctuates in response to various endo- and exo- stimulations, including growth temperature condition. Transgenic plants showed early flowering under LD/SD-30°C accompanying with drastic decrease of AsA content and redox states, but it is still unclear the orchestration and detail mechanism of AsA and heat-stimulation on flowering process.

Genetic approaches have identified a group of mutants whose flowering time is affected by AsA level, such as *vtc1*, *ao* and *OgPMEOX* plants (Yamamoto et al., 2005; Barth et al., 2006; Shen et al., 2009). For instance, some floral genes displayed higher level in AsA scarcity mutant *vtc1*, such as *LATE ELONGATED HYPOCOTYL (LHY)*, *TIMING OF CAB EXPRESSION (TOC1)*, *GIGANTEA(GI)*, *CONSTANS (CO)*, and *FLOWERING LOCUS C (FLC)* (Kotchoni et al., 2009). Moreover, the expression level

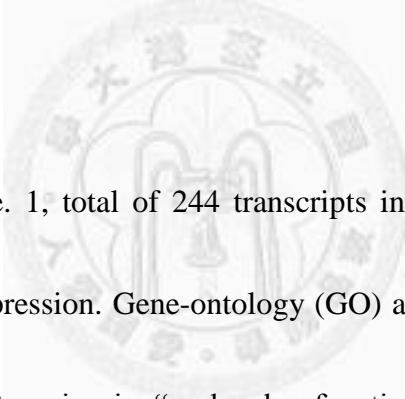
of *FLOWERING LOCUS M (FLM)*, a *FLC* paralogous gene, was repressed in *Arabidopsis* when growing under higher temperatures condition and figure out novel thermal-induced flowering pathway (Balasubramanian et al., 2006). The lower expression level of *AtFLM* was also present in *OgAPXOX* transgenic plants compared with wild type after 5 day under LD-30°C and figured out the role of AsA participating in flowering coordinating with thermal-induced pathway (Fig. 20).

2.2.2 Transcriptional Profiling of OgAPXOX Arabidopsis under Elevated Growth Temperature

To address this issue, we carried out an analyses of the expression profiling of *OgAPXOX* and control plants in response to the elevated growth temperature by 3' IVT Expression GeneChip (Affymetrix; *Arabidopsis* ATH1). All plants were growed under LD-22°C condition. Until they had 6 leaves, a half of transgenic lines and wild type would be cultivated under LD-30°C and sampled the leaves at 0 day under LD-30°C, at 1 day under LD-30°C and at 5 day under LD-30°C for further analysis. After normalization of the expression level with wild type growing under 22°C by Gene Spring GX10.5 (<http://www.genomics.agilent.com/homepage.aspx>), there were total of

860 transcripts selected from the other treatments displaying up- or down- regulated expression levels (>2 fold). The 860 transcripts were subsequently categorized into 10 clusters using *k*-means clustering in accordance with the pattern of their temporal change in the expression profile (Fig. 21A). The clusters consisted of transcripts that displayed overall trends of either increased (Fig. 21B, clusters 2-9) or decreased (Fig. 21B, cluster 1) gene expression over the different time points in the study. The detail of all clusters is interpreted:

Cluster 1:



In Fig. 21B and Table. 1, total of 244 transcripts in cluster 1 displayed overall trends of decreased gene expression. Gene-ontology (GO) analysis of genes in cluster 1 displayed the major subcategories in “molecular function” were function on DNA binding and provided with transcription regulator activity and transcription factor activity. The major subcategory in “cellular component” was located at endomembrane system. The major subcategories in “biological process” were related to transcription factor activity, stress response and response to hormone stimulus. Noteworthy, abundant genes in cluster 1 were predicted to encode various members of transcription factors, including *MYB*, *AP2* and protein in circadian clock. Three *MYBs*, *AtMYB48*

(At3g46130), *AtMYB3* (At1g22640), and *AtMYB60* (At1g08810), in cluster 1 belong to *R2R3-MYB* and have been characterized their function on anthocyanin biosynthesis. Four genes encoding AP2 protein in cluster 1 belong to RAP2.4 subgroup which mediating light and ethylene signaling, including At4g39780, At1g64380, At2g22200 and At1g74930. (Wang et al., 2008). Circadian clock genes, *LHY* (At1g01060) and *APRR9*(At2g46790), regulated flowering time through the canonical CO-dependent photoperiodic pathway (Nakamichi et al., 2007) and displayed drastically decreased expression levels under elevated growth temperature. Therefore, it suggests that antioxidant state (including anthocyanin and AsA), circadian rhythm and phytohormones level would be altered in response to the change of growth temperature and AsA state.

Cluster 2:

In Fig. 21B and Table. 2, total of 126 transcripts in cluster 2 displayed slightly decreased expression pattern after 1 day under LD-30°C, but significant increase in transgenic plants after 5 day under LD-30°C. GO analysis of genes in cluster 2 displayed the major subcategory in “molecular function” was function on nucleotide binding. The major subcategory in “cellular component” was located at plasma

membrane. The major subcategories in “biological process” were related to defense response, phosphate metabolic process, response to organic substance and nitrogen compound biosynthetic process. Noteworthy, abundant genes in cluster 2 were predicted to encode various members of stress-related transcription factors, including *AtMYB70* (At2g23290) and *AtWRKY11* (At4g31550). The transcription factor *AtWRKY11* acted as negative regulator for plant in susceptible to *Pseudomonas syringae* *pv* *tomato* (Kroj et al., 2006). Moreover, *AtMYB70* was likely to be associated with stress responses but still unclear about its detail function. All of them displayed striking increase in *OgAPXOX* under LD-30°C and suggests that their probable functions on coordination of elevated growth temperature and sensing the redox state change caused by *OgAPXOX*.

Cluster 3:

In Fig. 21B and Table. 3, cluster 3 contains 29 transcripts that displayed significantly decreased expression pattern after 1 day under LD-30°C, but significant increased after 5 day under LD-30°C. GO analysis of genes in cluster 3 displayed the major subcategory in “molecular function” was function on carbohydrate binding. The major subcategories in “cellular component” were located at plasma membrane and cell

wall. The major subcategories in “biological process” were related to defense response and response to organic substance. Noteworthily, abundant genes in cluster 3 were predicted to encode various members of stress-related transcription factors, including *AtGSTF3* (At2g02930) and *PR5* (At1g75040). *AtGSTF3* encoded glutathione transferase. *PR5* encoded thaumatin-like protein and involved in response to pathogens. Furthermore, they all displayed drastic decreased expression levels after 1 day under LD-30°C and increased after 5 day under LD-30°C. It suggests that they were response to temperature stimulus and response to pathogens at the late phase.

Cluster 4:

In Fig. 21B and Table. 4, there were 63 transcripts in cluster 4, and their expression levels increased highly in wild type compared with *OgAPXOX* after 5 day under LD-30°C. GO analysis of genes in cluster 4 displayed the major subcategory in “molecular function” was provided with transmembrane transporter activity. The major subcategory in “cellular component” was located at integral membrane. The major subcategories in “biological process” were related to temperature stimulus and response to reactive oxygen species. Noteworthily, abundant genes in cluster 4 were predicted to encode heat shock transcription factors, including, *At5g37670*, *AtHSP70* (At3g12580),

HSP70T-2, *At2g19310*, *HSP81-.1* (At5g52640). Furthermore, they all displayed striking increase expression levels in transgenic plants after 5 day under LD-30°C, and suggests that they promote trigger the heat response by sensing AsA state.

Cluster 5:

In Fig. 21B and Table. 5, there were 92 transcripts in cluster 5, and displayed overall tends of increased gene expression in control and transgenic plants under LD-30°C compared with cluster 4. GO analysis of genes in cluster 5 displayed the major subcategory in “molecular function” was response to oxidative stress. The major subcategory in “cellular component” was located at cell wall. The major subcategories in “biological process” were related to organic substance and response to oxidation reduction. Noteworthy, abundant genes in cluster 5 were predicted to detoxification process, including, *CYP96A4* (At5g52320), *CYP79B2* (At4g39950), *CYP81F4* (At4g37410), *CYP83B1* (At4g31500), *CYP71B3* (At3g26220), *CYP89A9* (At3g03470) and *CSD2* (At2g28190). Furthermore, they all displayed increased expression levels under LD-30°C and suggest oxidoreduction would be responsive to change of growth temperature and AsA state.

Cluster 6:

In Fig. 21B and Table. 6, total of 73 transcripts in cluster 6 displayed steady expression pattern in control and transgenic plants after 1 day under LD-30°C, but significant increased in transgenic plants after 5 day under LD-30°C. GO analysis of genes in cluster 6 displayed the major subcategory in “molecular function” was function on metal ion binding. The major subcategory in cellular component was located at external encapsulating structure. The major subcategories in “biological process” were related to oxidation reduction and response to organic substance. Noteworthy, At3g47480 was predicted to encode calcium-binding protein. Interestingly, At3g47480 displayed striking increase in *OgAPXOX* plants after 5 day under LD-30°C. It was suggested that calcium-triggered signal cascade could sense the redox state.

Cluster 7:

In Fig. 21B and Table. 7, total of 49 transcripts in cluster 7 displayed slightly decreased expression pattern after 1 day under LD-30°C, but significant increased after 5 day under LD-30°C. GO analysis of genes in cluster 7 displayed the major subcategories in “molecular function” were provided with transcription regulator activity and transcription factor activity. The major subcategory in “cellular component” was located at intrinsic membrane. The major subcategories in “biological process”

were related to endogenous stimulus, defense response, response to organic substance and response to carbohydrate stimulus. Noteworthy, abundant genes in cluster 7 were predicted to encode various members of stress response transcription factors, including *AtERF6* (At4g17490), *ATERF-2*(At5g47220), *AtACS11* (At4g08040) and *AtACS6* (At4g11280). All of them played important role in ACC synthesis. Interestingly, transgenic *Arabidopsis* overexpressing *AtMYB44* was more sensitive to ABA and had a more rapid ABA-induced stomatal closure response than wild type and *atmyb44* knockout plants. *AtMYB44* showed slightly decreased after 1 day under LD-30°C, but, induced drastically after 5 day under LD-30°C. It suggests that the stress phytohormones, including of ethylene and ABA, would be retrieved in response to AsA status under elevated growth temperature.

Cluster 8:

In Fig. 21B and Table. 8, cluster 8 contains 55 transcripts that displayed more significantly decreased expression pattern after 1 day under LD-30°C, but significantly increased after 5 day under LD-30°C compared with cluster 7. GO of genes in cluster 8 displayed the major subcategories in “molecular function” was function on ATP binding. The major subcategories in “cellular component” were located at plasma membrane,

cell wall. The major subcategories in “biological process” were related to defense response and response to organic substance. Noteworthy, abundant genes in cluster 8 were predicted to encode various members of pathogenesis-related transcription factors, including *AtPRI* (At2g14610), *AtPR4* (At3g04720), *PDF1.2* (At5g44420). Furthermore, they all displayed drastic decreased expression levels after 1 day under LD-30°C, and increased after 5 day under LD-30°C, and suggested that they were response to thermal-induced acclimation and sensing the redox state at the late phase to reduce injury by pathogen presumably.

Cluster 9:

In Fig. 21B and Table. 9, total of 62 transcripts in cluster 9 displayed steady expression pattern after 1 day under LD-30°C, but significantly increased in wild type after 5 day under LD-30°C. GO of genes in cluster 9 displayed the major subcategory in “molecular function” was function on cation binding. The major subcategory in “cellular component” was located at vacuole. The major subcategories in “biological process” were related to defense response, response to hormone stimulus and response to carbohydrate stimulus. Noteworthy, abundant genes among cluster 9 were predicted to encode various members of *MYB* transcription factors, including *AtMYB73*

(At4g37260), *MYB77* (At3g50060). Interestingly, *MYB77* modulated auxin signal transduction (Shin et al., 2007). *AtMYB73* was response to salicylic acid stimulus. *MYB77* was showed slightly decreased after 1 day under LD-30°C, but, induced drastically after 5 day under LD-30°C. It suggests that the auxin and salicylic acid stimulus in plant process was trigger by downstream genes under elevated growth temperature.

Cluster 10:

In Fig. 21B and Table. 10, cluster 10 contains 53 transcripts that displayed significantly decreased expression pattern after 1 day under LD-30°C, but, significant increased after 5 day under LD-30°C. GO of genes in cluster 10 displayed the major subcategories in “molecular function” was provided with serine/threonine kinase activity. The major subcategory in “cellular component” was located in cytosol. The major subcategories in “biological process” were elated to hormone stimulus and response to abiotic stimulus. Noteworthy, abundant genes in cluster 10 were predicted to encode putative protein kinase, including *CIPK20*, *AtCPK6* (At2g17290). Furthermore, they all displayed drastically decreased expression levels after 1 day under LD-30°C, and increased after 5 day under LD-30°C, and suggested response to

thermal-induced acclimation.

2.2.3 Functional Categories of Expression Clusters in Accordance with Genotypes and Growth Temperature Condition

Those transcripts in response to genotypes and growth temperature were functionally assigned to detail groups as shown in Fig. 22. The framework consists of the following:

Group I: Genes displayed up- /down- regulated by elevated growth temperature both in wild type and transgenic plants (cluster 4 and 5 / cluster 1). Genes in this group would be influenced by temperature and redox ratio, such as circadian clock genes, *MYB*, *HSP*, *RAP2.4* transcription factors, and *CYP*. The functions of these genes were suggested to regulation of anthocyanin biosynthesis, circadian rhythm, heat shock response and oxidative stress. Therefore, genes in Group I were suggested in response to redox ratio under elevated growth temperature.

Group II: Genes showed strikingly up-regulated after 5 day under LD-30°C by the coordination of elevated growth temperature condition and *OgAPXOX* background (cluster 2, 6). Genes in this group would be predicted to response to stress, such as *AtMYB70*, *AtWRKY11*. *At3g47480* was predicted to encode calcium-binding protein. It was suggested that genes in Group II were regulated calcium signal transduction and

stress response by sensing the redox state under elevated growth temperature.

Group III: Genes degraded immediately but de novo synthesis at late treatment period (cluster 3, 8 and 10). The functions of these genes were suggested to regulated pathogen defense, such as *PR* genes. It suggests that pathogen defense genes in Group III would be influenced by temperature at late period.

Group IV: Down-stream genes in response to elevated growth temperature condition (cluster 7 and 9). The functions of these genes were suggested to regulation of hormone stimulus, such as *AtMYB44*, *MYB77*. It suggests that hormone stimulus could be triggered as the down-stream genes under elevated growth temperature.

Noteworthy, the expression profiling of Group II indicates that *OgAPX* could act as a positive effector on their expression level under elevated growth temperature.

2.2.4 Transcription Profiling Revealed That Genes Encoding MYB and AP2 TFs Expressed with Higher/ Lower in OgAPXOX Plants under Elevated Growth Temperature

In accordance with above analysis, *MYB* and AP2 protein were the two TFs in response to elevated temperature or fluctuant redox ratio. The relative expression level

of genes in transgenic plant and wild type after different days under 30°C between wild type growing under LD-22°C were denoted T0/C0, T1/C0, T5/C0, C1/C0 and C5/C0, respectively). It showed that the expression level of *AtMYB70*, *AtMYB44* and *AtMYB77* were up-regulated 2.61, 6.82 and 4.25 fold in T5/C0, respectively. *AtMYB48*, *AtMYB3*, *AtMYB60* and *AtMYBL2* were down-regulated 3.03, 2.47, 2.29 and 1.95 fold in T5/C0, respectively (Table. 11). *MYB* proteins have been recognized key factors in regulatory networks controlling development, metabolism and responses to biotic and abiotic stresses (Dubos et al., 2010). The functions of *AtMYB3*, *AtMYBL2*, *AtMYB60*, *AtMYB111* were well-characterized on control anthocyanin biosynthesis (Lepiniec et al., 2008; Ohme-Takagi et al., 2008; Park et al., 2008; Stracke et al., 2010). *AtMYB77* regulated lateral root formation by modulating the expression of auxin-inducible genes (Shin et al., 2007). *AtMYB44* regulates ABA-mediated stomatal closure in response to abiotic stresses and *AtMYB70* are likely to be associated with stress responses (Cheong et al., 2008). But, the clear function of *AtMYB70* is still scant. The expression level of *AtMYB70* was increased in wild type under LD-30°C, and it would be enhanced in *OgAPXOX*. Therefore, we suggested the *AtMYB70* was a critical recipient sensing the drastic decreased redox status.

The AP2-type transcription factors including of At4g39780, At1g64380, At2g22200, At2g28550 and At2g44940 were down-regulated 2.68, 5.13, 2.84, 2.39 and 2.68 fold in T5/C0, respectively (Table. 12). At1g79700 and At1g74930 were up-regulated 1, 1.58 fold T5/C0, respectively. Noteworthily, *Rap2.4a* family genes which were identified the redox-sensitive transcription factors functioning on the control of antioxidant state, but the detail function is still unclear (Shaikhali et al., 2008). This analysis suggested that contain Rap2.4 domain (i.e., At4g39780, At1g64380, and At2g22200) might sense the drastic decrease of redox status.

2.2.5 Genes Involving in Circadian Rhythm and Starch Synthesis Were Significantly Altered in APXOX Plant under Elevated Growth Temperature

Several genes, including *LHY*, *PSEUDO-RESPONSE REGULATOR9 (APRR9)*, *SQUAMOSA PROMOTER BINDING PROTEINLIKE 3 (SPL3)* and *HEME ACTIVATOR PROTEIN 2B (ATHAP2B)* are robust markers for circadian rhythm (Nakamichi et al., 2007; Wu et al., 2007; Yamaguchi et al., 2009). The expression levels of *SPL3*, *ATHAP2B* were up-regulated 4, 1.49 folds T5/C0, respectively (Table. 13).

Oppositely, the expression levels of *LHY*, *APRR9* were down-regulated 2.14, 2.24 fold T5/C0, respectively.

Moreover, At3g30720, which encoding *QQS* functioning on starch metabolism showed drastic low level in transgenic plants (-8.60 in T0/C0, -7.73 in T5/C0 fold). It means that *QQS* would be responsive to AsA state rather than elevated growth temperature (Table. 14).

2.2.6 Quantification of Expression Level of Candidate Genes by Real-time

PCR

Candidate genes displaying 2-fold increased or decreased expression than wild type at day 0 (T5/C0) were further quantified for their expression level between different control and transgenic plant by real-time PCR. The expression level of *AtMYB70* in *OgAPXOX* plant was up-regulated 3 fold (T5/C0). But *AtMYB70* was slightly increased in wild type after 5 day under LD-30°C (Fig. 25). It was revealed facilitated *AtMYB70* expression level would be further enhanced in *OgAPXOX* (1.5 fold).

The expression level of *AP2* transcription factors (At4g39780, At1g64380,

At2g22200 and *TARGET OF EAT 1 (TOE1)* in *OgAPXOX* plant was significantly down-regulated when plant growing after 5 day under LD-30°C compared with wild type (Fig. 23). It also reveals that decrease of expression level would be severe in *OgAPXOX*.

The expression level of *LHY* in *OgAPXOX* and wild type were up-regulated when plant growing after 1 day under LD-30°C, but, down-regulated after 5 day under LD-30°C (Fig. 24). The expression level of *APRR9* in *OgAPXOX* and wild type were down-regulated when plant growing under LD-30°C, but, significantly down-regulated in *OgAPXOX* (Fig. 24) (0.7 fold). In Fig. 24, the expression level of *SPL3* in *OgAPXOX* was up-regulated >2fold (T1/C0), but, significantly down-regulated about 0.7 fold (T5/T1). The expression level of *AtHAP2B* in wild type were up-regulated when plant growing under LD-30°C >2.5 fold (C5/C0), but, the expression level in transgenic plant displayed steady state under LD-30°C (Fig. 24). It is interesting that the transcript level of *QQS* showed the steady drastic low level in transgenic plants (0.1 fold) (Fig 25). It should be noted that the expression level of *QQS* in other independent line also showed lower than control plants and indicated that *QQS* was highly responsive to AsA status rather than ambient temperature (Fig 26). Moreover, *QQS* functions on starch

biosynthesis and revealed that AsA status may cross-talk with sugar on flowering process.

2.2.7 Expression Profiling of Candidate Genes in AsA Deficient or Accumulated Mutants

Identification of candidate genes in response to endogenous AsA status, their expression level were monitored in AsA-deficient mutant *vtc1* which exhibited the 40% AsA level of wild type and AsA-accumulated transgenic plants (*OgPMEOX*) which exhibited 2 fold AsA level of wild type (Smirnoff, 2000; Shen et al., 2009). *VTC1* and *PME* encode GDP- D -mannose pyrophosphorylase and pectin methylesterase in the Smirnoff-Wheeler pathway and galacturonate pathway for AsA biosynthesis, respectively. Total RNAs were extracted from the 1-week-old seedling of each mutant and transcript levels were determined by real-time PCR. It showed that the transcript levels of *AtMYB70*, circadian genes (*ATHAP2B*, *LHY*) and *AP2* transcription factors (*At4g39780*, *At2g22200*, *TOE1*) and *At3g30720* were higher in the AsA-deficient mutant *vtc1* background than in wild type (about 2 fold), while the circadian genes (*SPL3*, *ATHAP2B*) and *AP2* gene (*At1g64380*) showed steady state (Fig 27, 28, 29). Next, all of them were investigated further in AsA-accumulated transgenic plants

OgPMEOX. The relative transcript levels of all genes were substantially repressed in AsA accumulated mutants (about 0.1 fold), apart from At1g64380 and *LHY* (Fig 27, 28).

3. Discussion

Arabidopsis overexpressing *OgAPX* exhibited superior capacity for scavenging H₂O₂ and displayed the same flowering time under 22°C (Fig.12, 14) but accelerated flowering under 30°C compared with wild type (Fig. 16,19). APX affecting the AsA status was well-characterized in thermal response and desirable to detail address its function in orchestration of AsA and temperature on flowering process. Transcriptional profiling elucidated versatile hierarchies in response to AsA and temperature coordinating flowering, including oxidoreductases, heat response proteins, phytohormone response proteins, and numerous transcription factors. The temporal expression pattern at 30°C and expression levels under different AsA level mutants speculated the critical role of stress-related *MYBs* and *AP2* participating in redox state functioning on a mechanism prior to sugar and miRNAs affecting flowering process.

The activity of APX would be accelerated when plant undergoing elevated temperature condition and brought about severe deprivation of AsA (Bonifacio et al.,

2011). *OgAPXOX* transgenic plants displayed similar AsA redox ratio at 22°C but decreased pattern at 30°C compared with wild type in LD photoperiod (Fig. 10). It reveals that utilization of AsA by APX would be reinforced swiftly under LD-30°C and brought about early flowering in transgenic plants compared with wild type. *MYBs*, such as *AtMYB11*, *AtMYB12* and *AtMYB111* were validated their function in response to the fluctuate of redox ratio resulting from change of environment (Weisshaar et al., 2007; Grotewold et al., 2010). The expression level of *AtMYB70* was increased in wild type under LD-30°C, and it would be enhanced in *OgAPXOX* (Fig. 25). Therefore, we suggested the *AtMYB70* was a critical recipient sensing the drastic decreased redox status and function on flowering. Redox control in R2R3-MYB was through to alter Cys residues to form an intra-molecular S-S bond to influence MYB domain structure. *AtMYB70* belongs to R2R3-MYB. Therefore, *OgAPXOX* displaying drastic decrease of redox status under elevated growth temperature would carry out significant alteration of Cys residues for influencing the expression of responsible genes.

Furthermore, a validated MYB binding *cis* element locating on *QQS* promoter region (Li et al., 2009), and it infers that *QQS* transcription is also regulated by direct binding of MYB within *QQS* gene promoter.

Moreover, earlier studies have shown that flowering induction might be caused by a combination of sugar import and mobilization of various polysaccharides (Lejeune et al., 1993; Sulpice et al., 2009). *QQS* functioning on starch biosynthesis (Li et al., 2009). *OgAPXOX* displayed drastic decrease of expression level of *QQS* than wild type under LD-22/30°C (Fig. 25,26). It infers that starch content is presumable also less than wild type. Noteworthy, *QQS* would be responsive to AsA state rather than elevated growth temperature. It might indicate that AsA play a vital importance for thermal-induced flowering and carbohydrate homeostasis.

Interestingly, the flowering process was regulated by *miR156* level and carbohydrate metabolism (Schmid and Srikanth, 2011). It is tempting to speculate that *miR156* and its target *SQUAMOSA PROMOTER BINDING PROTEINLIKE (SPL)* would be response to the carbohydrate status of plant under endo- or exo- environmental events. It suggests that *QQS* regulated by AsA state provides a prior regulatory hierarchy in the cross-talk miRNA and carbohydrate on flowering process.

Moreover, phase transition in *Arabidopsis* would be promoted when plant presented decreasing *miR156* level and further trigger *SPL3* expression level (Wu and Poethig, 2006). *SPL3* was direct upstream activator of *LEAFY (LFY)* (Yamaguchi et al.,

2009). The expression level of *SPL3* was significantly increased in *OgAPXOX* after 1 day under LD-30°C (Fig. 24). It suggests that the increasing *SPL3* is a consequence of decrease in *miR156* level presumably. SPL protein promoted the *miR172* transcription to trigger downstream signal cascade for phase transition (Wu et al., 2009; Zhu and Helliwell, 2011).

MiR172 acted as downstream of *SPLs* to repress six *AP2-like* transcription factor, such as TARGET OF EAT (TOE) proteins (TOE1, TOE2, and TOE3), SMZ and its paralog SCHNARCHZAPFEN (SNZ) (Mathieu et al., 2009). The expression level of *TOE1* was significantly down-regulated in *OgPMEOX* but up-regulated in *vtc1* (Fig. 27). However, *OgAPXOX* displayed drastic decrease of expression level of *TOE1* than wild type after 5 day under LD-30°C (Fig. 23). It suggests that *TOE1* would be regulated by AsA in different genotype background.

SMZ, other target gene of *miR172*, would require FLM to repress *FT*. In Fig. 20, the lower expression level of *AtFLM* was present in *OgAPXOX* transgenic plants compared with wild type after 5 day under LD-30°C and figured out the role of AsA participating in flowering coordinating with thermal-induced pathway.

In summarize, the genetic network of *OgAPXOX* provide a complex regulatory

mechanism of flowering by altering the redox state under elevated growth temperature (Fig. 30).

Noteworthy, the clock-associated gene *PSEUDO-RESPONSE REGULATOR9* (*APRR9*) has been validated in activation of *CO* expression and antagonistic to *LATE ELONGATED HYPOCOTYL* (*LHY*) during the daytime (Nakamichi et al., 2007). The expression levels of *APRR9* and *HEME ACTIVATOR PROTEIN 2B* (*ATHAP2B*) were significantly down-regulated in *OgPEMOX* whereas *LHY* was up-regulated in *vtc1* (Fig. 28). However, *OgAPXOX* showed lower AsA level under elevated growth temperature, but the flowering positive regulator *APRR9* and *AtHAP2B* showed decrease and steady pattern, respectively (Fig. 24). It suggests that these clock genes were not all response to AsA status and brought about the differential expression pattern under different genotype backgrounds. This results also support the previous evidence declaring elevated growth temperature would not require the photoperiod effector *CO* to act upstream of the floral integrator *FT* (Balasubramanian et al., 2006).

Moreover, the *AP2* transcription factors in *OgAPXOX* transgenic plants displayed striking decreased gene expression compared with wild type under LD-30°C day 5 (Fig. 23). It reveals that *AP2* transcription factors were regulated by the homeostasis of ROS

and AsA in *Oncidium* and *Arabidopsis* (Shaikhali et al., 2008; Wang et al., 2008b). In previous studies showed that RAP2.4 type genes were down-regulated by light but up-regulated by salt and drought stresses (Wang et al., 2008b). However, transgenic plant overexpressing RAP2.4 would present early flowering compared with wild type (Lin et al., 2008). Although these RAP2.4 type AP2 validated in response to oxidative stress were not be monitored in *OgAPXOX* transgenic plant under different conditions, the expression levels of different RAP2.4 genes displayed significant relevancy with AsA status, including of At4g39780, At1g64380 and At2g22200 , and speculates their probable function on thermal-induced flowering.

The shorter inflorescence was another significant phenotype in *OgAPXOX* transgenic plants. Moreover, the starch is provided energy to sustain floral development (Wang et al., 2008a). In Fig. 25, we speculate the higher expression level of *AtMYB70* in *OgAPXOX* would bring about the decreasing *AtQQS* and further affected the starch biosynthesis. Therefore, the damage of inflorescence growth could be presumably perceived to the work of APX on carbohydrate mobilization under elevated growth temperature condition (Fig. 17). Accordingly, we suggest that *AtMYB70* is not only function on flowering but also regulate the inflorescence growth

attributing to carbohydrate metabolism. Moreover, *adgl-1/tpt-1* double mutant displaying severe impairment in starch biosynthesis and triose phosphate / phosphate translocator not only resulted in decline maximum photosynthetic electron transport rate but also diminished chlorophyll contents compared with wild type (Hausler et al., 2009). It also appears that the chlorosis phenotype in *OgAPXOX* transgenic plants can be attributed to the total concentration of starch in *OgAPXOX* is less than control plants presumably (Fig. 3).

In summarize, the genetic network of *OgAPXOX* provides a complex regulatory mechanism of flowering by altering the redox state prior to miRNA and sugar-affected flowering under elevated growth temperature.

4. Prospective

Dissection of phase transition is an important issue to improve our knowledge for breeding and manipulation of horticulture crop efficiently. To ensure reproductive success, plants evolved an elaborate genetic network that integrates environmental signals (day length and temperature) and endogenous substance such as AsA and carbohydrate. The increasing expression level of *AtMYB70* would be reinforced in *OgAPXOX* compared with wild type under LD-30°C. Therefore, we suggested the *AtMYB70* was a critical recipient sensing the drastic decreased redox status and functions on flowering. There were several *cis*-elements in response to redox ratio have been assigned in upstream region of promoter of scavenging enzymes in mammal, but the validated transcription activator is still uncertain in plants. In order to address this model, scanning the antioxidant response element (ARE) element in *AtMYB70* promoter and identification of the regulatory proteins on it could further figure out the detail signal cascade of flowering associated with redox homeostasis.

Moreover, *QQS* acting on starch biosynthesis which expression level was suppressed by overexpressing *OgAPX*. However, in transgenic plants fine-tune carbohydrate homeostasis mechanism was still unknown. Therefore, we will also

analyze the *QQS* expression levels and carbohydrate contents in *apx*-knockout mutant to dissect the mechanism. In previous studies showed that *miR156* would be response the carbohydrate state and function on flowering. However, the correlation between *miR156* and carbohydrate status was poorly understood. We will perform overexpression of *AtQQS* in *Arabidopsis* to understand that how does carbohydrate homeostasis regulate *miR156*.



5. Materials and Methods

5.1 Plant Materials and Growth Conditions

Wild-type *Arabidopsis thaliana* plants Columbia-0 (Col-0) were grown in solidified Murashige and Skoog (MS) medium (following the protocol of Shen et al., 2009). All seed was sterilized with 75% ethanol and 50% bleach(contain tween 20) separately, for 10 min, washed three times with sterilized H₂O, and then spread onto 0.4% (w/v) phytagel plates containing MS medium and 1% sucrose. The seeds were placed in darkness for 3 day at 4°C and then incubating in growth chambers under 16 h of 100 $\mu\text{mol photons m}^{-2} \text{s}^{-1}$ light and 8 h of darkness at 23°C. After the germination, all plants were transferred to growth room under short-day photoperiod condition (8 h of light/16 h of dark) or long-day photoperiod condition (16 h of light/8 h of dark). Plant were further transferred to elevated growth temperature condition (30°C) under LD/SD condition for following analyses. Fifteen plants per genotype/condition were dissected and flash frozen before transfer (Day 0) or on the following days 1 and 5. Flowering time was measured by scoring the number of rosette leaves when each plant consisting of 30-50 individual at bolting. To generate *OgAPX* overexpressing plants (*OgAPXOX*), a complete cDNA of *Oncidium ascorbate*

peroxidase was amplified by PCR and cloned into a destination vector harboring the cauliflower mosaic virus (CaMV) 35S promoter. The recombinant plasmid was introduced into wild-type Columbia plants using the floral dip method (Clough and Bent, 1998). Homozygous plants in the T3 generation were used to analyze the flowering time, expression patterns and numerous analyses.

5.2 RNA Extraction, Microarray and qPCR

1. Total RNAs were extracted from transgenic plants and wild type under different conditions by flowering with “Pine tree” method. (Chang et al., 1993)
2. Total RNAs have been validated by capillary electrophoresis (O.D. 260/230 \geq 1.8, 260/280 \geq 1.9 and the concentration: 1.5 – 3 $\mu\text{g}/\mu\text{g}$ l).
3. The cDNAs of each samples would be generated and further hybridized to Affymetrix 3'-Expression array ATH1 chip for following analyses.
www.affymetrix.com (service by Academia Sinica, Taiwan)
4. Raw data displaying the intensity of signals which aimed to different genes would be further normalized in Gene Spring 10.5 and resulting the relative gene expression level. (Agilent Technologies).

(<http://www.genomics.agilent.com/homepage.aspx>) (service by TechComm center,

College of Life Science, NTU)

5. The genes displaying significant alteration on expression level compared with LD-22°C condition (more than 2-fold up- or down-regulation) would further monitor their expression level by qPCR.
6. Total RNAs with high-quality (A260/A280>1.8 and A260/A230>2.0) were used for qPCR.
7. mRNAs among total RNA (1 mg) converting to first-strand cDNA by using reverse transcriptase with the oligo-dT primer was in accordance with the manufacturer's instructions. (Fermentas) (<http://www.fermentas.com/en/home>)
8. qPCR was performed using Applied Biosystems 7500 Fast Real-Time PCR System and KAPA SYBR Green PCR[®] master mixture universal.
9. The primers for qPCR were listed in Appendix 1.

5.3 Ascorbate Peroxidase Activity Analysis

Preparation:

Equipments: spectrophotometer, centrifuge.

Materials: 1.5/2mL microcentrifuge tubes.

Reagents:

1. Substrate Buffer: 0.4mL 0.75mM EDTA plus 1mL 1.5mM ascorbate and 1mL 150mM potassium phosphate buffer (PH 7.0).

Procedures:

1. Mix 100 μ L crude protein with 2.4mL substrate Buffer and measure the absorbance at 290nm immediately (A_0).
2. Add 250 μ L 0.03% H₂O₂ to the above mixture and mix well.
3. Incubate the mixture for 2 min at 25°C and measure the absorbance at 290nm immediately (A_2).
4. The decrease of absorbance is the cause of the oxidation of ascorbate by ascorbate peroxidase, and it can be estimated through the linear regression equation from the A_{260} of the ascorbate standards.
5. One unit of ascorbate peroxidase was defined as the activity that consumed 1 μ mole AsA min⁻¹mg⁻¹ total protein.

Principles:

Ascorbate peroxidase was assayed from the decrease in absorbance at 290nm as ascorbate was oxidized. We used 290nm in place of 265nm because the absorbance of

our assay mixture was too high at the absorption maximum of ascorbate in Hitachi spectrophotometer. (Mukherjee and Choudhuri, 1981)

Notes:

Although the ascorbate oxidase present in the crude protein would interfere the result of the decrease of ascorbate by ascorbate peroxidase, the ascorbate in symplast is oxidized mainly by ascorbate peroxidase.

5.4 Ascorbate Measurement

Preparation:

Equipment: spectrophotometer, centrifuge (4°C), oven (37°C), mortar and pestle.

Material: liquid nitrogen, 1.5mL and 2mL microcentrifuge tubes, 96well microplate.

Reagents:

Fresh 1M ascorbate (AsA) and dithiothreitol (DTT).

Procedures:

1. Homogenize tissue (0.5g) by pre-chilled mortar and pestle with liquid nitrogen.
2. Mix 1mL 6% trichloroacetate (TCA) well and transfer the mixture to a 2mL microcentrifuge tubes.

3. Vortex well for 10 second and keep the mixtures on the ice.
4. Delaminate by centrifugating with 13000rpm for 5min at 4°C and transfer the supernatants to the new 1.5mL microcentrifuge tubes.
5. Transfer 200 μ L supernatant to new 2 mL microcentrifuge tubes labeled total AsA.
6. Transfer 200 μ L supernatant to new 2 mL microcentrifuge tubes labeled reduced AsA.
7. Prepare 200 μ L 6% TCA as blank and 200 μ L AsA standards (0.15-1 mM) in the mL microcentrifuge tubes.
8. Add 100 μ L 75 mM sodium phosphate buffer (pH7.0) to all above microcentrifuge tubes.
9. Add 100 μ L 10 mM DTT to the total AsA microcentrifuge tubes and incubate at room temperature for 10 min. DTT would reduce the oxidized AsA.
10. Add 100 μ L 0.5% *N*-ethylmaleimide (NEM) to the total AsA tubes for removing the excess DTT and incubate for 30 second.
11. Add 200 μ L ddH₂O to the reduced AsA microcentrifuge tubes.
12. Add 500 μ L 10%TCA, 400 μ L 43% phosphoric acid (H₃PO₄), 400 μ L 4% α - α' -bipyridyl and 200 μ L 3% ferric chloride (FeCl₃) to all microcentrifuge tubes.

13. Incubate the microcentrifuge tubes at 37°C for 1hr.
14. Load 200 μ L samples, blank and standards in a 96-well microplate and measure the absorbance at 525nm.
15. Calculate a linear regression curve from the A_{525} of the AsA standards.
16. Concentration of total AsA and reduced AsA of samples can be estimated through the linear regression equation.
17. Oxidized AsA can be estimated by subtracting the reduced portion from the total ascorbate pool.

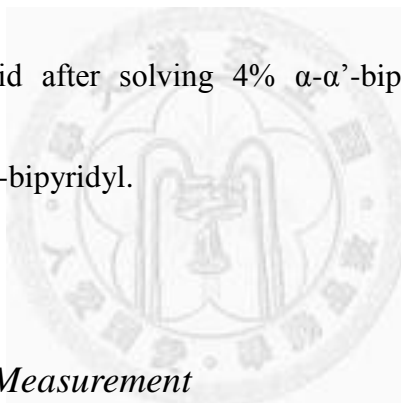
Principles:

This protocol describes a microplate-adapted colorimetric ascorbate assay, in which ferric ion (Fe^{3+}) is reduced by ascorbate to the ferrous ion (Fe^{2+}). The ferrous ion reacts with α - α' -bipyridyl to form a complex with characteristic absorbance at 525 nm.

With the DTT reduction of any dehydroascorbate (DHA) in a sample, total ascorbate can be assayed using the α - α' -bipyridyl method, and DHA can be estimated by subtracting the reduced portion from the total ascorbate pool. (Ainsworth and Gillespie, 2007)

Notes:

- a. Reagents would work at room temperature for avoid the precipitation of α - α' -bipyridyl and storage them at 4°C.
- b. All sample and standards were prone to keep on ice and avoid the light.
- c. 10% TCA, 400 μ L 43% phosphoric acid (H₃PO₄), 400 μ L 4% α - α' -bipyridyl and 200 μ L 3% ferric chloride (FeCl₃) could be mixed in order before use.
- d. α - α' -bipyridyl is prepared in or higher 4% phosphoric acid.
- e. Mix the 3% ferric acid after solving 4% α - α' -bipyridyl completely to avoid precipitation of 4% α - α' -bipyridyl.



5.5 Hydrogen Peroxide Measurement

Preparation:

Equipments: spectrophotometer, centrifuge (4°C), mortar and pestle.

Materials: 2 mL microcentrifuge tubes 96well microplate, liquid nitrogen.

Reagents:

1. Buffer 1: 10mM 3-amino-1,2,4-triazole in 50mM sodium phosphate buffer (pH 6.5).
2. Buffer 2: Titanium (IV) oxysulfate-sulfuric acid solution.

3. 30% (9.8M) H₂O₂.

Procedures:

1. Prepare the hydrogen peroxide standard (9.8 mM~9.8 nM) to confirm the efficiency of the buffers before assay.
2. Homogenize tissue (0.5 g) with liquid nitrogen in pre-chilled mortar and pestle.
3. Add 1.8 mL Buffer 1 to extract and transfer the mixture to the 2 mL microcentrifuge tubes.
4. The samples were centrifugated with 13000 rpm for 5 min at 4°C and transfer the supernatants to the new 1.5 mL microcentrifuge tubes.
5. Repeat the centrifugation.
6. Preparation 200 µL Buffer 2 to the new microcentrifuge tubes.
7. Add 600 µL supernatant and H₂O₂ (9.8 mM~9.8 nM) to above microcentrifuge tubes and mix well.
8. All mixtures were centrifugated with 13000 rpm for 5 min at 4°C.
9. Take 500 µL supernatant (yellow or light pink) to the new microcentrifuge tubes and discard the pellet (white).
10. The supernatants were centrifugated with 13000 rpm for 5 min at 4°C to remove

excess Titanium chelate.

11. Load 200 μL samples, blank and standards in 96-well microplate and measure the absorbance at 410 nm.

12. Calculate a linear regression curve from the A_{410} of the H_2O_2 standards.

13. H_2O_2 amount in each sample can be estimated through the linear regression equation.

Principles:

Ti (IV) in sulfuric acid is present as $[\text{Ti}(\text{OH})_2]^{2+}$ and $[\text{Ti}(\text{OH})_3]$ + colorless ions.

However, it would be converted into $[\text{Ti}(\text{O})_2\text{OH}]$ + yellow-orange ion. This chelate is soluble in sulfuric acid and could be separated with excess Ti ion by a simple

centrifugation. The limit of detection of hydrogen peroxide is 10 nM. (Jana and Choudhuri, 1982)

Notes:

a. The color is dark red when add excess H_2O_2 as standard, and the optimal standard concentration ranges from 9.8 mM~9.8 nM and display the colour in yellow.

b. (samples or standard mixing with Buffer1) / (Buffer 2) = 3:1 (v/v).

5.6 Hydrogen Peroxide Staining

Preparation:

Equipments: microscope, vacuum dryer, water bath.

Materials: knives (razor), tweezers, glass slides, 50 mL microcentrifuge tubes.

Reagents:

1. DAB buffer (0.5 mg mL⁻¹): 50 mg 3,3'-diaminobenzidine in 100 mL 50 mM sodium phosphate buffer (pH 7.0).
2. Wash buffer: 95 mL 70% ethanol plus 5 mL NH₄OH ACS reagent.
3. Ethanol.

Procedures:

1. Samples were sliced to form 2 mm section.
2. Sections were incubated in DAB buffer.
3. Increase the efficiency of the fixation by evacuation for 2 min twice.
4. Keep the sections in the dark at room temperature for 24 h.
5. Boil the sections with ethanol (96%, v/v) until remove the chlorophyll completely.
6. Keep the sections in the 100% ethanol.
7. Photograph the sections.

Principles:

The staining was based on the instant polymerization of DAB (to form a reddish-brown complex which is stable in most solvents), as soon as it comes into contact with H₂O₂ in the presence of peroxidase. (ThordalChristensen et al., 1997)

Notes:

Keep the DAB buffer in the dark and storage at 4°C

5.7 Quantitative Analysis of Protein Concentration

Bio-Rad Protein Assay Kit.

Preparation:

Equipment: spectrophotometer.

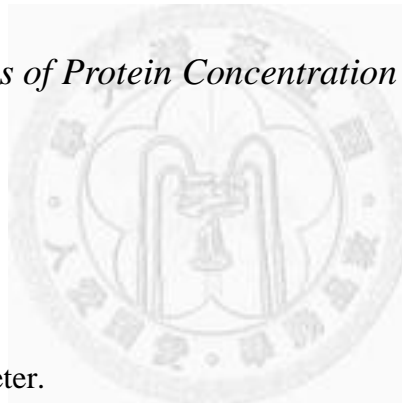
Material: 96 well microplate.

Reagents:

1. Bio-Rad Protein Assay kit.
2. BSA(1 µg µL⁻¹).

Procedures:

1. Mix dye and ddH₂O by 4:1 (v/v).



2. Add 1,2,4,8,16 μL bovine serum albumin (BSA) and 1 μL ~5 μL crude proteins with above mixture to 200 μL and incubate at room temperature for at least 5 min.
3. Measure the absorbance at 595 nm and calculate a linear regression curve from the A_{595} of the BSA standards.
4. Protein concentration of crude protein can be estimated through the linear regression equation.

Principles:

This assay is based on the method of Bradford. The absorbance maximum for an acidic solution of Coomassie Brilliant Blue G-250 dye shifts from 465 nm to 595 nm when binding to protein occurs. The Coomassie blue dye binds to primarily basic and aromatic amino acid residues, especially arginine.

Notes:

Absorbance will increase over time; samples should incubate at room temperature for no more than 1 hr.

5.8RNA Extraction

Preparation:

Equipments: mortar and pestle, centrifuge, water bath (65°C), refrigerator (4,-80°C), 30 mL centrifuge tubes.

Materials: liquid nitrogen, 5 mL tip.

Reagents:

1. Extraction buffer (500 mL): 10 g polyvinylpyrrolidone (PVP, average mol wt 40000) + 10 g hexadecyltrimethylammonium bromide (CTAB) + 4.653 g EDTA + 58.44 g NaCl + 0.25 g spermidine.
2. 10X MOPS (200 mL): 8.372 g MOPS + 0.8203 g sodium acetate + 0.7448 g EDTA.
3. Denature buffer: 600 µL formamide + 210 µL formaldehyde + 10X MOPS buffer + 7 µL ethidium bromide (EtBr; 10 mg mL⁻¹).
4. RNase free ddH₂O: 1 mL diethylpyrocarbonate (DEPC) in 1 L water and sterilize in autoclave with 2 atm for 40 min.

Procedures:

1. Grind 1 g sample in the mortar treated with liquid nitrogen.
2. Add 10 mL extraction buffer with fresh 200 µL β-mercaptoethanol into the mortar.
3. After thawing the mixture, transfer the slurry to the centrifugation tube.
4. Incubate the mixture at 65°C in water bath for 10 min.

5. Delaminate by centrifugating with 13000rpm at 25°C for 15min.
6. Transferring the supernatant into a new centrifugation tube.
7. Add equal volume chloroform/isoamyl alcohol (24:1) and gently mix it for 1 min.
8. Repeat step 5 to step 7.
9. Delaminate by centrifugating with 13000 rpm at 25°C for 15 min.
10. Transferring the supernatant into a new centrifugation tube.
11. Add one fourth fold volume 10 M lithium chloride (LiCl).
12. Incubate the mixture at 4°C overnight.
13. Collect the RNA by centrifugating with 13000 rpm at 4°C for 15 min.
14. Wash the pellet by 75% ethanol two times.
15. Remove the excess alcohol in the pellet by vacuum dryer.
16. Resuspend the pellet with optimal volume RNase free ddH₂O.
17. Check the quality of RNA by electrophoresis.
18. The remaining RNA samples were immediately steeped in liquid nitrogen and keep
in -80°C for long time storage.
19. RNA electrophoresis (e.g. 25mL volume):
 - (1) 25 g agar + 25 mL RNase free ddH₂O.

- (2) Melt the agar by microwave oven.
- (3) Until the mixture cool down to 40~50°C and add 2.5 mL 10X 3-(N-morpholino)propanesulfonic acid, 4-morpholinepropanesulfonic acid (MOPS) and 0.75 mL 37% formaldehyde.
- (4) Solidify the agar in the suitable tank.
- (5) Electrophoresis in 50 mV 1 hr.
- (6) Photograph the gel under UV exposure.

Note:

- a. There are three methods for RNA precipitation:

- (1) LiCl: For precipitation of RNA which molecular weight is longer than 200 bp.

The optimal precipitation condition is at 4°C.

Supernatant: 10M LiCl = 4:1 (v/v)

- (2) 100% ethanol: The optimal precipitation condition is at -20°C.

Supernatant: 100% EtOH: 10M NH₄OAc = 1:2.5:0.25 (v/v/v)

- (3) 100% Isopropanol: The optimal precipitation condition is at -20°C.

Supernatant: Isopropanol: 10M NH₄OAc = 1: 0.25 (v/v)

- b. All material including motars, pistils, reagents, etc should be remove the RNase by

rinsing with 1% DEPC and then sterilize in autoclave with 2 atm for 40 min.

- c. The chemicals for extraction buffer should be mixed in order and sterilize in autoclave with 2 atm for 40 min after stirring with 0.5mL DEPC overnight.

5.9 RT PCR for Gene Expression (One-step RT PCR)

(1) Add the following reagents to a 0.2 mL microcentrifuge tube in order

RNase Free ddH ₂ O	24 μ L
10 X One Step RNA PCR Buffer	5 μ L
25 mM MgCl ₂	10 μ L
10 mM dNTP	5 μ L
10 μ M Gene specific forward primer	1 μ L
10 μ M Gene specific reverse primer	1 μ L
RNA (1 μ g μ L ⁻¹)	1 μ L
RNase Inhibitor (40 units mL ⁻¹)	1 μ L
AMV RTase XL (5 units mL ⁻¹)	1 μ L
AMV-Optimized Taq (5 units mL ⁻¹)	1 μ L

(2) Setup a PCR reaction following the below condition:

50°C	45 min	
94°C	2 min	
94°C	30 sec	} 12~25 cycles
50~60°C	30 sec	
72°C	30 sec	
72°C	10 min	
16°C	∞	

(2) The expression level of gene in different samples was quantificated by the intensity of PCR product which displayed in the electrophoresis.

5.10 Construction of Functional Plasmid for Overexpressing the Interested Genes in Arabidopsis

Preparation:

Equipments: Electrophoresis set, centrifuge (4/-20°C), heating plate (65/50/42°C), refrigerator, oven (80/37°C), PCR machine, electroporation machine and cuvette.

Materials: Ligation Kit, Gel elution Kit, pCAMBIA 2300 vector, 15mL centrifuge tube, 1.5mL microcentrifuge tubes, restriction enzymes,

Reagents:

1. LB medium (1L): Mix 15g (Luria-Bertani) medium and 25g agar (for bacteria culture) and sterilize at 2 atm for 20 min.
2. LB broth (1L): Mix 15g (Luria-Bertani) medium and sterilize at 20 atm for 20 min.
3. Solution 1: 50mM glucose, 10mM EDTA in 25mM Tris-HCl (pH8.0).
4. Solution 2 (Fresh): 880 μ L ddH₂O, 100 μ L 10%SDS and 20 μ L 10N sodium hydroxide.

Keep at room temperature.

5. Solution 3: 60mL 5M potassium acetate +11.5mL glacial acetic acid and 28.5mL H₂O.
6. RNase: 0.1g RNase A solves in 10 μ L H₂O, and then boils it for 10min. Filter sterilize the solution by passing it through 0.22 micron filter and storage at -20°C.
7. PCI: phenol/chloroform/isoamylalcohol (25:24:1)
8. CI: chloroform/isoamylalcohol (24:1).
9. X-gal: 1g of X-gal in 10 mL of dimethyl formamide (DMF).
10. IPTG: Isopropyl Thiol-D-Galactoside, 0.2g IPTG solves in 10mL H₂O and filter sterilize the solution by passing it through 0.22 micron filter and store them in -20°C.

Procedures:

1. Elute the DNA product from the electrophoresis by following the elution kit protocol.
2. Check and quantify the elution product by electrophoresis.
3. Ligate the DNA fragment with T-A cloning vector (e.g. pGEM-T easy)

DNA fragment	3 μ L
2X ligation buffer	5 μ L
pGEM-T easy vector	1 μ L
T ₄ DNA ligase	1 μ L

4. Incubate the mixture at 4°C overnight.
5. Transformation by heat shock method following below steps:

(1) Mix above mixture with 100 μ L *E.coli* (DH5 α) competence cell and keep on ice for 30 min.

(2) Heat the above mixture at 42°C for 90 sec.

(3) Keep on ice for 2 min.

(4) Add 100 μ L LB broth to above mixture and incubate at 37°C for 30 min.

(5) Spread the mixture with 40 μ L 10% X-gel and 7 μ L 20% IPTG for Blue White

screening on the 100ppm ampicillin LB medium plate.

- (6) Incubate the plate at 37°C overnight.
6. Subculture several single colony in a new plate and operate a colony-PCR to select the colonies transformed successfully.
7. Sequence the plasmid to confirm and analyze the interested gene by bioinformatics approach.
8. Generation of single colony from the accurate colony by streaking plate method.
9. Extraction the plasmids from the colony by following the below steps:
 - (1) Culture the single colony in 5mL LB broth with 100ppm ampicillin at 37°C overnight.
 - (2) Collect the bacteria by centrifugation with 3000 rpm at room temperature for 10 min.
 - (3) Discard the supernatant and resuspend the pellet with 100µL solution I.
 - (4) Incubate at room temperature for 5 min.
 - (5) Add the solution II and vortex gently until the mixture becomes clear.
 - (6) Keep on ice for 5 min.
 - (7) Add 150µL solution III and vortex gently until appearance of white slurry.

- (8) Delaminate the above mixture by centrifugating with 13000 rpm at 4°C for 15 min.
- (9) Transfer the 400 μL supernatant to a new 1.5 mL microcentrifuge tube and add 4 μL RNase (10mg mL^{-1}).
- (10) Incubate the mixture at 50 °C for 1 hr.
- (11) Add 400 μL PCI and vortex vigorously.
- (12) Delaminate the above mixture by centrifugating with 13000 rpm at 4 °C for 15 min.
- (13) Transfer 300 μL supernatant to a new microcentrifuge tube.
- (14) Add 300 μL CI and vortex vigorously.
- (15) Delaminate the above mixture by centrifugating with 13000 rpm at 4°C for 5 min.
- (16) Transfer 200 μL supernatant to a new centrifugating tube.
- (17) Add 50 μL 10M ammonium acetate (NH_4OAc ; pH 6.5) and 500 μL 100% ethanol.
- (18) Keep at -20 °C for 2 hr.
- (19) Collect the plasmid by centrifugating with 13000 rpm at 4°C for 20 min.

- (20) Remove the excess salt from the plasmid by washing with 70% ethanol twice.
- (21) Remove the ethanol from the plasmid by vacuuming.
- (22) Resuspend the pellet with ddH₂O.

10. Digestion of plasmid with optimal restriction enzymes following the below steps:

Plasmid (50µg)	85 µL
Restriction enzymes (less than 5% of total volume)	4 µL
10X Digestion buffer	10 µL
100X BSA	0-1 µL

11. Incubate the above mixture at 37 °C overnight.

12. Check the digestion product by electrophoresis.

13. Elute the DNA product from the electrophoresis by following the elution kit protocol.

14. Check and quantify the elution product by electrophoresis.

15. Ligate the DNA fragment with pCAPMBIA 2300 vector

DNA fragment	6 µL
2X ligation buffer	9 µL
Vector	1 µL

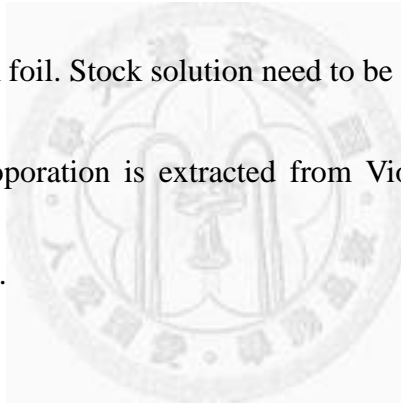
T₄ DNA ligase

1 μL

16. Incubate the mixture at 4°C overnight.
17. Transformation, colony PCR and sequencing to confirm the accuracy of the functional plasmid.
18. Transformation of *Agrobacterium tumefaciens* by electroporation method.
 - (1) Keep the electroporation cuvette in the oven (80°C) for 15 min to remove the excess ethanol.
 - (2) Capping and keep on ice for 5 min.
 - (3) Keep the competence cell on ice for 5 min.
 - (4) Add the 2 μL pure plasmid to the competent cell and incubate on ice for 5 min.
 - (5) Transfer the above mixture to the electroporation cuvette.
 - (6) Charge and trigger the pulse.
 - (7) Add 900 μL LB broth and incubate at 28 °C for 1 hr.
 - (8) Spread 200 μL mixture on the 100 ppm kanamycin plate and incubate at 28°C for two day.
19. Subculture several signal colony in a new plate and operate a colony-PCR to select the colonies transformed successfully.

Notes:

- a. The pH of the phenol as shipped is 6.6 ± 0.2 . After addition of the Tris alkaline buffer, the pH is confirmed to be 7.9 ± 0.2 , and it is suitable for deproteinization of nucleic acids.
- b. The rotational speed when collection of the bacteria by centrifuging should not higher than 5000 rpm to prevent the damage of bacteria.
- c. X-gal is light sensitive and hence store in a glass or polypropylene containers wrapped with aluminum foil. Stock solution need to be store in $-20\text{ }^{\circ}\text{C}$.
- d. The plasmid for electroporation is extracted from Viogene Mini Plus TM Plasmid DNA Extraction System.



5.11 *Agrobacterium* Infiltration (Host: *Arabidopsis thaliana* Col.)

Preparation:

Equipment: Oven (28°C), centrifuge.

Materials: *Arabidopsis* with inflorescence, 50/250 mL centrifuge tubes, triangle flask,

Reagents:

1. Infiltration broth (1L; pH5.7): 2.2g MS with vitamin, 50g sucrose, 0.5g MES, 0.1mL

Silweet L-77.

2. 100 ppm kanamycin

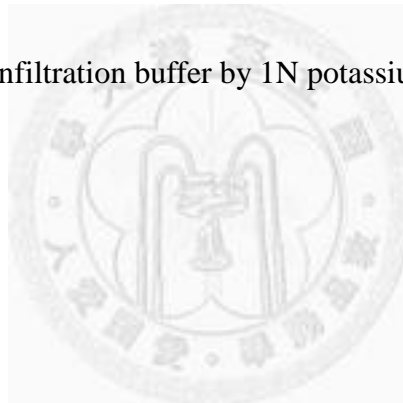
Procedure:

1. Subculture the colony containing the plasmid in the kanamycin-selected plate and incubate it at 28°C for 2 days.
2. Select a single colony from the plate and culture it with 40 mL LB broth in 50 mL centrifuge tube (Agro in anaerobic) overnight.
3. Transfer the bacteria solution to 500 mL LB and culture it at 28 °C overnight.
4. While the absorbance at 600 nm is higher than 0.8, collect the bacteria by centrifugating with 5000 rpm at 4°C for 10 min.
5. Resuspend the pellet with 250 mL infiltration broth.
6. Dip the optimal plants in the 250 mL infiltration broth for 45 sec.
7. Repeat step 6.
8. Seal the plant with the plastic wrap at the dark overnight.
9. Remove the plastic wrap.
10. Until the whole plant product the fully mature siliques, collect and sieve the seed in the 1.5 mL microcentrifuge tubes.

11. Remove the water on the surface of the seeds by keep in the humidity-controlled oven.

Notes:

- a. Remove the growing siliques from the Arabidopsis inflorescence before the dipping could decrease the population of wild-type seeds in the later collection of seeds.
- b. 250 mL infiltration broth is enough for dipping 30 plants.
- c. Infiltration broth is not necessary to sterilize.
- d. Adjust the pH value of infiltration buffer by 1N potassium hydroxide.



References

- Agius, F., Gonzalez-Lamothe, R., Caballero, J.L., Munoz-Blanco, J., Botella, M.A., and Valpuesta, V.** (2003). Engineering increased vitamin C levels in plants by overexpression of a D-galacturonic acid reductase. *Nat Biotechnol* **21**: 177-181.
- Ainsworth, E.A., and Gillespie, K.M.** (2007). Measurement of reduced, oxidized and total ascorbate content in plants. *Nature Protocols* **2**: 871-874.
- Attolico, A.D., and De Tullio, M.C.** (2006). Increased ascorbate content delays flowering in long-day grown *Arabidopsis thaliana* (L.) Heynh. *Plant Physiol Biochem* **44**: 462-466.
- Ausin, I., Alonso-Blanco, C., Jarillo, J.A., Ruiz-Garcia, L., and Martinez-Zapater, J.M.** (2004). Regulation of flowering time by *FVE*, a retinoblastoma-associated protein. *Nat Genet* **36**: 162-166.
- Badiani, M., Paolacci, A.R., Miglietta, F., Kimball, B.A., Pinter, P.J., Garcia, R.L., Hunsaker, D.J., LaMorte, R.L., and Wall, G.W.** (1996). Seasonal variations of antioxidants in wheat (*Triticum aestivum*) leaves grown under field conditions. *Aust J Plant Physiol* **23**: 687-698.
- Balasubramanian, S., Sureshkumar, S., Lempe, J., and Weigel, D.** (2006). Potent induction of *Arabidopsis thaliana* flowering by elevated growth temperature. *PLoS Genet* **2**: e106.
- Barth, C., Moeder, W., Klessig, D.F., and Conklin, P.L.** (2004). The timing of senescence and response to pathogens is altered in the ascorbate-deficient *Arabidopsis* mutant *vitamin c-1*. *Plant Physiol* **134**: 1784-1792.
- Blanchard, M.G., and Runkle, E.S.** (2006). Temperature during the day, but not during the night, controls flowering of *Phalaenopsis* orchids. *J Exp Bot* **57**: 4043-4049.
- Barth, C., De Tullio, M., and Conklin, P.L.** (2006). The role of ascorbic acid in the control of flowering time and the onset of senescence. *J Exp Bot* **57**: 1657-1665.
- Blazquez, M.A., Green, R., Nilsson, O., Sussman, M.R., and Weigel, D.** (1998). Gibberellins promote flowering of *Arabidopsis* by activating the *LEAFY* promoter. *Plant Cell* **10**: 791-800.
- Bond, D.M., Dennis, E.S., Pogson, B.J., and Finnegan, E.J.** (2009). Histone acetylation, *VERNALIZATION INSENSITIVE 3*, *FLOWERING LOCUS C*, and

- the vernalization response. *Mol Plant* **2**: 724-737.
- Cheong, J.J., Jung, C., Seo, J.S., Han, S.W., Koo, Y.J., Kim, C.H., Song, S.I., Nahm, B.H., and Do Choi, Y.** (2008). Overexpression of *AtMYB44* enhances stomatal closure to confer abiotic stress tolerance in transgenic *Arabidopsis*. *Plant Physiology* **146**: 623-635.
- Chen, Z., and Gallie, D.R.** (2004). The ascorbic acid redox state controls guard cell signaling and stomatal movement. *Plant Cell* **16**: 1143-1162.
- Clough, S.J., and Bent, A.F.** (1998). Floral dip: a simplified method for *Agrobacterium*-mediated transformation of *Arabidopsis thaliana*. *Plant J* **16**: 735-743.
- Conklin, P.L., and Barth, C.** (2004). Ascorbic acid, a familiar small molecule intertwined in the response of plants to ozone, pathogens, and the onset of senescence. *Plant Cell and Environment* **27**: 959-970.
- Conklin, P.L., Pallanca, J.E., Last, R.L., and Smirnoff, N.** (1997). L-ascorbic acid metabolism in the ascorbate-deficient *arabidopsis* mutant *vtc1*. *Plant Physiol* **115**: 1277-1285.
- Conklin, P.L., Norris, S.R., Wheeler, G.L., Williams, E.H., Smirnoff, N., and Last, R.L.** (1999). Genetic evidence for the role of GDP-mannose in plant ascorbic acid (vitamin C) biosynthesis. *P Natl Acad Sci USA* **96**: 4198-4203.
- Dat, J., Vandenabeele, S., Vranova, E., Van Montagu, M., Inze, D., and Van Breusegem, F.** (2000). Dual action of the active oxygen species during plant stress responses. *Cell Mol Life Sci* **57**: 779-795.
- Davletova, S., Rizhsky, L., Liang, H.J., Zhong, S.Q., Oliver, D.J., Coutu, J., Shulaev, V., Schlauch, K., and Mittler, R.** (2005). Cytosolic *ascorbate peroxidase 1* is a central component of the reactive oxygen gene network of *Arabidopsis*. *Plant Cell* **17**: 268-281.
- de Pinto, M.C., Paradiso, A., Leonetti, P., and De Gara, L.** (2006). Hydrogen peroxide, nitric oxide and cytosolic ascorbate peroxidase at the crossroad between defence and cell death. *Plant J* **48**: 784-795.
- De Tullio, M.C., and Arrigoni, O.** (2004). Hopes, disillusion and more hopes from vitamin C. *Cell Mol Life Sci* **61**: 209-219.
- Dubos, C., Stracke, R., Grotewold, E., Weisshaar, B., Martin, C., and Lepiniec, L.** (2010). *MYB* transcription factors in *Arabidopsis*. *Trends in Plant Science* **15**: 573-581.
- Gao, Q., and Zhang, L.** (2008). Ultraviolet-B-induced oxidative stress and antioxidant

- defense system responses in ascorbate-deficient *vtc1* mutants of *Arabidopsis thaliana*. *J Plant Physiol* **165**: 138-148.
- Gocal, G.F.W., Sheldon, C.C., Gubler, F., Moritz, T., Bagnall, D.J., MacMillan, C.P., Li, S.F., Parish, R.W., Dennis, E.S., Weigel, D., and King, R.W.** (2001). *GAMYB-like* genes, flowering, and gibberellin signaling in *Arabidopsis*. *Plant Physiology* **127**: 1682-1693.
- Hartmann, U., Hohmann, S., Nettesheim, K., Wisman, E., Saedler, H., and Huijser, P.** (2000). Molecular cloning of *SVP*: a negative regulator of the floral transition in *Arabidopsis*. *Plant J* **21**: 351-360.
- Hirai, N., Kojima, Y., Shinozaki, M., Koshimizu, K., Murofushi, N., and Takimoto, A.** (1995). Accumulation of ascorbic-acid in the cotyledons of morning glory (*pharbitis-nil*) seedlings during the induction of flowering by low-temperature treatment and the effect of prior exposure to high-intensity light. *Plant and Cell Physiology* **36**: 1265-1271.
- Jana, S., and Choudhuri, M.A.** (1982). Glycolate metabolism of 3 submersed aquatic angiosperms during aging. *Aquat Bot* **12**: 345-354.
- Johanson, U., West, J., Lister, C., Michaels, S., Amasino, R., and Dean, C.** (2000). Molecular analysis of *FRIGIDA*, a major determinant of natural variation in *Arabidopsis* flowering time. *Science* **290**: 344-347.
- Kardailsky, I., Shukla, V.K., Ahn, J.H., Dagenais, N., Christensen, S.K., Nguyen, J.T., Chory, J., Harrison, M.J., and Weigel, D.** (1999). Activation tagging of the floral inducer *FT*. *Science* **286**: 1962-1965.
- Kobayashi, Y., Kaya, H., Goto, K., Iwabuchi, M., and Araki, T.** (1999). A pair of related genes with antagonistic roles in mediating flowering signals. *Science* **286**: 1960-1962.
- Koornneef, M., Alonso-Blanco, C., Blankestijn-de Vries, H., Hanhart, C.J., and Peeters, A.J.M.** (1998). Genetic interactions among late-flowering mutants of *Arabidopsis*. *Genetics* **148**: 885-892.
- Kotchoni, S.O., Larrimore, K.E., Mukherjee, M., Kempinski, C.F., and Barth, C.** (2009). Alterations in the endogenous ascorbic acid content affect flowering time in *Arabidopsis*. *Plant Physiol* **149**: 803-815.
- Koussevitzky, S., Suzuki, N., Huntington, S., Armijo, L., Sha, W., Cortes, D., Shulaev, V., and Mittler, R.** (2008). Ascorbate peroxidase 1 plays a key role in the response of *Arabidopsis thaliana* to stress combination. *J Biol Chem* **283**: 34197-34203.

- Kroj, T., Journot-Catalino, N., Somssich, I.E., and Roby, D.** (2006). The transcription factors *WRKY11* and *WRKY17* act as negative regulators of basal resistance in *Arabidopsis thaliana*. *Plant Cell* **18**: 3289-3302.
- Larkindale, J., Hall, J.D., Knight, M.R., and Vierling, E.** (2005). Heat stress phenotypes of *Arabidopsis* mutants implicate multiple signaling pathways in the acquisition of thermotolerance. *Plant Physiol* **138**: 882-897.
- Lee, J.H., Yoo, S.J., Park, S.H., Hwang, I., Lee, J.S., and Ahn, J.H.** (2007). Role of *SVP* in the control of flowering time by ambient temperature in *Arabidopsis*. *Genes Dev* **21**: 397-402.
- Lee, J.H., Lee, J.S., and Ahn, J.H.** (2008). Ambient temperature signaling in plants: an emerging field in the regulation of flowering time. *J Plant Biol* **51**: 321-326.
- Leferink, N.G., van Duijn, E., Barendregt, A., Heck, A.J., and van Berkel, W.J.** (2009). Galactonolactone dehydrogenase requires a redox-sensitive thiol for optimal production of vitamin C. *Plant Physiol* **150**: 596-605.
- Lepiniec, L., Dubos, C., Le Gourrierc, J., Baudry, A., Huel, G., Lanet, E., Debeaujon, I., Routaboul, J.M., Alboresi, A., and Weisshaar, B.** (2008). *MYBL2* is a new regulator of flavonoid biosynthesis in *Arabidopsis thaliana*. *Plant Journal* **55**: 940-953.
- Long, S.P., and Ort, D.R.** (2010). More than taking the heat: crops and global change. *Current Opinion in Plant Biology* **13**: 241-248.
- Lorence, A., Chevone, B.I., Mendes, P., and Nessler, C.L.** (2004). *myo*-inositol oxygenase offers a possible entry point into plant ascorbate biosynthesis. *Plant Physiol* **134**: 1200-1205.
- Millar, A.A., and Gubler, F.** (2005). The *Arabidopsis* *GAMYB-like* genes, *MYB33* and *MYB65*, are MicroRNA-regulated genes that redundantly facilitate anther development. *Plant Cell* **17**: 705-721.
- Millar, A.A., Alonso-Peral, M.M., Li, J.Y., Li, Y.J., Allen, R.S., Schnippenkoetter, W., Ohms, S., and White, R.G.** (2010). The *MicroRNA159*-regulated *GAMYB-like* genes inhibit growth and promote programmed cell death in *Arabidopsis*. *Plant Physiology* **154**: 757-771.
- Miller, G., Suzuki, N., Ciftci-Yilmaz, S., and Mittler, R.** (2010). Reactive oxygen species homeostasis and signalling during drought and salinity stresses. *Plant Cell and Environment* **33**: 453-467.
- Miller, G., Suzuki, N., Rizhsky, L., Hegie, A., Koussevitzky, S., and Mittler, R.** (2007). Double mutants deficient in cytosolic and thylakoid ascorbate

- peroxidase reveal a complex mode of interaction between reactive oxygen species, plant development, and response to abiotic stresses. *Plant Physiol* **144**: 1777-1785.
- Mouradov, A., Cremer, F., and Coupland, G.** (2002). Control of flowering time: interacting pathways as a basis for diversity. *Plant Cell* **14 Suppl**: S111-130.
- Mukherjee, S.P., and Choudhuri, M.A.** (1981). Effect of water-stress on some oxidative-enzymes and senescence in vigna seedlings. *Physiol Plantarum* **52**: 37-42.
- Muller-Moule, P., Golan, T., and Niyogi, K.K.** (2004). Ascorbate-deficient mutants of *Arabidopsis* grow in high light despite chronic photooxidative stress. *Plant Physiol* **134**: 1163-1172.
- Nakamichi, N., Kita, M., Niinuma, K., Ito, S., Yamashino, T., Mizoguchi, T., and Mizuno, T.** (2007). *Arabidopsis* clock-associated pseudo-response regulators *PRR9*, *PRR7* and *PRR5* coordinately and positively regulate flowering time through the canonical *CONSTANS*-dependent photoperiodic pathway. *Plant Cell Physiol* **48**: 822-832.
- Noctor, G., and Foyer, C.H.** (1998). Ascorbate and glutathione: keeping active oxygen under control. *Annu Rev Plant Physiol Plant Mol Biol* **49**: 249-279.
- Ohme-Takagi, M., Matsui, K., and Umemura, Y.** (2008). *AtMYBL2*, a protein with a single *MYB* domain, acts as a negative regulator of anthocyanin biosynthesis in *Arabidopsis*. *Plant Journal* **55**: 954-967.
- Park, J.S., Kim, J.B., Cho, K.J., Cheon, C.I., Sung, M.K., Choung, M.G., and Roh, K.H.** (2008). *Arabidopsis* R2R3-MYB transcription factor *AtMYB60* functions as a transcriptional repressor of anthocyanin biosynthesis in lettuce (*Lactuca sativa*). *Plant Cell Rep* **27**: 985-994.
- Pignocchi, C., and Foyer, C.H.** (2003). Apoplastic ascorbate metabolism and its role in the regulation of cell signalling. *Curr Opin Plant Biol* **6**: 379-389.
- Pnueli, L., Liang, H., Rozenberg, M., and Mittler, R.** (2003). Growth suppression, altered stomatal responses, and augmented induction of heat shock proteins in cytosolic ascorbate peroxidase (*Apx1*)-deficient *Arabidopsis* plants. *Plant J* **34**: 187-203.
- Schomburg, F.M., Patton, D.A., Meinke, D.W., and Amasino, R.M.** (2001). *FPA*, a gene involved in floral induction in *Arabidopsis*, encodes a protein containing RNA-recognition motifs. *Plant Cell* **13**: 1427-1436.
- Shaikhali, J., Heiber, I., Seidel, T., Stroher, E., Hiltcher, H., Birkmann, S., Dietz,**

- K.J., and Baier, M.** (2008). The redox-sensitive transcription factor Rap2.4a controls nuclear expression of 2-Cys peroxiredoxin A and other chloroplast antioxidant enzymes. *Bmc Plant Biol* **8**: 48.
- Shen, C.H., and Yeh, K.W.** (2010a). Hydrogen peroxide mediates the expression of ascorbate-related genes in response to methanol stimulation in *Oncidium*. *J Plant Physiol* **167**: 400-407.
- Shen, C.H., and Yeh, K.W.** (2010b). The signal network of ascorbate homeostasis. *Plant Signal Behav* **5**.
- Shen, C.H., Krishnamurthy, R., and Yeh, K.W.** (2009). Decreased L-ascorbate content mediating bolting is mainly regulated by the galacturonate pathway in *Oncidium*. *Plant Cell Physiol* **50**: 935-946.
- Shin, R., Burch, A.Y., Huppert, K.A., Tiwari, S.B., Murphy, A.S., Guilfoyle, T.J., and Schachtman, D.P.** (2007). The *Arabidopsis* transcription factor *MYB77* modulates auxin signal transduction. *Plant Cell* **19**: 2440-2453.
- Smirnoff, N.** (2000). Ascorbate biosynthesis and function in photoprotection. *Philos Trans R Soc Lond B Biol Sci* **355**: 1455-1464.
- Srikanth, A., and Schmid, M.** (2011). Regulation of flowering time: all roads lead to Rome. *Cellular and Molecular Life Sciences* **68**: 2013-2037.
- Stracke, R., Jahns, O., Keck, M., Tohge, T., Niehaus, K., Fernie, A.R., and Weisshaar, B.** (2010). Analysis of *PRODUCTION OF FLAVONOL GLYCOSIDES*-dependent flavonol glycoside accumulation in *Arabidopsis thaliana* plants reveals *MYB11*-, *MYB12*- and *MYB111*-independent flavonol glycoside accumulation. *New Phytol* **188**: 985-1000.
- Tan, J., Wang, H.L., and Yeh, K.W.** (2005). Analysis of organ-specific, expressed genes in *Oncidium* orchid by subtractive expressed sequence tags library. *Biotechnol Lett* **27**: 1517-1528.
- ThordalChristensen, H., Zhang, Z.G., Wei, Y.D., and Collinge, D.B.** (1997). Subcellular localization of H₂O₂ in plants. H₂O₂ accumulation in papillae and hypersensitive response during the barley-powdery mildew interaction. *Plant Journal* **11**: 1187-1194.
- Wang, C.Y., Chiou, C.Y., Wang, H.L., Krishnamurthy, R., Venkatagiri, S., Tan, J., and Yeh, K.W.** (2008). Carbohydrate mobilization and gene regulatory profile in the pseudobulb of *Oncidium* orchid during the flowering process. *Planta* **227**: 1063-1077.
- Wang, H.Y., Lin, R.C., and Park, H.J.** (2008). Role of *Arabidopsis* RAP2.4 in

regulating light- and ethylene-mediated developmental processes and drought stress tolerance. *Mol Plant* **1**: 42-57.

Wolucka, B.A., and Van Montagu, M. (2003). GDP-mannose 3',5'-epimerase forms GDP-L-gulose, a putative intermediate for the de novo biosynthesis of vitamin C in plants. *Journal of Biological Chemistry* **278**: 47483-47490.

Wu, Y.J., Cai, X.N., Ballif, J., Endo, S., Davis, E., Liang, M.X., Chen, D., DeWald, D., Kreps, J., and Zhu, T. (2007). A putative CCAAT-binding transcription factor is a regulator of flowering timing in *Arabidopsis*. *Plant Physiology* **145**: 98-105.

Yamaguchi, A., Wu, M.F., Yang, L., Wu, G., Poethig, R.S., and Wagner, D. (2009). The microRNA-regulated SBP-Box transcription factor *SPL3* is a direct upstream activator of *LEAFY*, *FRUITFULL*, and *APETALA1*. *Dev Cell* **17**: 268-278.

Yamamoto, A., Bhuiyan, M.N., Waditee, R., Tanaka, Y., Esaka, M., Oba, K., Jagendorf, A.T., and Takabe, T. (2005). Suppressed expression of the apoplastic ascorbate oxidase gene increases salt tolerance in tobacco and *Arabidopsis* plants. *J Exp Bot* **56**: 1785-1796.

Yong, J.W.H., and Hew, C.S. (1995). The importance of photoassimilate contribution from the current shoot and connected back shoots to inflorescence size in the thin-leaved sympodial orchid *Oncidium-Goldiana*. *Int J Plant Sci* **156**: 450-459.

Table 1. GO analysis of cluster 1

Biological Process	Count	%
regulation of transcription	34	14.8
response to organic substance	31	13.5
response to hormone stimulus	29	12.6
response to endogenous stimulus	29	12.6
response to abiotic stimulus	24	10.4
transcription	22	9.6
regulation of transcription, DNA-dependent	19	8.3
regulation of RNA metabolic process	19	8.3
response to ethylene stimulus	13	5.7
response to salicylic acid stimulus	12	5.2
response to salt stress	12	5.2
response to osmotic stress	12	5.2
hormone-mediated signaling	12	5.2
cellular response to hormone stimulus	12	5.2
response to inorganic substance	12	5.2
two-component signal transduction system	11	4.8
response to abscisic acid stimulus	11	4.8
response to metal ion	10	4.3
lipid catabolic process	9	3.9
cell wall organization	9	3.9
external encapsulating structure organization	9	3.9
carboxylic acid biosynthetic process	9	3.9
organic acid biosynthetic process	9	3.9
response to gibberellin stimulus	8	3.5
response to jasmonic acid stimulus	8	3.5
chromatin organization	8	3.5
chromosome organization	8	3.5
response to cadmium ion	8	3.5
response to auxin stimulus	8	3.5
nucleosome organization	7	3
nucleosome assembly	7	3
chromatin assembly	7	3
protein-DNA complex assembly	7	3

Table 1. continued

chromatin assembly or disassembly	7	3
cellular macromolecular complex assembly	7	3
cellular macromolecular complex subunit organization	7	3
macromolecular complex assembly	7	3
response to oxidative stress	7	3
macromolecular complex subunit organization	7	3
response to cytokinin stimulus	6	2.6
lipid transport	6	2.6
lipid localization	6	2.6
ethylene mediated signaling pathway	6	2.6
cell division	6	2.6
amine biosynthetic process	6	2.6
cytokinin mediated signaling	5	2.2
plant-type cell wall organization	5	2.2
cell wall modification	5	2.2
stomatal complex development	4	1.7
plant-type cell wall loosening	4	1.7
plant-type cell wall modification	4	1.7
biogenic amine biosynthetic process	3	1.3
nicotianamine biosynthetic process	2	0.9
nicotianamine metabolic process	2	0.9

Cellular Component	Count	%
endomembrane system	46	20
extracellular region	23	10
cell wall	13	5.7
external encapsulating structure	13	5.7
chromosome	8	3.5
nucleosome	7	3
protein-DNA complex	7	3
chromatin	7	3
chromosomal part	7	3
extracellular region part	3	1.3

Table 1. continued

Molecular Function	Count	%
DNA binding	38	16.5
transcription regulator activity	30	13
transcription factor activity	25	10.9
carboxylesterase activity	9	3.9
lipid binding	6	2.6
two-component response regulator activity	5	2.2
nicotianamine synthase activity	2	0.9
growth factor activity	2	0.9

*Count: The number of gene counted in the population.



Table 2. GO analysis of cluster 2

Biological Process	Count	%
defense response	15	11.9
phosphate metabolic process	15	11.9
phosphorus metabolic process	15	11.9
protein amino acid phosphorylation	14	11.1
response to organic substance	14	11.1
phosphorylation	14	11.1
nitrogen compound biosynthetic process	10	7.9
carboxylic acid biosynthetic process	9	7.1
organic acid biosynthetic process	9	7.1
secondary metabolic process	9	7.1
response to wounding	8	6.3
aromatic compound biosynthetic process	7	5.6
response to bacterium	7	5.6
response to chitin	6	4.8
cellular amino acid biosynthetic process	6	4.8
response to carbohydrate stimulus	6	4.8
amine biosynthetic process	6	4.8
aromatic amino acid family metabolic process	5	4
dicarboxylic acid metabolic process	5	4
programmed cell death	5	4
death	5	4
cell death	5	4
cellular amino acid derivative metabolic process	5	4
immune response	5	4
aromatic amino acid family biosynthetic process	4	3.2
chorismate metabolic process	4	3.2
cellular amino acid derivative biosynthetic process	4	3.2
indole derivative biosynthetic process	3	2.4
auxin metabolic process	3	2.4
indole and derivative metabolic process	3	2.4
indole derivative metabolic process	3	2.4
plant-type hypersensitive response	3	2.4

Table 2. continued

host programmed cell death induced by symbiont	3	2.4
abscisic acid mediated signaling	3	2.4
L-phenylalanine biosynthetic process	2	1.6
aromatic amino acid family biosynthetic process, prephenate pathway	2	1.6
L-phenylalanine metabolic process	2	1.6

Cellular Component	Count	%
plasma membrane	26	20.6
extracellular region	12	9.5
apoplast	6	4.8

Molecular Function	Count	%
nucleotide binding	29	23
adenyl nucleotide binding	26	20.6
purine nucleoside binding	26	20.6
nucleoside binding	26	20.6
purine nucleotide binding	26	20.6
ATP binding	22	17.5
adenyl ribonucleotide binding	22	17.5
purine ribonucleotide binding	22	17.5
ribonucleotide binding	22	17.5
protein kinase activity	14	11.1
protein serine/threonine kinase activity	10	7.9
coenzyme binding	7	5.6
cofactor binding	7	5.6
carboxylesterase activity	6	4.8
FAD binding	4	3.2
NAD or NADH binding	3	2.4
hydro-lyase activity	3	2.4

*Count: The number of gene counted in the population.

Table 3. GO analysis of cluster 3

Biological Process	Count	%
response to organic substance	6	20.7
response to salicylic acid stimulus	5	17.2
defense response	5	17.2
innate immune response	4	13.8
immune response	4	13.8
defense response, incompatible interaction	3	10.3
response to bacterium	3	10.3
systemic acquired resistance	2	6.9

Cellular Component	Count	%
plasma membrane	10	34.5
cell wall	5	17.2
external encapsulating structure	5	17.2
vacuole	5	17.2
extracellular region	5	17.2
apoplast	4	13.8
plant-type cell wall	3	10.3

Molecular Function	Count	%
sugar binding	3	10.3
carbohydrate binding	3	10.3

*Count: The number of gene counted in the population.

Table 4. GO analysis of cluster 4

Biological Process	Count	%
response to abiotic stimulus	11	16.9
response to heat	8	12.3
response to temperature stimulus	8	12.3
response to inorganic substance	8	12.3
response to oxidative stress	7	10.8
response to reactive oxygen species	6	9.2
response to high light intensity	5	7.7
response to light intensity	5	7.7
response to hydrogen peroxide	5	7.7
protein folding	5	7.7
generation of precursor metabolites and energy	5	7.7
response to light stimulus	5	7.7
response to radiation	5	7.7
oxidative phosphorylation	4	6.2
nucleotide biosynthetic process	4	6.2
response to water deprivation	4	6.2
nucleobase, nucleoside and nucleotide biosynthetic process	4	6.2
nucleobase, nucleoside, nucleotide and nucleic acid biosynthetic process	4	6.2
response to water	4	6.2
carbohydrate biosynthetic process	4	6.2
ATP synthesis coupled proton transport	3	4.6
energy coupled proton transport, down electrochemical gradient	3	4.6
ion transmembrane transport	3	4.6
proton transport	3	4.6
hydrogen transport	3	4.6
ATP metabolic process	3	4.6
ATP biosynthetic process	3	4.6
ribonucleoside triphosphate biosynthetic process	3	4.6
ribonucleoside triphosphate metabolic process	3	4.6
purine ribonucleoside triphosphate metabolic process	3	4.6
purine nucleoside triphosphate metabolic process	3	4.6

Table 4. continued

purine nucleoside triphosphate biosynthetic process	3	4.6
purine ribonucleoside triphosphate biosynthetic process	3	4.6
nucleoside triphosphate biosynthetic process	3	4.6
nucleoside triphosphate metabolic process	3	4.6
purine ribonucleotide metabolic process	3	4.6
purine ribonucleotide biosynthetic process	3	4.6
purine nucleotide biosynthetic process	3	4.6
purine nucleotide metabolic process	3	4.6
ribonucleotide biosynthetic process	3	4.6

Cellular Component	Count	%
integral to membrane	11	16.9
mitochondrion	8	12.3
cytosol	6	9.2
mitochondrial inner membrane	4	6.2
mitochondrial membrane	4	6.2
organelle inner membrane	4	6.2
mitochondrial envelope	4	6.2
mitochondrial part	4	6.2
proton-transporting ATP synthase complex	3	4.6
proton-transporting two-sector ATPase complex	3	4.6
proton-transporting ATP synthase complex, coupling factor F(o)	2	3.1
proton-transporting two-sector ATPase complex, proton-transporting domain	2	3.1

Molecular Function	Count	%
inorganic cation transmembrane transporter activity	5	7.7
hydrogen ion transmembrane transporter activity	4	6.2
inorganic cation transmembrane transporter activity	4	6.2

*Count: The number of gene counted in the population.

Table 5. GO analysis of cluster 5

Biological Process	Count	%
response to organic substance	17	17.9
oxidation reduction	15	15.8
transcription	13	13.7
response to abiotic stimulus	12	12.6
response to endogenous stimulus	11	11.6
response to oxidative stress	9	9.5
response to carbohydrate stimulus	8	8.4
response to chitin	7	7.4
response to wounding	7	7.4
response to jasmonic acid stimulus	6	6.3
cellular amino acid derivative metabolic process	6	6.3
response to temperature stimulus	6	6.3
cellular response to stress	6	6.3
aging	4	4.2
cell wall modification	4	4.2
response to reactive oxygen species	4	4.2
defense response to bacterium	4	4.2
cellular amino acid derivative biosynthetic process	4	4.2
cell wall thickening	3	3.2
biogenic amine metabolic process	3	3.2
cellular response to oxidative stress	3	3.2
response to iron ion	2	2.1
indoleacetic acid biosynthetic process	2	2.1
indoleacetic acid metabolic process	2	2.1
removal of superoxide radicals	2	2.1
response to oxygen radical	2	2.1
response to superoxide	2	2.1
superoxide metabolic process	2	2.1
callose deposition in cell wall during defense response	2	2.1
cell wall thickening during defense response	2	2.1
callose deposition in cell wall	2	2.1
response to copper ion	2	2.1
callose deposition during defense response	2	2.1

Table 5. continued

Cellular Component	Count	%
cell wall	7	7.4
external encapsulating structure	7	7.4
plant-type cell wall	6	6.3

Molecular Function	Count	%
metal ion binding	23	24.2
cation binding	23	24.2
ion binding	23	24.2
transition metal ion binding	19	20
transcription factor activity	14	14.7
iron ion binding	9	9.5
electron carrier activity	8	8.4
heme binding	7	7.4
tetrapyrrole binding	7	7.4
oxygen binding	6	6.3
antiporter activity	4	4.2
superoxide dismutase activity	2	2.1
oxidoreductase activity, acting on superoxide radicals as acceptor	2	2.1
glycerol-3-phosphate O-acyltransferase activity	2	2.1

*Count: The number of gene counted in the population.

Table 6. GO analysis of cluster 6

Biological Process	Count	%
oxidation reduction	18	25
response to organic substance	13	18.1
response to endogenous stimulus	10	13.9
defense response	9	12.5
response to wounding	6	8.3
aromatic compound biosynthetic process	6	8.3
response to bacterium	6	8.3
response to oxidative stress	6	8.3
response to fungus	6	8.3
secondary metabolic process	5	6.9
response to chitin	4	5.6
response to heat	4	5.6
response to jasmonic acid stimulus	4	5.6
electron transport chain	4	5.6
cellular amino acid derivative biosynthetic process	4	5.6
response to carbohydrate stimulus	4	5.6
cellular amino acid derivative metabolic process	4	5.6
jasmonic acid metabolic process	3	4.2
oxylipin metabolic process	3	4.2
response to light intensity	3	4.2
phenylpropanoid biosynthetic process	3	4.2
jasmonic acid biosynthetic process	2	2.8
salicylic acid mediated signaling pathway	2	2.8

Cellular Component	Count	%
external encapsulating structure	6	8.3
cell wall	5	6.9
anchored to membrane	4	5.6

Molecular Function	Count	%
metal ion binding	20	27.8

Table 6. continued

ion binding	20	27.8
transition metal ion binding	18	25
iron ion binding	12	16.7
electron carrier activity	7	9.7
oxidoreductase activity, acting on single donors with incorporation of molecular oxygen, incorporation of two atoms of oxygen	5	6.9
oxidoreductase activity, acting on single donors with incorporation of molecular oxygen	5	6.9
oxidoreductase activity, acting on sulfur group of donors	4	5.6
oxidoreductase activity, acting on paired donors, with incorporation or reduction of molecular oxygen, 2-oxoglutarate as one donor, and incorporation of one atom each of oxygen into both donors	3	4.2
sugar binding	3	4.2
lipoxygenase activity	2	2.8
oxidoreductase activity, acting on sulfur group of donors, disulfide as acceptor	2	2.8

*Count: The number of gene counted in the population.

Table 7. GO analysis of cluster 7

Biological Process	Count	%
response to organic substance	19	38.8
response to endogenous stimulus	14	28.6
defense response	14	28.6
response to hormone stimulus	11	22.4
response to carbohydrate stimulus	9	18.4
response to chitin	8	16.3
regulation of transcription, DNA-dependent	8	16.3
regulation of RNA metabolic process	8	16.3
response to abiotic stimulus	8	16.3
transcription	8	16.3
response to jasmonic acid stimulus	7	14.3
response to ethylene stimulus	7	14.3
response to wounding	6	12.2
response to bacterium	6	12.2
immune response	6	12.2
intracellular signaling cascade	6	12.2
innate immune response	5	10.2
defense response to fungus	5	10.2
secondary metabolic process	5	10.2
hormone-mediated signaling	5	10.2
cellular response to hormone stimulus	5	10.2
response to fungus	5	10.2
ethylene mediated signaling pathway	4	8.2
sulfur metabolic process	4	8.2
defense response to bacterium	4	8.2
two-component signal transduction system (phosphorelay)	4	8.2
response to cold	4	8.2
response to oxidative stress	4	8.2
response to auxin stimulus	4	8.2
response to temperature stimulus	4	8.2
response to salicylic acid stimulus	3	6.1
response to water deprivation	3	6.1
response to water	3	6.1

Table 7. continued

camalexin biosynthetic process	2	4.1
response to singlet oxygen	2	4.1
positive regulation of programmed cell death	2	4.1
positive regulation of cell death	2	4.1
camalexin metabolic process	2	4.1
indole phytoalexin metabolic process	2	4.1
phytoalexin biosynthetic process	2	4.1
indole metabolic process	2	4.1
phytoalexin metabolic process	2	4.1
indole phytoalexin biosynthetic process	2	4.1
ripening	2	4.1
response to mechanical stimulus	2	4.1
ethylene metabolic process	2	4.1
ethylene biosynthetic process	2	4.1
cellular alkene metabolic process	2	4.1
alkene biosynthetic process	2	4.1
regulation of programmed cell death	2	4.1
positive regulation of innate immune response	2	4.1
positive regulation of immune response	2	4.1
activation of innate immune response	2	4.1
activation of immune response	2	4.1
positive regulation of immune system process	2	4.1
regulation of cell death	2	4.1
senescence	2	4.1
positive regulation of defense response	2	4.1
systemic acquired resistance	2	4.1
regulation of innate immune response	2	4.1
indole derivative biosynthetic process	2	4.1
indole and derivative metabolic process	2	4.1
indole derivative metabolic process	2	4.1

Cellular Component	Count	%
intrinsic to membrane	11	22.4

Table 7. continued		
cell wall	7	14.3
external encapsulating structure	7	14.3
extracellular region	6	12.2

Molecular Function	Count	%
transcription factor activity	10	20.4
transcription regulator activity	10	20.4
1-aminocyclopropane-1-carboxylate synthase activity	3	6.1
carbon-sulfur lyase activity	3	6.1
transferase activity, transferring nitrogenous groups	3	6.1
vitamin B6 binding	3	6.1
pyridoxal phosphate binding	3	6.1
transcription activator activity	3	6.1
vitamin binding	3	6.1

*Count: The number of gene counted in the population.

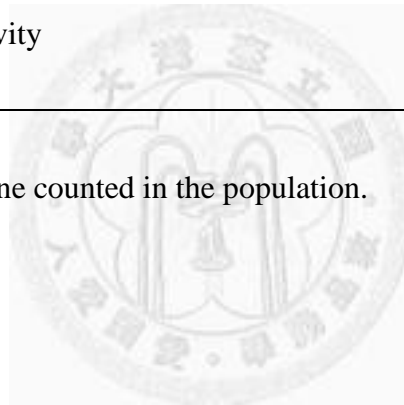


Table 8. GO analysis of cluster 8

Biological Process	Count	%
defense response	18	32.7
response to organic substance	11	20
immune response	10	18.2
defense response to bacterium	9	16.4
response to bacterium	9	16.4
innate immune response	9	16.4
response to endogenous stimulus	8	14.5
protein amino acid phosphorylation	7	12.7
phosphorylation	7	12.7
response to abiotic stimulus	7	12.7
response to wounding	6	10.9
response to hormone stimulus	6	10.9
defense response, incompatible interaction	5	9.1
response to salt stress	5	9.1
defense response to fungus	5	9.1
response to osmotic stress	5	9.1
response to fungus	5	9.1
response to jasmonic acid stimulus	4	7.3
programmed cell death	4	7.3
cell death	4	7.3
death	4	7.3
response to ethylene stimulus	4	7.3
carboxylic acid biosynthetic process	4	7.3
organic acid biosynthetic process	4	7.3
cellular response to stress	4	7.3
systemic acquired resistance	3	5.5
response to virus	3	5.5
plant-type hypersensitive response	3	5.5
host programmed cell death induced by symbiont	3	5.5
response to salicylic acid stimulus	3	5.5
salicylic acid biosynthetic process	2	3.6
salicylic acid metabolic process	2	3.6
negative regulation of defense response	2	3.6

Table 8. continued

defense response to virus	2	3.6
immune effector process	2	3.6
oxylipin biosynthetic process	2	3.6
oxylipin metabolic process	2	3.6
regulation of innate immune response	2	3.6
jasmonic acid mediated signaling pathway	2	3.6

Cellular Component	Count	%
plasma membrane	12	21.8

Molecular Function	Count	%
ATP binding	10	18.2
adenyl ribonucleotide binding	10	18.2
adenyl nucleotide binding	10	18.2
purine nucleoside binding	10	18.2
nucleoside binding	10	18.2
ribonucleotide binding	10	18.2
purine ribonucleotide binding	10	18.2
protein kinase activity	7	12.7
protein serine/threonine kinase activity	6	10.9
calmodulin binding	3	5.5

*Count: The number of gene counted in the population.

Table 9. GO analysis of cluster 9

Biological Process	Count	%
response to organic substance	16	25.8
defense response	13	21
regulation of transcription	11	17.7
response to endogenous stimulus	10	16.1
response to carbohydrate stimulus	9	14.5
response to chitin	8	12.9
response to hormone stimulus	8	12.9
regulation of transcription, DNA-dependent	8	12.9
regulation of RNA metabolic process	8	12.9
response to abiotic stimulus	8	12.9
response to ethylene stimulus	7	11.3
transcription	7	11.3
response to salicylic acid stimulus	6	9.7
intracellular signaling cascade	6	9.7
response to wounding	5	8.1
response to jasmonic acid stimulus	5	8.1
response to gibberellin stimulus	4	6.5
ethylene mediated signaling pathway	4	6.5
two-component signal transduction system (phosphorelay)	4	6.5
response to cold	4	6.5
innate immune response	4	6.5
response to abscisic acid stimulus	4	6.5
immune response	4	6.5
response to temperature stimulus	4	6.5
response to metal ion	4	6.5
cellular response to hormone stimulus	4	6.5
hormone-mediated signaling	4	6.5
response to absence of light	2	3.2

Cellular Component	Count	%
vacuole	6	9.7

Table 9. continued

Molecular Function	Count	%
cation binding	14	22.6
ion binding	14	22.6
metal ion binding	13	21
DNA binding	11	17.7
transcription factor activity	10	16.1
transcription regulator activity	10	16.1
calcium ion binding	7	11.3
poly(A)-specific ribonuclease activity	2	3.2
3'-5'-exoribonuclease activity	2	3.2
exoribonuclease activity, producing 5'-phosphomonoesters	2	3.2
exoribonuclease activity	2	3.2
exonuclease activity, active with either ribo- or deoxyribonucleic acids and producing 5'-phosphomonoesters	2	3.2

*Count: The number of gene counted in the population.

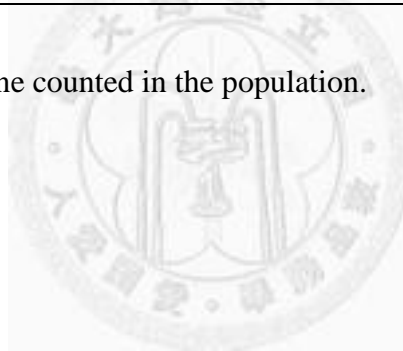


Table 10. GO analysis of cluster 10

Biological Process	Count	%
response to organic substance	8	15.1
response to hormone stimulus	7	13.2
response to endogenous stimulus	7	13.2
oxidation reduction	7	13.2
response to abiotic stimulus	7	13.2
defense response	6	11.3
protein amino acid phosphorylation	6	11.3
response to osmotic stress	5	9.4
defense response to fungus	5	9.4
response to fungus	5	9.4
pigment biosynthetic process	4	7.5
pigment metabolic process	4	7.5
response to cold	4	7.5
response to temperature stimulus	4	7.5
response to salt stress	4	7.5
hormone-mediated signaling	4	7.5
cellular response to hormone stimulus	4	7.5
chlorophyll biosynthetic process	3	5.7
chlorophyll metabolic process	3	5.7
porphyrin biosynthetic process	3	5.7
tetrapyrrole biosynthetic process	3	5.7
flavonoid biosynthetic process	3	5.7
flavonoid metabolic process	3	5.7
porphyrin metabolic process	3	5.7
tetrapyrrole metabolic process	3	5.7
phenylpropanoid biosynthetic process	3	5.7
heterocycle biosynthetic process	3	5.7
regulation of post-embryonic development	3	5.7
cofactor biosynthetic process	3	5.7
phenylpropanoid metabolic process	3	5.7
cellular amino acid derivative biosynthetic process	3	5.7
aromatic compound biosynthetic process	3	5.7
anthocyanin biosynthetic process	2	3.8

Table 10. continued

cell wall macromolecule catabolic process	2	3.8
hyperosmotic salinity response	2	3.8
response to brassinosteroid stimulus	2	3.8

Cellular Component	Count	%
cytosol	6	11.3

Molecular Function	Count	%
protein serine/threonine kinase activity	6	11.3
protein kinase activity	6	11.3
protochlorophyllide reductase activity	2	3.8
oxidoreductase activity, acting on the CH-CH group of donors, NAD or NADP as acceptor	2	3.8

*Count: The number of gene counted in the population.

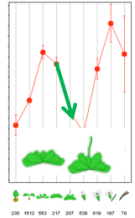
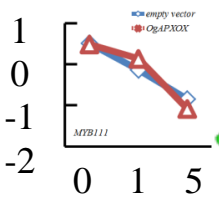
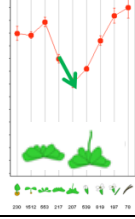
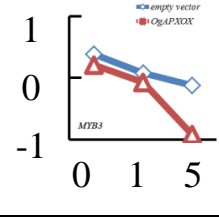
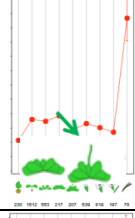
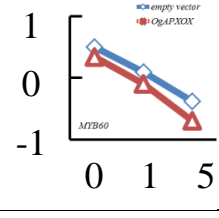
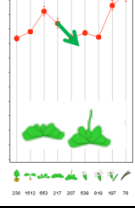
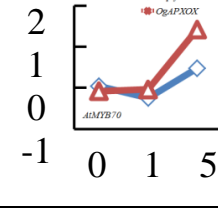
Cluster	Gene Symbol	Gene ID	C1/C0	C5/C0	T0/C0	T1/C0	T5/C0	Gene Expression Level of Development
1	<i>MYB111</i>	At3g46130	-1.56	-2.56	-1.02	-1.30	-3.03	  <p> ◆ empty vector ▲ <i>OgAPXOX</i> — Empty vector — <i>OgAPXOX</i> Vegetative to Reproductive stage </p>
1	<i>MYB3</i>	At1g22640	-1.24	-1.42	-1.13	-1.37	-2.47	  <p> ◆ empty vector ▲ <i>OgAPXOX</i> — Empty vector — <i>OgAPXOX</i> </p>
1	<i>MYB60</i>	At1g08810	-1.32	-1.84	-1.12	-1.51	-2.29	  <p> ◆ empty vector ▲ <i>OgAPXOX</i> — Empty vector — <i>OgAPXOX</i> </p>
2	<i>AtMYB70</i>	At2g23290	-1.21	1.36	-1.08	-1.05	2.61	  <p> ◆ empty vector ▲ <i>OgAPXOX</i> — Empty vector — <i>OgAPXOX</i> </p>

Table 11. Transcriptional profiling of MYB or MYB-like transcription factors. Gene symbol and Gene ID was following NCBI database.

<http://www.ncbi.nlm.nih.gov/> Gene expression level of development was adapted from TAIR. <http://www.arabidopsis.org/>

Table 11. continued

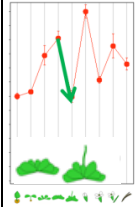
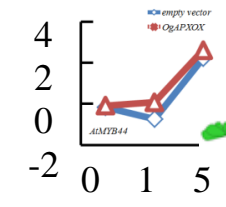
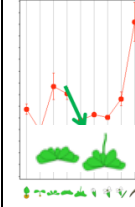
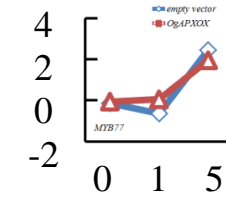
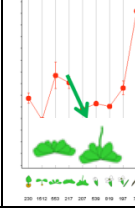
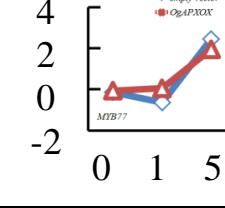
Cluster	Gene Symbol	Gene ID	C1/C0	C5/C0	T0/C0	T1/C0	T5/C0	Gene Expression Level of Development
7	<i>AtMYB44</i>	At5g67300	-1.50	5.25	1.05	1.18	6.82	 
9	<i>MYB77</i>	At3g50060	-1.42	6.02	1.06	1.14	4.25	 
10	<i>ATMYBL2</i>	At1g71030	-2.21	-1.11	1.03	1.96	-1.95	 

Table 11. Transcriptional profiling of *MYB* or *MYB-like* transcription factors. Gene symbol and Gene ID was following NCBI database.

<http://www.ncbi.nlm.nih.gov/> Gene expression level of development was adapted from TAIR. <http://www.arabidopsis.org/>

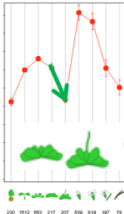
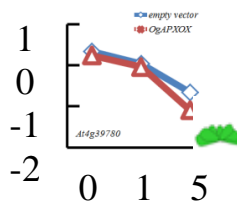
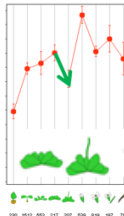
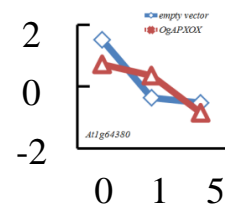
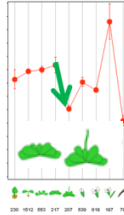
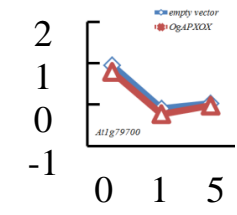
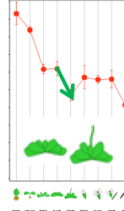
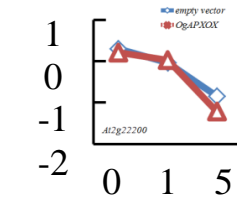
Cluster	Gene Symbol	Gene ID	<i>C1/C0</i>	<i>C5/C0</i>	<i>T0/C0</i>	<i>T1/C0</i>	<i>T5/C0</i>	Gene Expression Level of Development
1		At4g39780	-1.22	-1.98	-1.06	-1.30	-2.68	 
1		At1g64380	-3.65	-4.12	-1.73	-2.22	-5.13	 
1		At1g79700	-2.05	-1.90	-1.11	-2.26	-1.96	 
1		At2g22200	-1.25	-2.21	-1.06	-1.20	-2.84	 

Table 12. Transcriptional profiling of AP2-like transcription factors. Gene symbol and Gene ID was following NCBI database.

<http://www.ncbi.nlm.nih.gov/> Gene expression level of development was adapted from TAIR. <http://www.arabidopsis.org/>

Table 12. continued

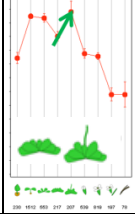
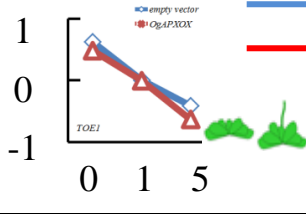
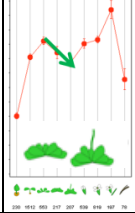
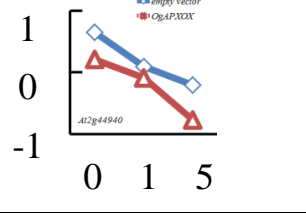
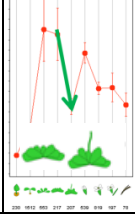
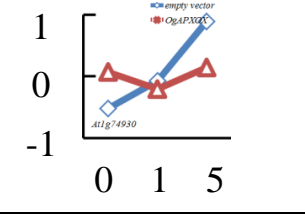
Cluster	Gene Symbol	Gene ID	C1/C0	C5/C0	T0/C0	T1/C0	T5/C0	Gene Expression Level of Development
1	<i>TOEI</i>	At2g28550	-1.53	-2.05	-1.10	-1.54	-2.39	 
1		At2g44940	-1.47	-1.81	-1.35	-1.67	-2.68	 
5		At1g74930	1.36	2.65	1.51	1.24	1.58	 

Table 12. Transcriptional profiling of *AP2-like* transcription factors. Gene symbol and Gene ID was following NCBI database.

<http://www.ncbi.nlm.nih.gov/> Gene expression level of development was adapted from TAIR. <http://www.arabidopsis.org/>

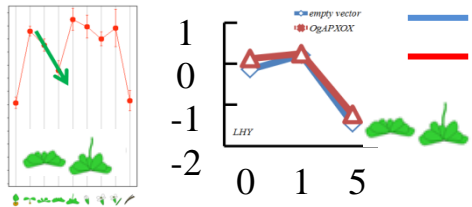
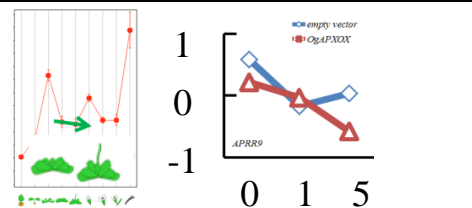
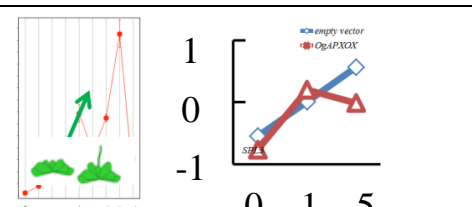
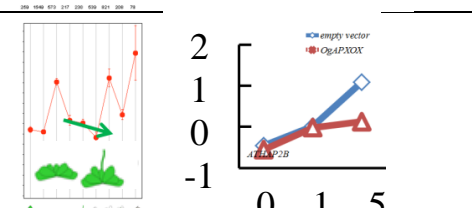
Cluster	Gene Symbol	Gene ID	<i>C1/C0</i>	<i>C5/C0</i>	<i>T0/C0</i>	<i>T1/C0</i>	<i>T5/C0</i>	Gene Expression Level of Development
1	At1g01060	<i>LHY</i>	1.27	-2.51	1.20	1.30	-2.14	
1	At2g46790	<i>APRR9</i>	-1.69	-1.46	-1.29	-1.54	-2.24	
4	At2g33810	<i>SPL3</i>	1.47	2.15	-1.17	1.68	1.44	
5	At3g05690	<i>ATHAP2B</i>	1.38	2.90	-1.07	1.35	1.49	

Table 13. Transcriptional profiling of circadian genes. Gene symbol and Gene ID was following NCBI database. <http://www.ncbi.nlm.nih.gov/> Gene expression level of development was adapted from TAIR. <http://www.arabidopsis.org/>

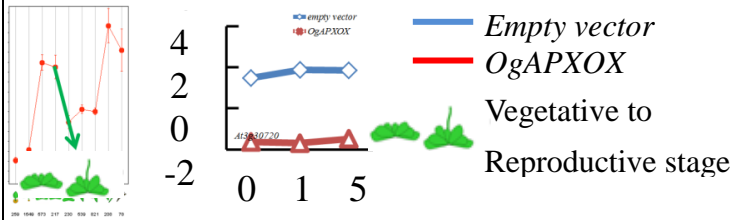
Cluster	Gene Symbol	Gene ID	C1/C0	C5/C0	T0/C0	T1/C0	T5/C0	Gene Expression Level of Development
4	At3g30720	QQS	1.33	1.29	-8.60	-8.97	-7.73	

Table 14. Transcriptional profiling of *QQS*. Gene symbol and Gene ID was following NCBI database. <http://www.ncbi.nlm.nih.gov/> Gene expression level of development was adapted from TAIR. <http://www.arabidopsis.org/>



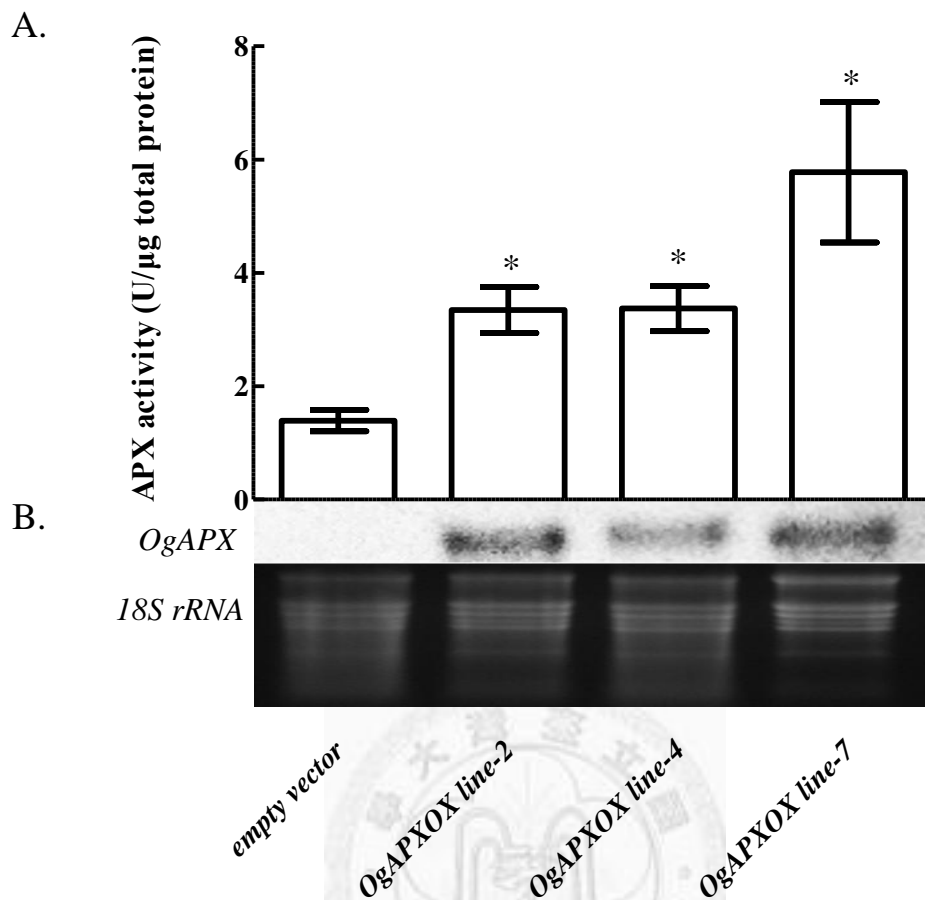


Figure 1. The enzymatic activity and expression level of APX in several independent lines.

- A. The APX activity in mature leaves of 24-d-old control and transgenic *Arabidopsis* plants growing under long-day photoperiod (16 h light and 8 h dark) and 22°C. One unit of APX was defined as the activity that consumed $1 \mu \text{mol AsA min}^{-1} \mu \text{g}^{-1}$ total protein. The data was means \pm SD from three independent experiments (n =6; three measurements on each of the six plants). Means were considered to be significant difference which were indicated by asterisks (*) when $P < 0.001$
- B. The expression level of *OgAPX* in each independent transgenic *Arabidopsis* plants. In the lower panel, ethidium bromide-stained total RNA was shown as a loading control.

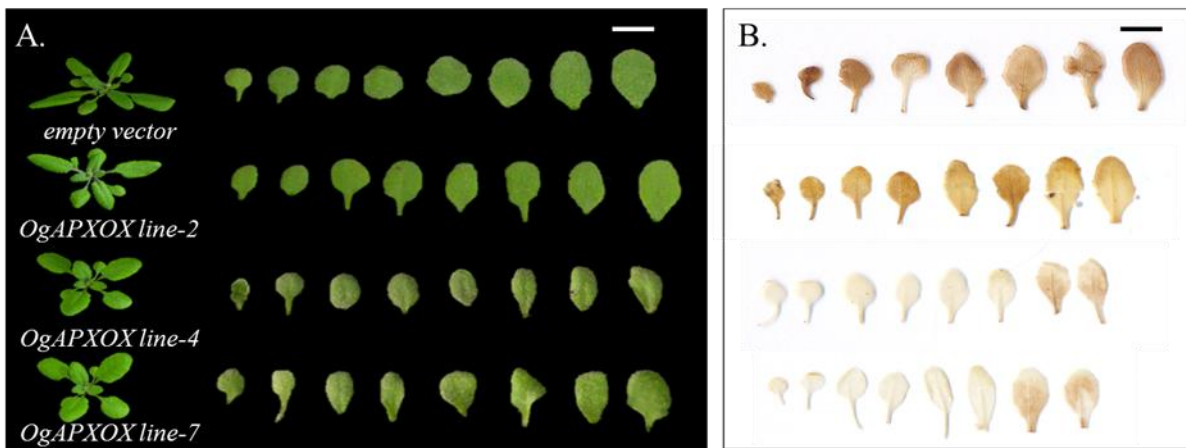
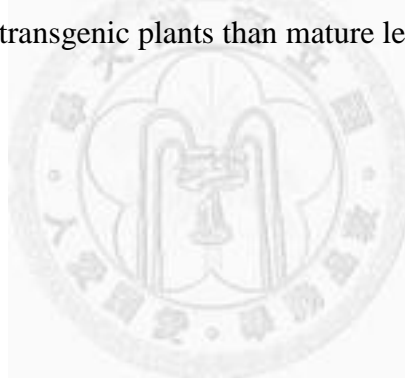


Figure 2. The foliar phenotype and H_2O_2 content in transgenic and control plants growing under long-day photoperiod and 22°C condition.

A. The phenotype of transgenic and control plants. Scale bar indicated 1cm.

B. Histological stain of H_2O_2 with 3,3'-diaminobenzidine displayed that less H_2O_2 level was present in young leaves of transgenic plants than mature leaves. Scale bar indicated 1cm.



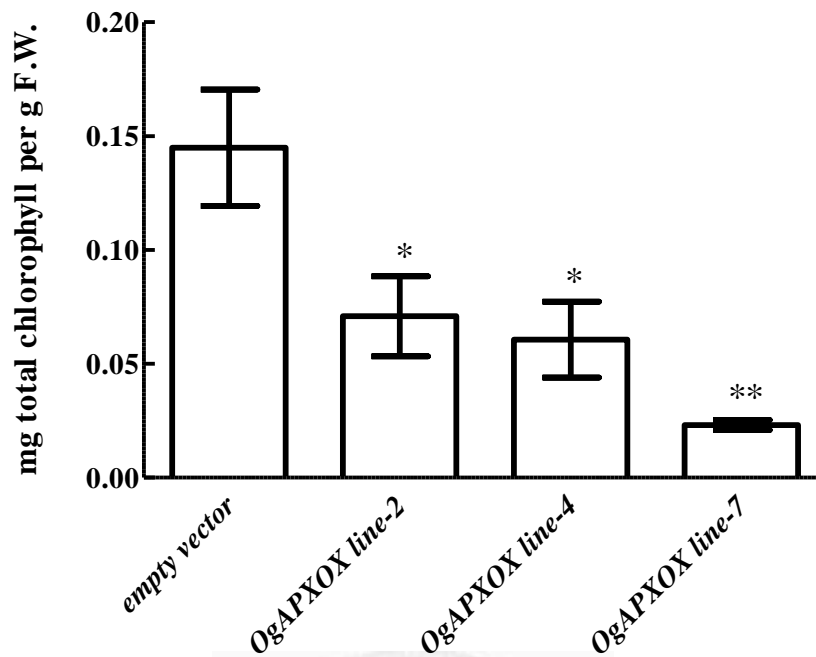


Figure 3. The chlorophyll content of control and transgenic plants.

Transgenic plants accumulated less chlorophyll in mature leaves of 24-d-old growing under long-day photoperiod and 22°C condition. The data was means \pm SD from three independent experiments (n =6; three measurements on each of the six plants). Means were considered to be significant difference which were indicated by asterisks (*) when $P < 0.05$ and $P < 0.01$ (**).

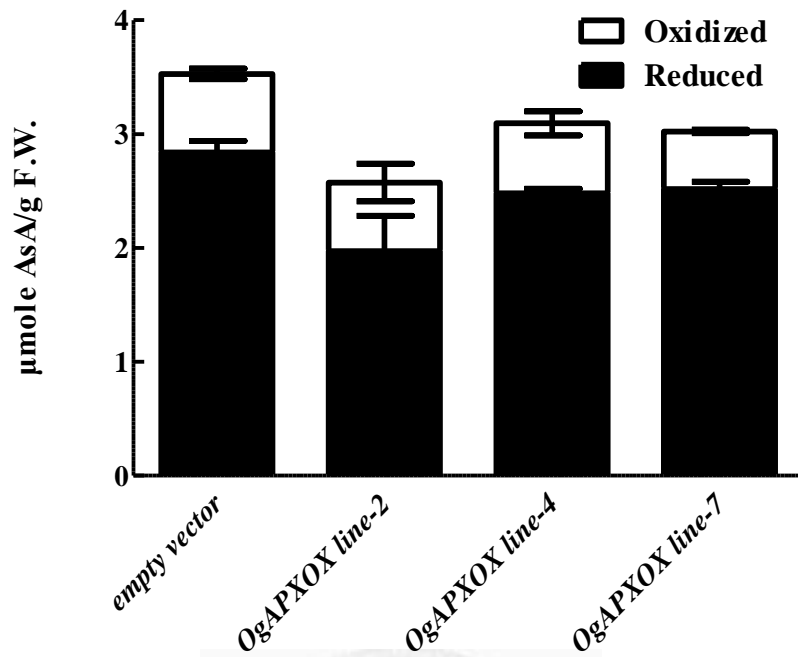


Figure 4. The AsA level in transgenic and control plants growing under 22°C condition and long-day photoperiod. AsA content in 4 leaves of transgenic and control plants growing under 22°C condition and long-day photoperiod. The data was means \pm SD from three independent experiments (n =6; three measurements on each of the six plants).

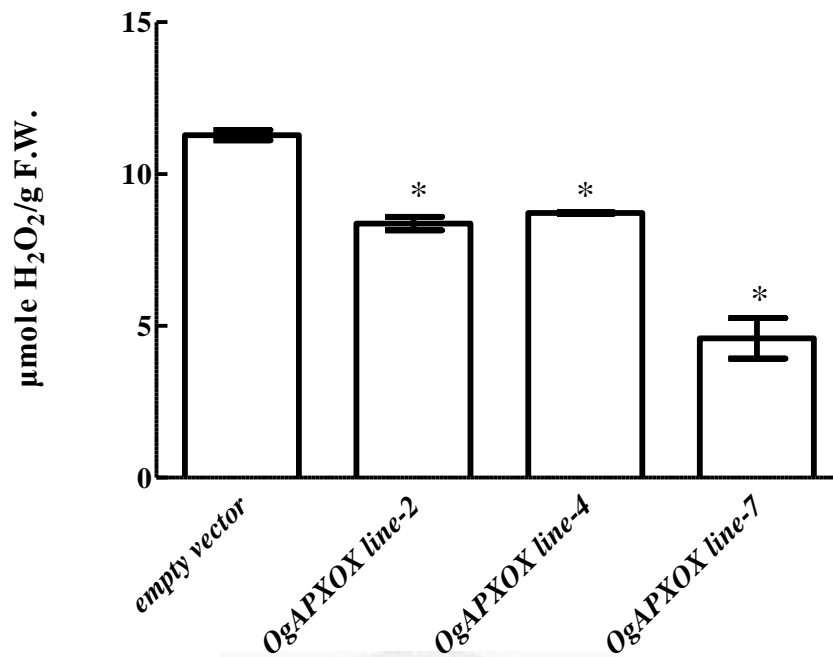


Figure 5. The H₂O₂ content in transgenic and control plants growing under long-day photoperiod and 22°C condition.

Transgenic plants exhibited the less H₂O₂ level with control plants.

The data was means \pm SD from three independent experiments (n =6; three measurements on each of the six plants). Means were considered to be significantly different when $P < 0.005$, which were indicated by asterisks (*).

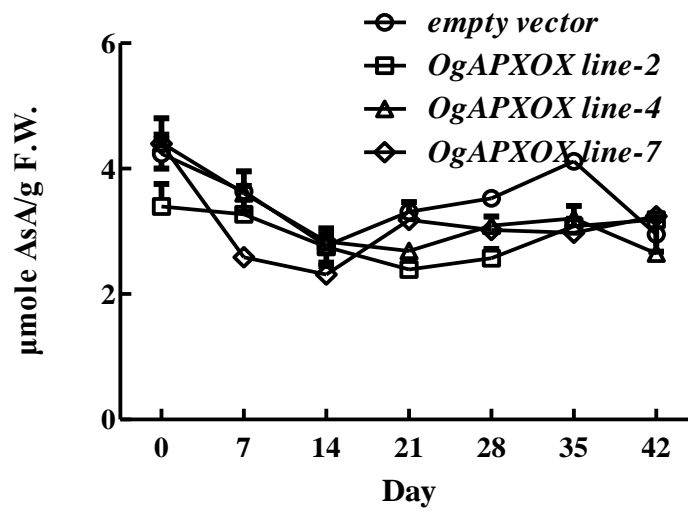


Figure 6. The AsA level in transgenic and control plants growing under 22°C condition and short-day photoperiod. Control and transgenic plants showed the steady pattern of AsA level under 22°C condition and short-day photoperiod. Day 0 means the initiatory day for detecting AsA level when plants consisted of six leaves. The data was means \pm SD from three independent experiments (n =6; three measurements on each of the six plants).

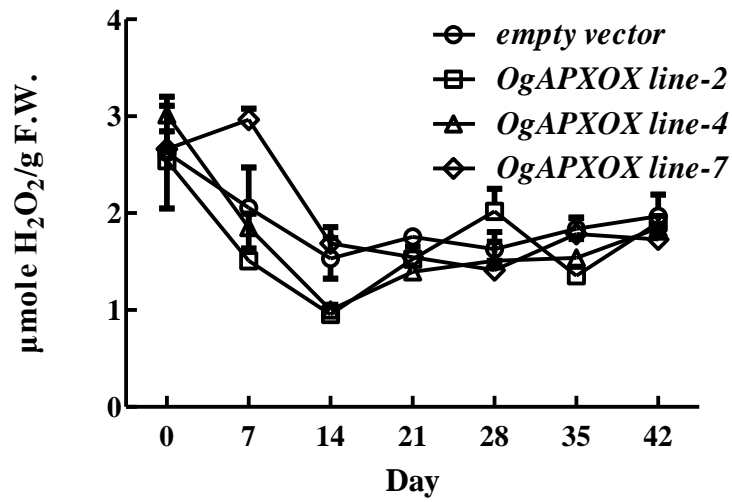
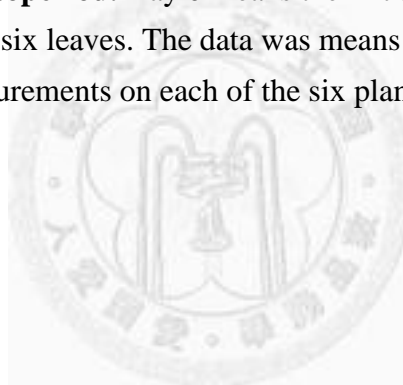


Figure 7. The H₂O₂ content in transgenic and control plants growing under 22°C condition and short-day photoperiod. Day 0 means the initiatory day for detecting H₂O₂ level when plants consisted of six leaves. The data was means \pm SD from three independent experiments (n =6; three measurements on each of the six plants).



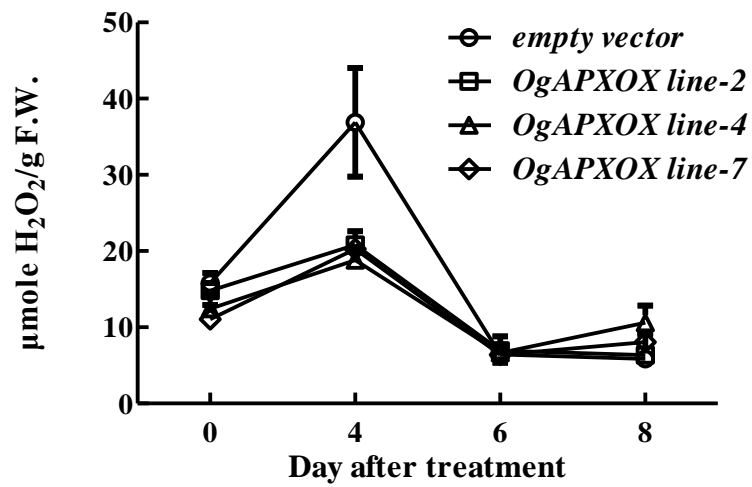


Figure 8. H₂O₂ level in wild type and *OgAPXOX* transgenic *Arabidopsis* after elevating growth temperature to 30°C. The H₂O₂ level in wild type increased significantly under elevated growth temperature condition compared with *OgAPXOX* transgenic plants displaying mild increased pattern. Day 0 means the initiatory day for detecting H₂O₂ level when plants consisted of six leaves. The data was means \pm SD from three independent experiments (n =6; three measurements on each of the six plants).

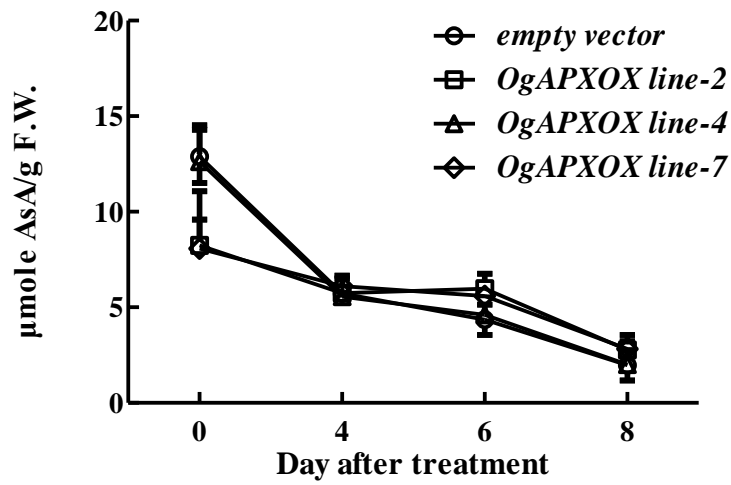


Figure 9. AsA content in transgenic plants *OgAPXOX* after heat treatment.

AsA content in transgenic and control plants were monitored after elevating growth temperature to 30°C.

The higher growth temperature brought about striking decrease of AsA level in transgenic plants and wild type. The data was means \pm SD from three independent experiments (n =6; three measurements on each of the six plants).

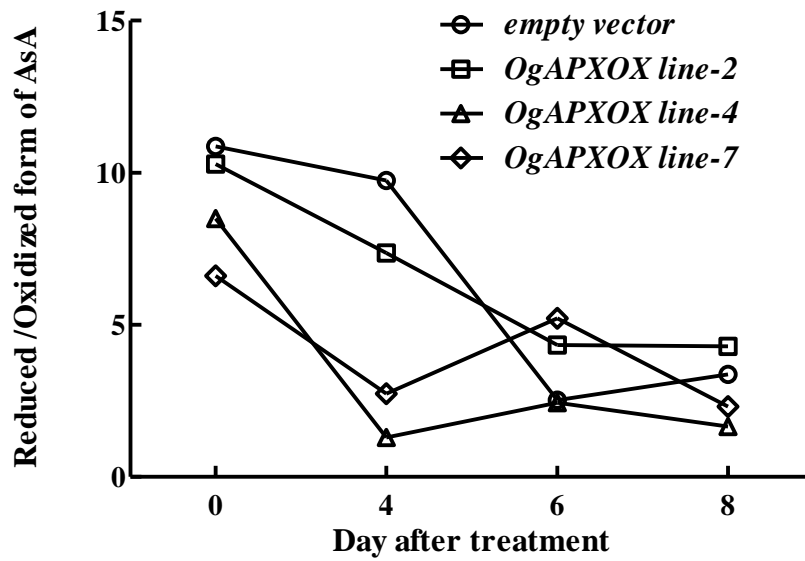


Figure 10. The AsA redox ratio in transgenic plants *OgAPXOX* after elevating growth temperature to 30°C.

The higher growth temperature brought about striking decrease of AsA redox state in transgenic plants and wild type. Day 0 means the initiatory day for detecting AsA redox state when plants consisted of six leaves. The data was means \pm SD from three independent experiments (n =6; three measurements on each of the six plants).

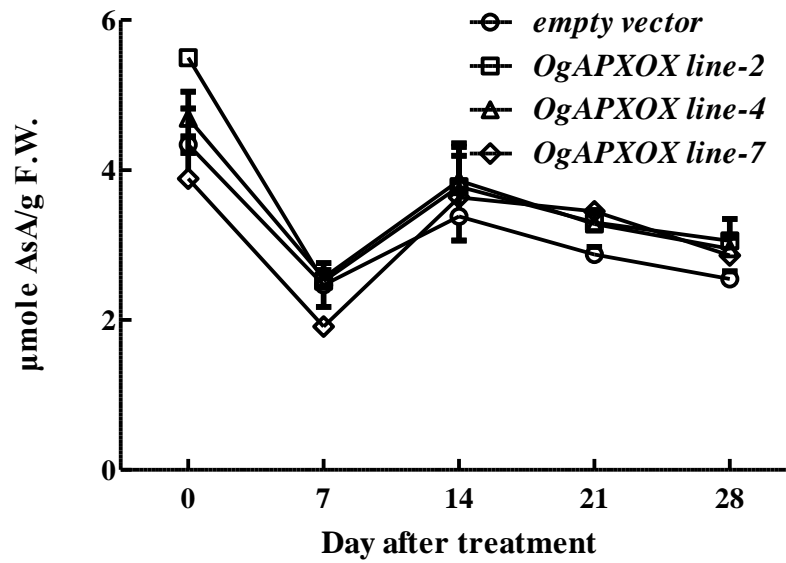


Figure 11. The higher growth temperature brought about drastic decrease of AsA level in wild type and transgenic plants. The AsA level in wild type and transgenic plants decrease significantly when growing under elevated growth temperature for 7 day. Day 0 means the initiatory day for detecting AsA level when plants consisted of six leaves. The data was means \pm SD from three independent experiments (n =6; three measurements on each of the six plants).

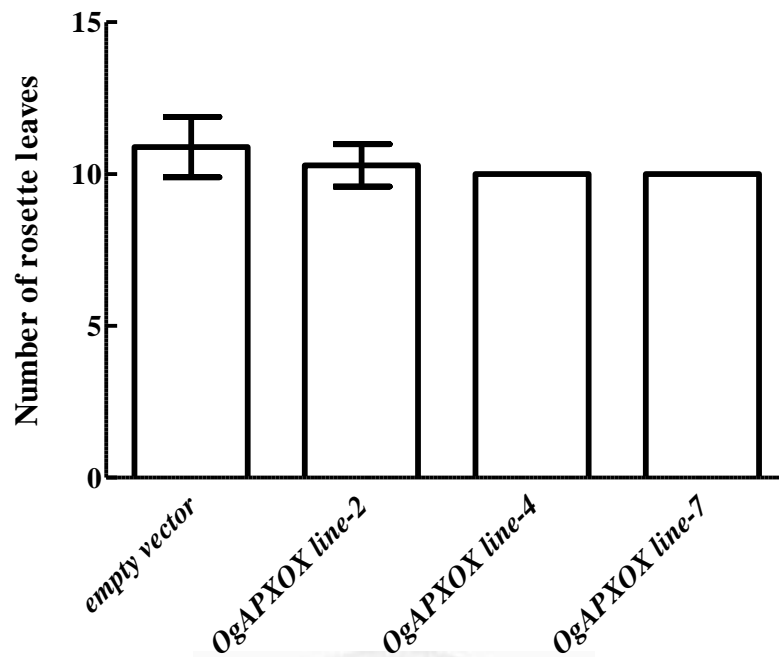


Figure 12. The number of rosette leaves at the time of flowering in *OgAPXOX* and control plants. *OgAPXOX* transgenic *Arabidopsis* displayed similar flowering time with wild type under $22 \pm 2^\circ\text{C}$ and a long-day photoperiod (16 h light and 8 h dark). The flowering of each plant was monitored in the T3 generation. ($n_{\text{empty vector}} > 20$, $n_{\text{OgAPXOX line-2,4,7}} > 20$).



Figure 13. The phenotype of transgenic *Arabidopsis* and control plants growing under short-day photoperiod and 22°C condition. Scale bar indicated 1 cm.

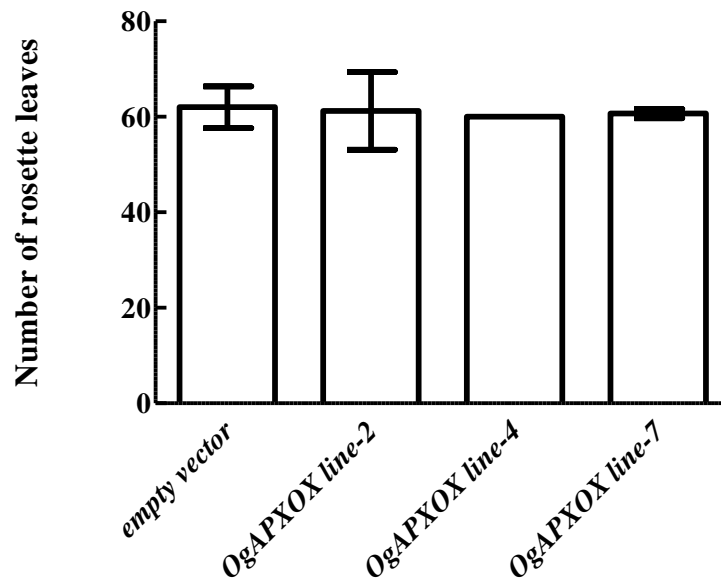


Figure 14. The flowering time of transgenic *Arabidopsis* and control plants growing under 22°C condition and short-day photoperiod.

OgAPXOX transgenic *Arabidopsis* displayed similar flowering time with wild type under 22°C condition and short-day photoperiod. ($n_{empty\ vector} > 30$, $n_{OgAPXOX\ line-2,4,7} > 30$).

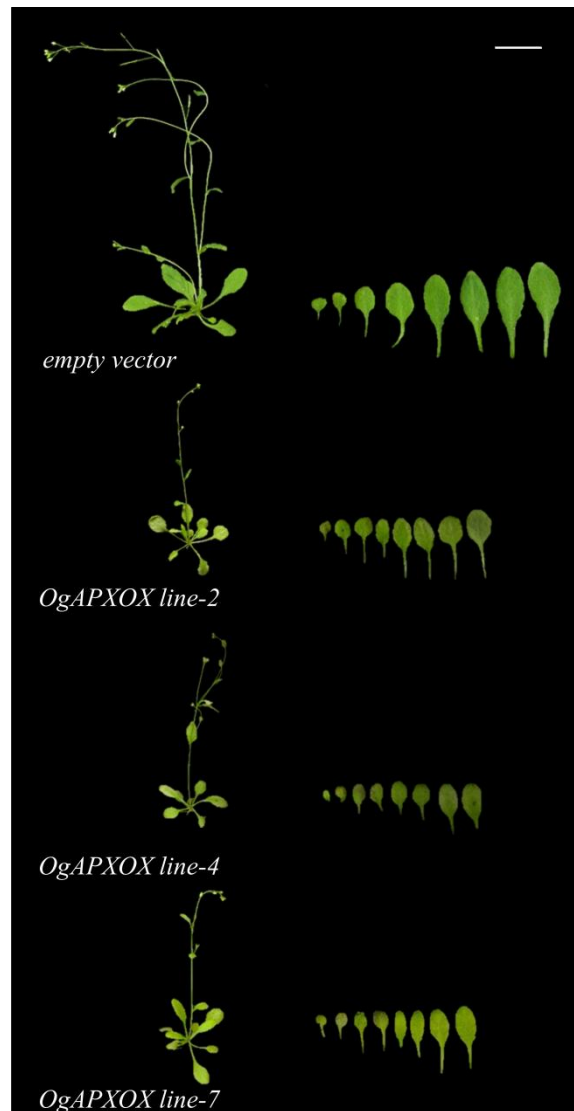


Figure 15. The phenotype of transgenic *Arabidopsis* and control plants growing under 30°C condition and long-day photoperiod.

The shorter inflorescence length was present in *OgAPXOX* transgenic plants after growing under long-day photoperiod and 30°C condition for 3 weeks. ($n_{\text{empty vector}} > 70$, $n_{\text{OgAPXOX line-2,4,7}} > 70$). Scale bar indicates 1cm.

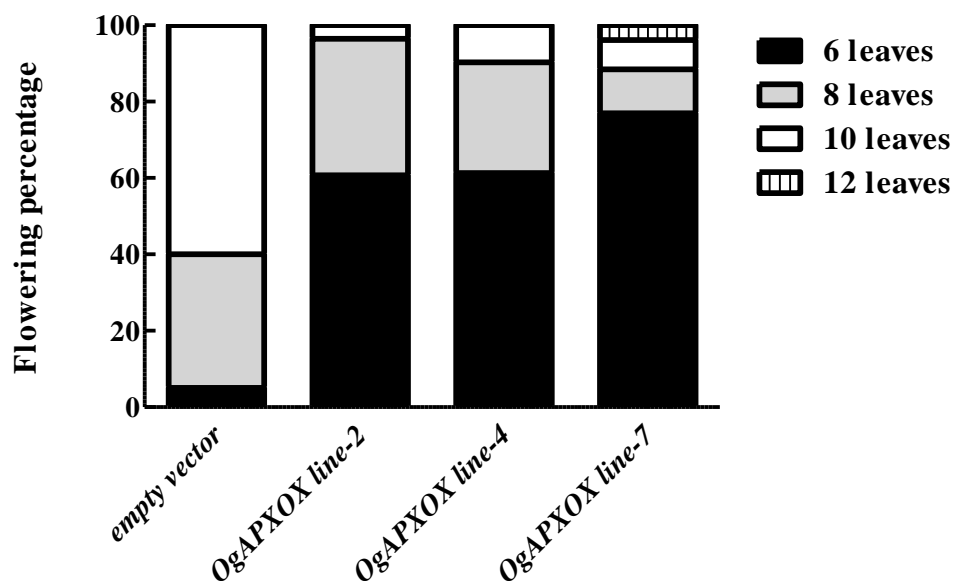


Figure 16. The percentage of rosette leaf number when flowering in transgenic *Arabidopsis* and control plants growing under 30°C condition and long-day photoperiod.

The major number of leaves (>50%) at the time of flowering in wild type and transgenic plants were six and eight, respectively. Noteworthy, over a half of wild type flowered when leaves number higher than eight. *OgAPXOX* transgenic *Arabidopsis* displayed early flowering time with wild type under 30°C condition and long-day photoperiod. ($n_{empty\ vector} > 50$, $n_{OgAPXOX\ line-2,4,7} > 50$).

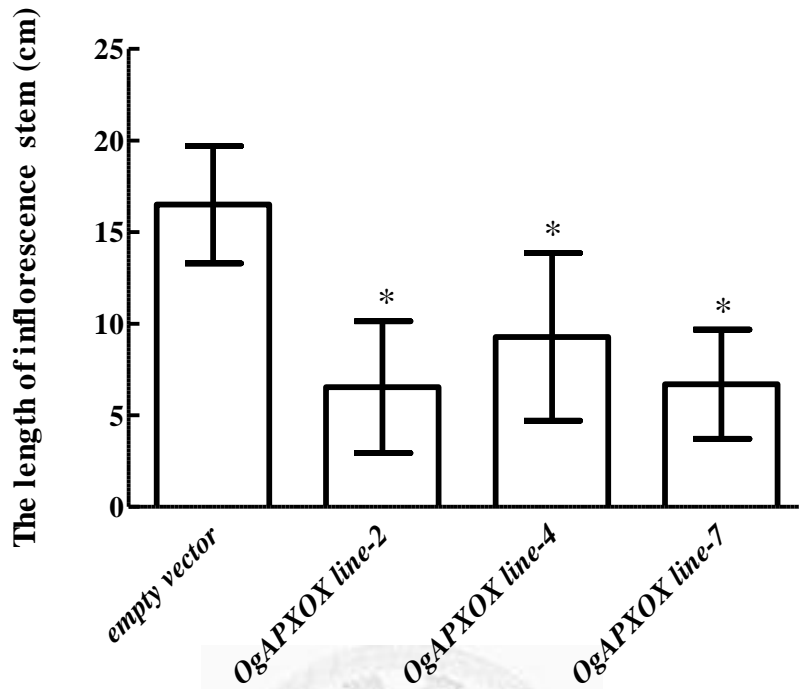


Figure 17. *OgAPXOX* transgenic plants exhibited the shorter length of inflorescence stem.

Vertical bars represent the standard deviation. Each plant was monitored using transgenic plants in the T3 generation. ($n_{empty\ vector} > 50$, $n_{OgAPXOX\ line-2,4,7} > 50$). Means were considered to be significant difference which were indicated by asterisks (*) when $P < 0.0005$.



Figure 18. The phenotype of transgenic *Arabidopsis* and control plants growing under 30°C condition and short-day photoperiod. Scale bar indicates 1cm.



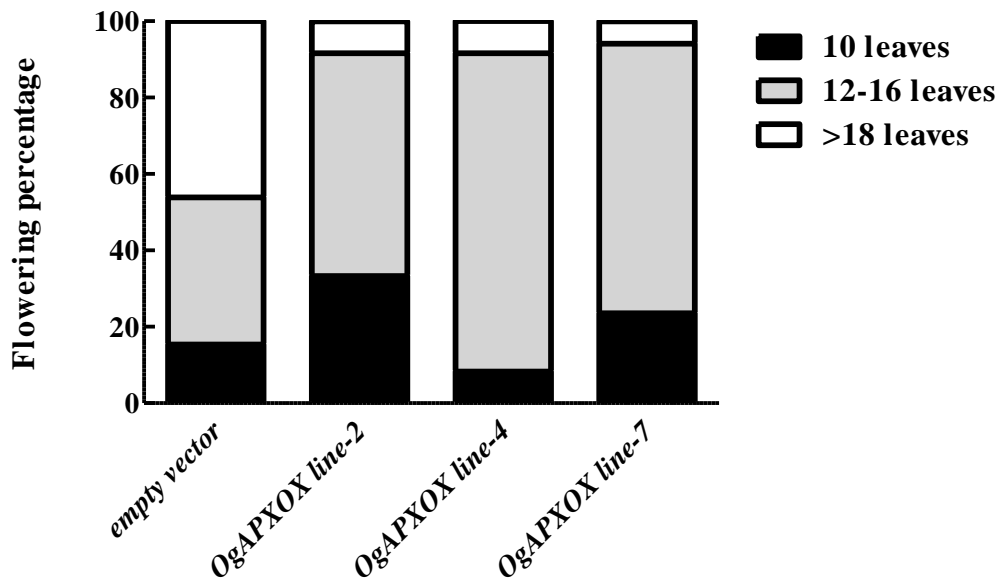


Figure 19. The percentage of rosette leaf number when flowering in *OgAPXOX* and control plants growing under 30°C condition and short-day photoperiod. Vertical bars represent the standard deviation. Each plant was monitored using transgenic plants in the T3 generation. ($n_{empty\ vector} > 50$, $n_{OgAPXOX\ line-2,4,7} > 50$).

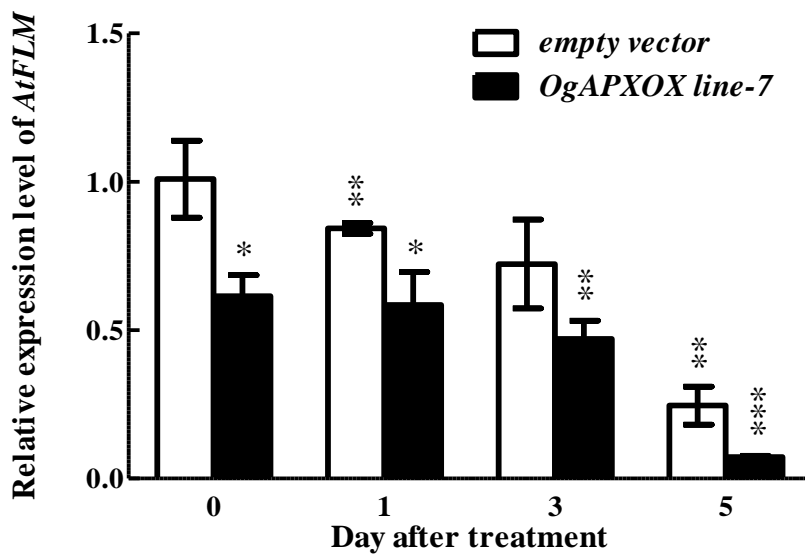


Figure 20. Relative expression levels of thermal sensitivity gene *FLOWERING LOCUS M* (*FLM*) in wild type and transgenic plants under elevated growth temperature.

Comparing to wild type, lower *FLM* expression level was present in the transgenic plants. Means were considered to be significant difference which were indicated by asterisks (*) when $P < 0.05$, $P < 0.01$ (**) and $P < 0.001$ (***)

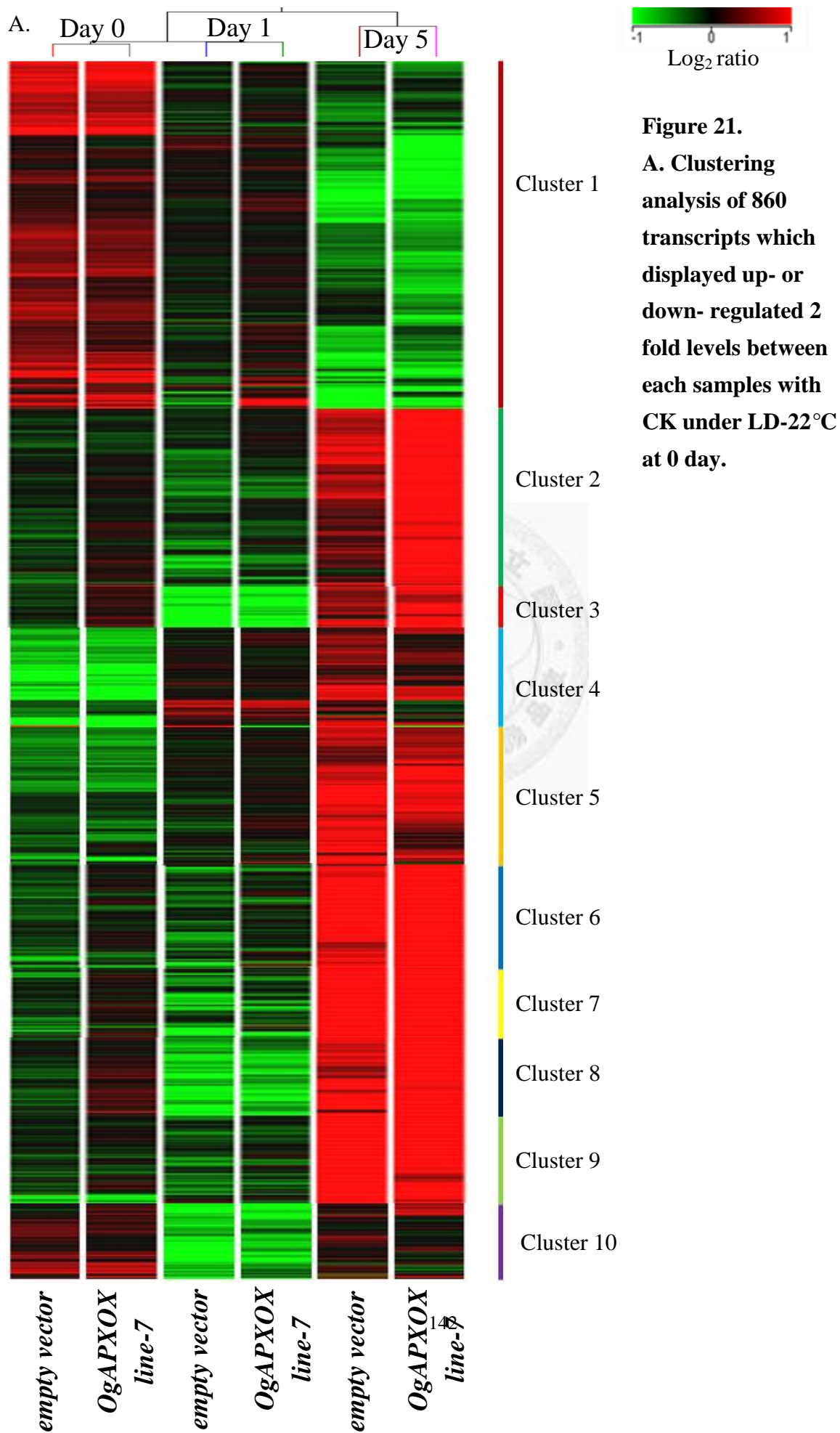
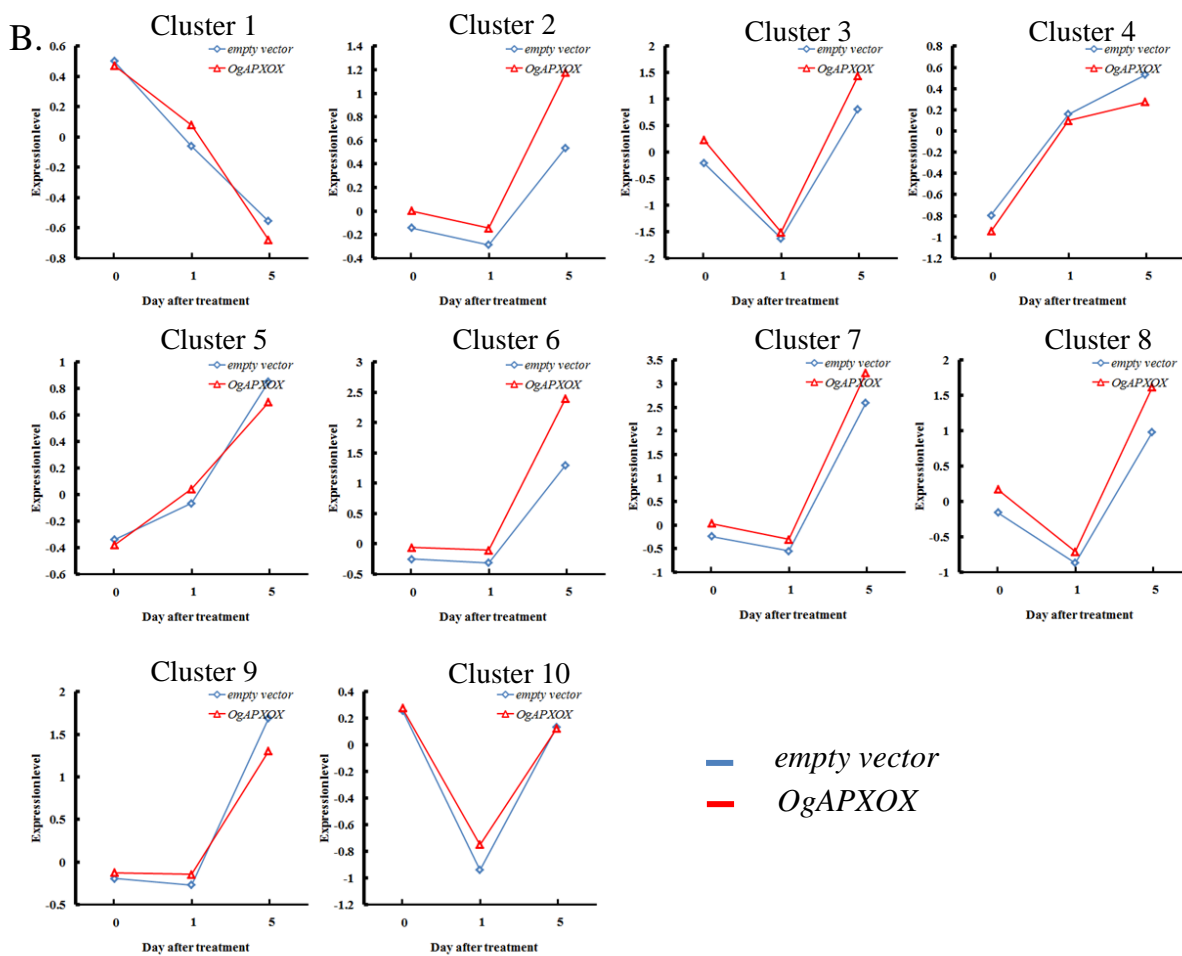


Figure 21.
A. Clustering analysis of 860 transcripts which displayed up- or down- regulated 2 fold levels between each samples with CK under LD-22°C at 0 day.



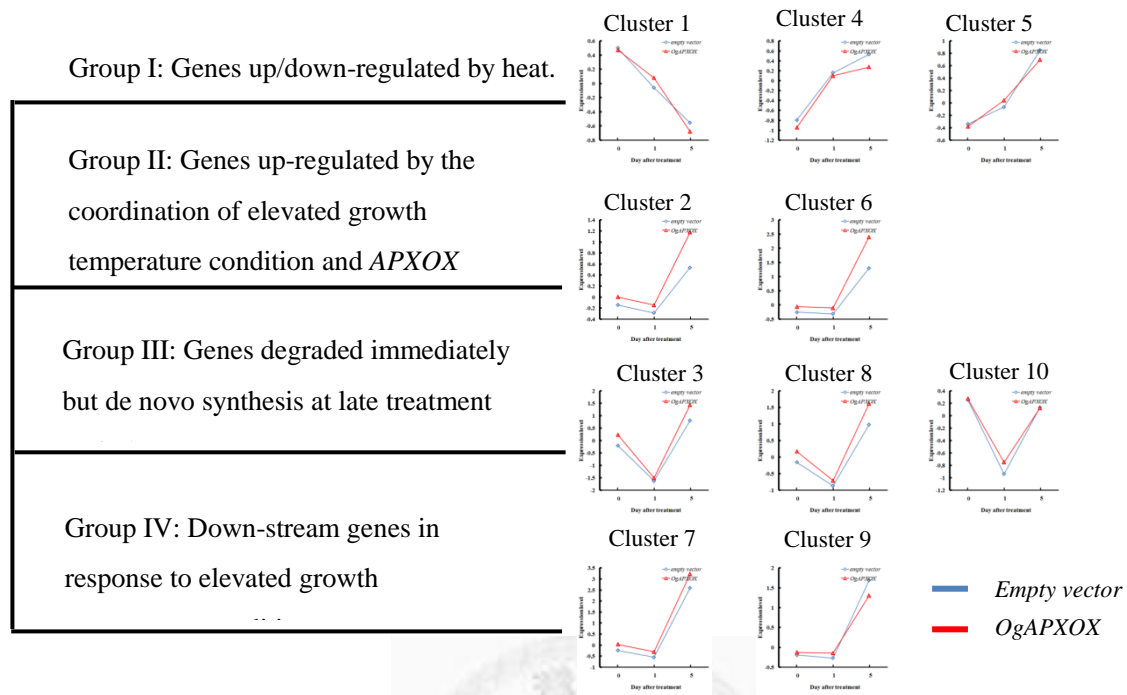


Figure 22. Functional categories of expression clusters in accordance with genotypes and growth temperature condition. The *x*-axis indicates the time points at which heat treatment following 0, 1 and 5 long days (LDs), whereas the *y*-axis represents the average values of the normalized by CK under LD-22°C at 0 day and \log_2 transformed signal intensity values of the transcripts in the cluster.

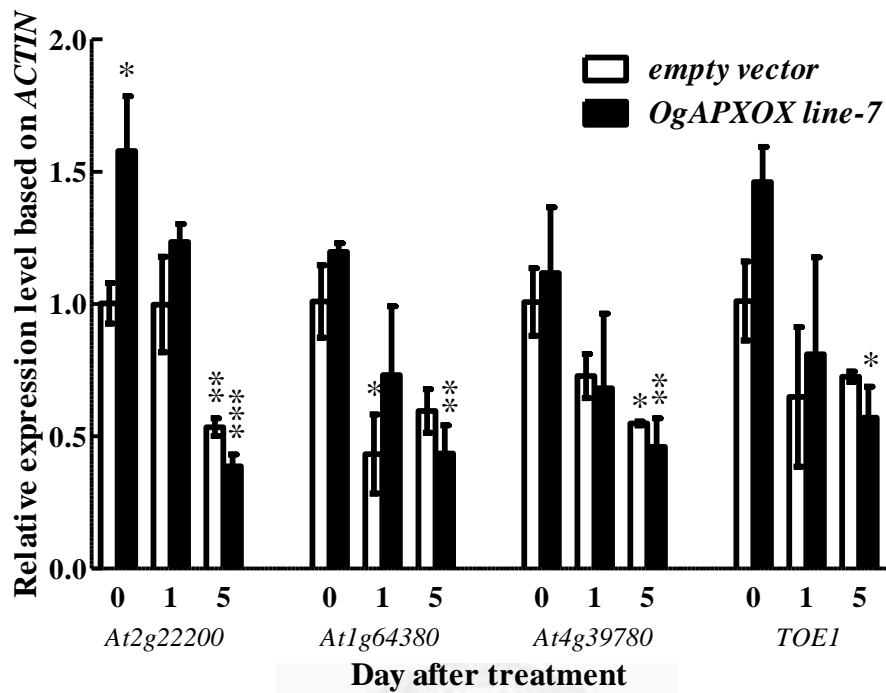


Figure 23. Relative expression levels of AP2 transcription factors in wild type and transgenic plants under elevated growth temperature. Means were considered to be significant difference which were indicated by asterisks (*) when $P < 0.05$, $P < 0.001$ (**) and $P < 0.0001$ (***). (n =6; three measurements on each of the six plants).

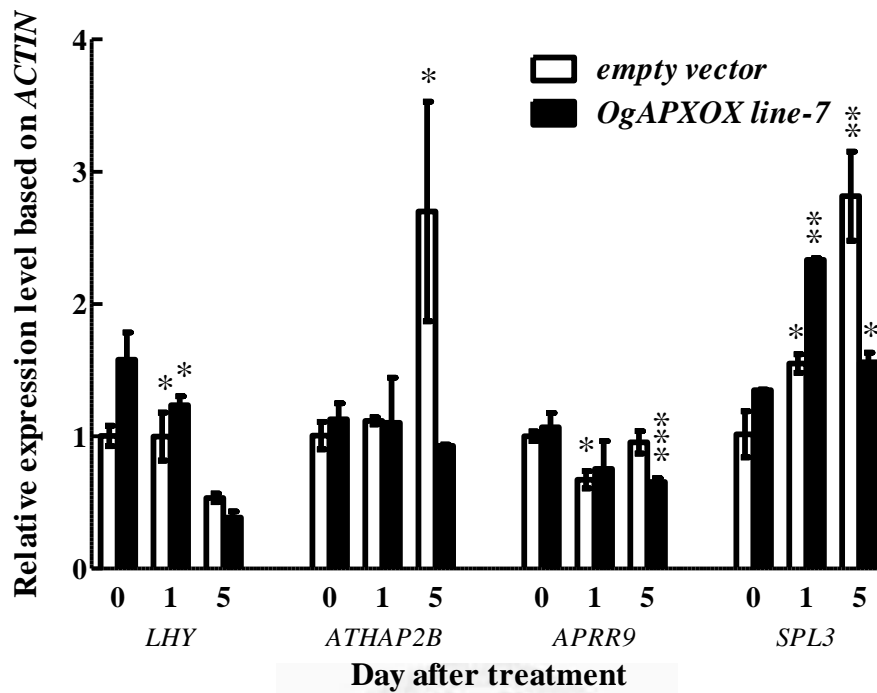


Figure 24. Relative expression levels of circadian genes in wild type and transgenic plants under elevated growth temperature. Means were considered to be significant difference which were indicated by asterisks (*) when $P < 0.05$, $P < 0.001$ (**) and $P < 0.0001$ (***) . (n=6; three measurements on each of the six plants).

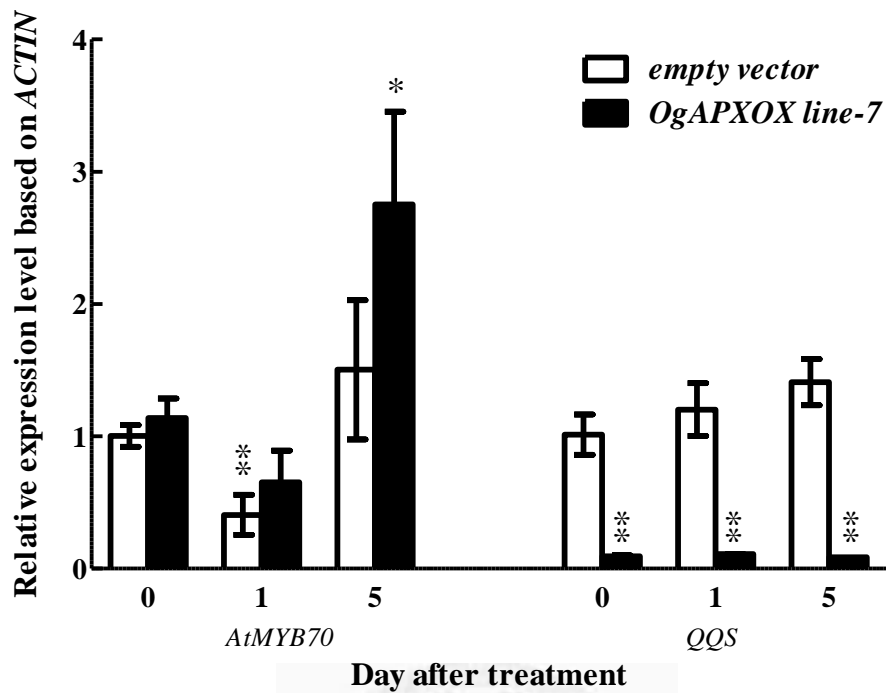


Figure 25. Relative expression levels of *AtMYB70* and *QQS* in wild type and transgenic plants under elevated growth temperature. Means were considered to be significant difference which were indicated by asterisks (*) when $P < 0.05$, $P < 0.001$ (**). (n =6; three measurements on each of the six plants).

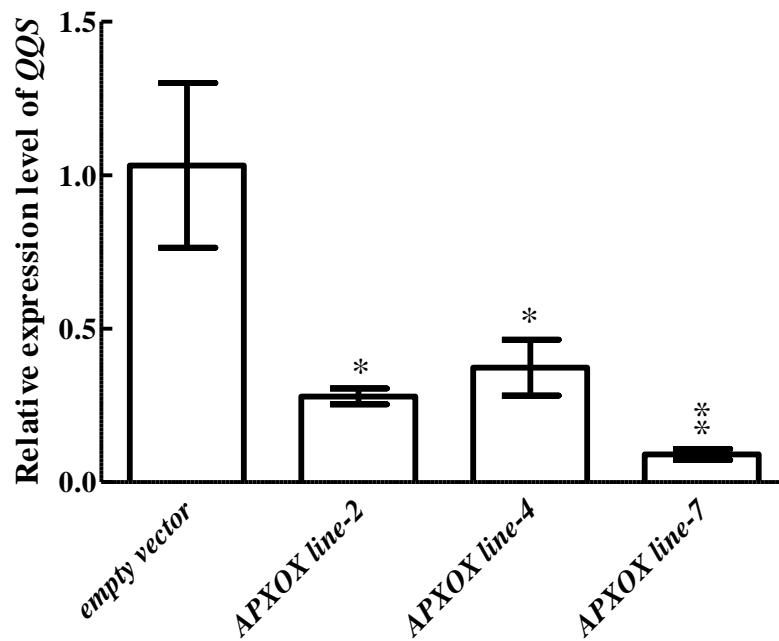


Figure 26. Relative expression levels of *qua-quine starch* (*QQS*) in three independent lines. In comparison with wild type, lower *QQS* expression level was present in the transgenic plants. Means were considered to be significant difference which were indicated by asterisks (*) when $P < 0.05$ and $P < 0.001$ (**). (n=6; three measurements on each of the six plants).

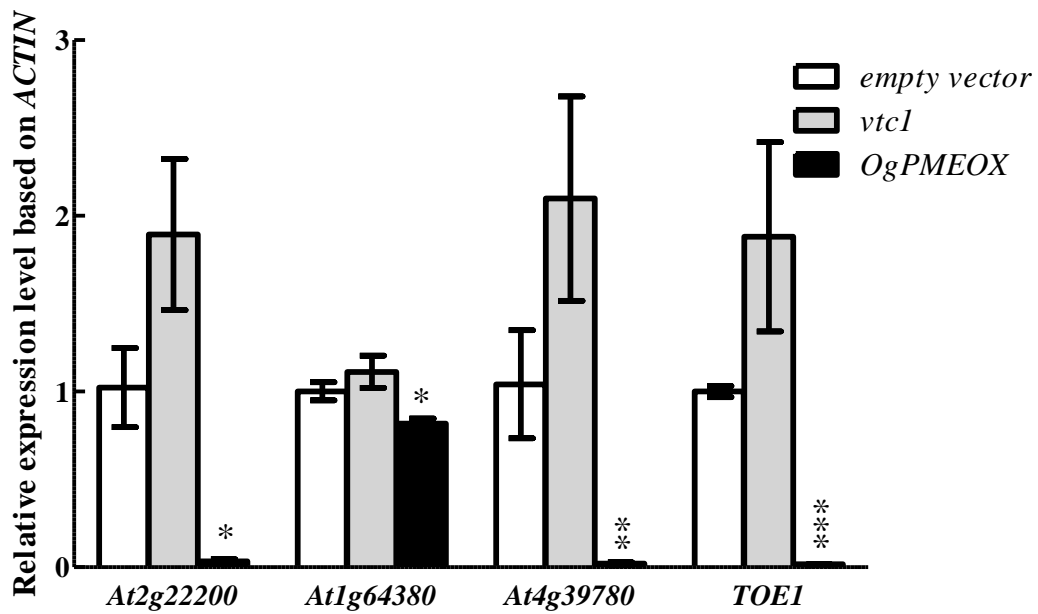


Figure 27. Relative expression levels of AP2 transcription factors in *vtc1* or *OgPMEOX* mutants. Means were considered to be significant difference which were indicated by asterisks (*) when $P < 0.05$, $P < 0.001$ (**) and $P < 0.0001$ (***). (n =6; three measurements on each of the six plants).

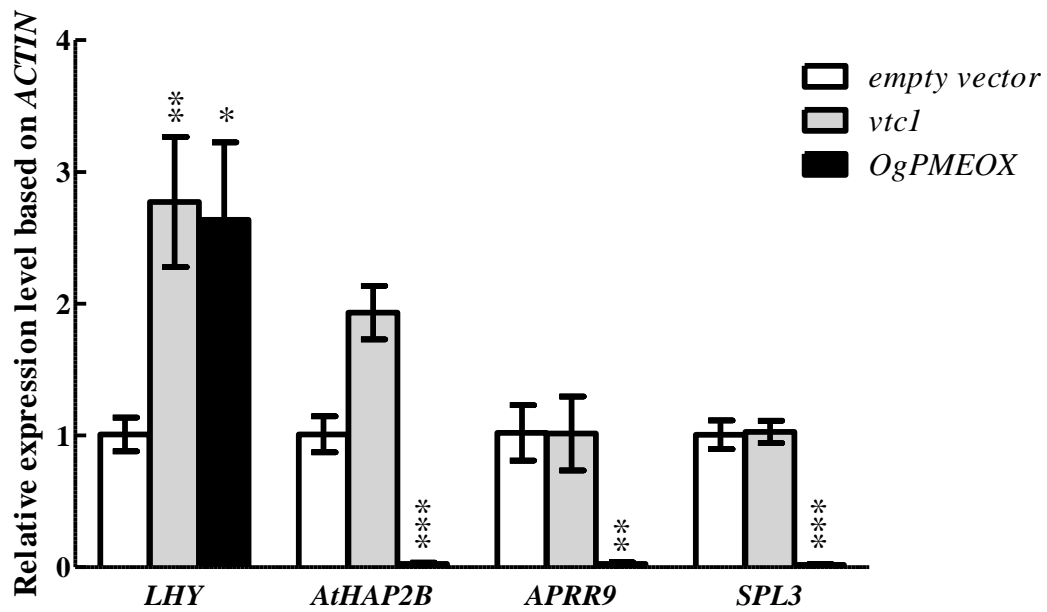


Figure 28. Relative expression levels of circadian genes in *vtc1* or *OgPMEOX* mutants.

Means were considered to be significant difference which were indicated by asterisks (*) when $P < 0.05$, $P < 0.001$ (**) and $P < 0.0001$ (***). (n = 6; three measurements on each of the six plants).

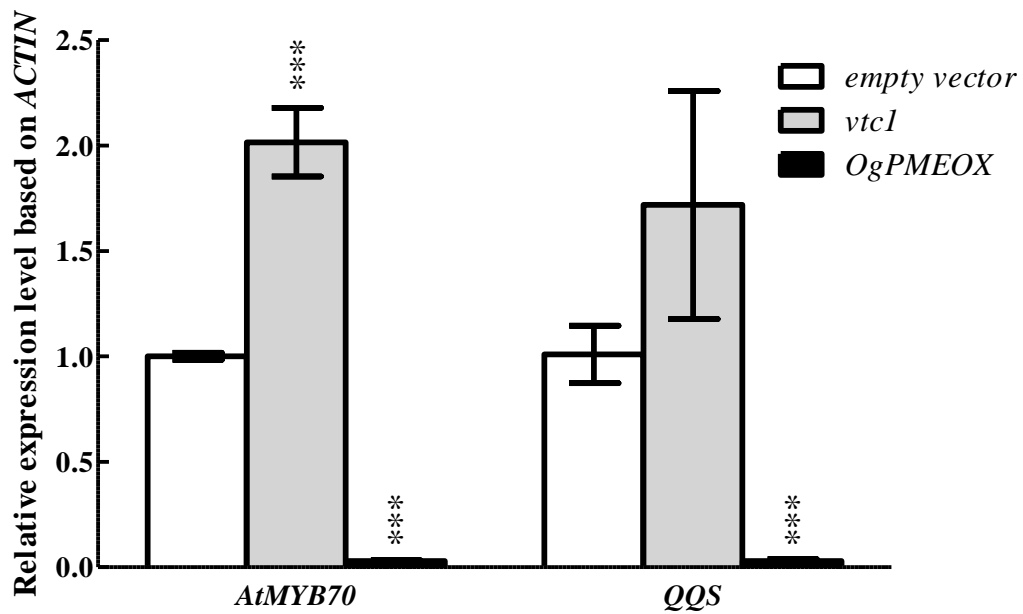


Figure 29. Relative expression levels of *AtMYB70* and *QQS* in *vtc1* or *OgPMEOX* mutants. Means were considered to be significant difference which were indicated by asterisks (*) when $P < 0.05$, $P < 0.001$ (**) and $P < 0.0001$ (***). (n =6; three measurements on each of the six plants).

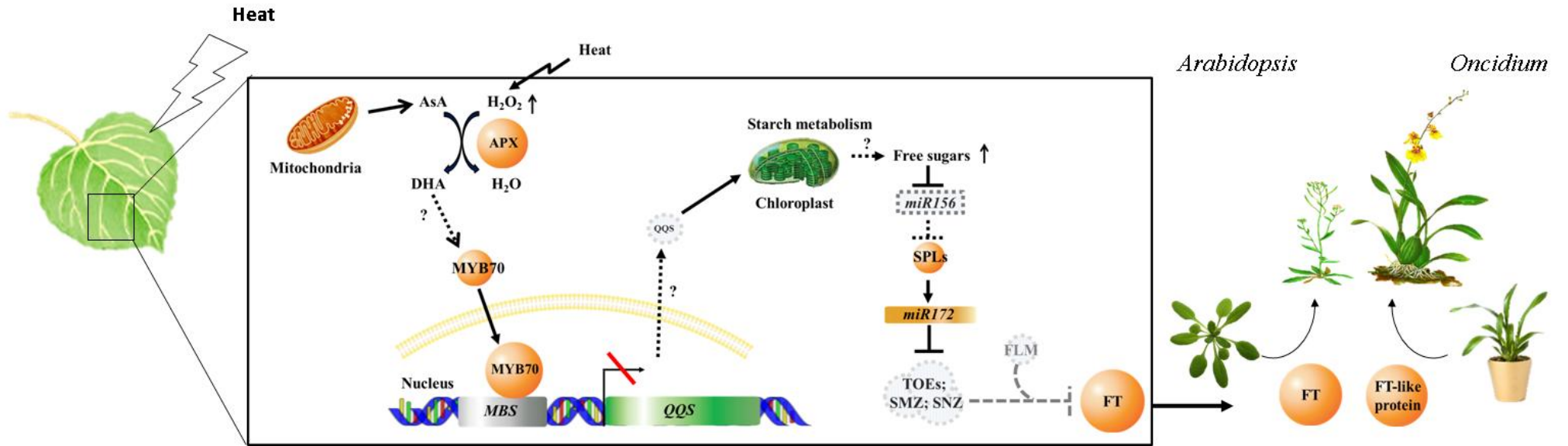
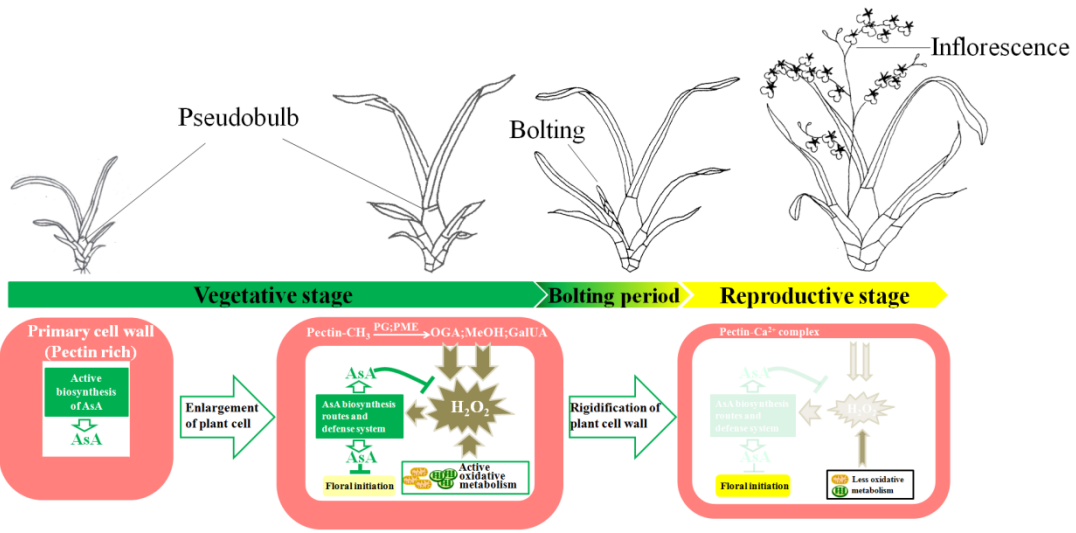


Figure 30. Proposal model of genetic network for activated APX in modulating flowering process.

Appendix 1. The oligonucleotides used for RT-PCR and qRT-PCR.

Gene	T _m	Sequence
OgAPX-F	55.2°C	5'-GCAACTGTATCTCTCGTGTCATC-3'
OgAPX-R	52.3°C	5'-TGACCCAAGTTGTCAAGTCCA-3'
AtFLM-F	54.3°C	5'-TCAGAATTATCTTCCACACAAGGAG-3'
AtFLM-R	52.9°C	5'-TTCCTCTCTCATCATCTGTTGC-3'
AtSPL3-F	51.7°C	5'-CGTTTCTGCCAACAATGCAG-3'
AtSPL3-R	51.7°C	5'-TGTGCTTTTCCGCCTTCTCT-3'
AtLHY-F	53.7°C	5'-GCGTTTCAGGCTCTCTTTGC-3'
AtLHY-R	49.6°C	5'-CACCGATCATTACTACTCCT-3'
AtHAP2B-F	57.3°C	5'-CAGCCTAAGCCTCAGCAAAGTAAC-3'
AtHAP2B-R	51.7°C	5'-GCATTACCATGCCACCAAGA-3'
At3g30720-F	53.7°C	5'-CAGCGACCAGTTGGTGTTTG-3'
At3g30720-R	56.6°C	5'-TTGAGCCTTGCGACACCTGATG-3'
APRR9-F	54.7°C	5'-AAGCCGTCGTTGCTTTAGAGGA-3'
APRR9-R	57.8°C	5'-GTTGCTGCTCGTTGTGGCGC-3'
TOE1-F	59.2°C	5'-ATCATCGCCTTTACTGGAACGGAGC-3'
TOE1-R	52.3°C	5'-CCCAGTTACTCATCATCCCTT-3'
At4g39780-F	50.3°C	5'-GGTATTACTACGTTCTTGGAC-3'
At4g39780-R	54.3°C	5'-CAARCAATCTCCACAGAAGGAAACT-3'
At2g22200-F	54.2°C	5'-AGCGATGAGACCTCGTTGTTG-3'
At2g22200-R	54.7°C	5'-CATCCAATCAATCTCCACCGA-3'
At1g64380-F	59.0°C	5'-CTCCGGTGACGACA ACTACTACTG-3'
At1g64380-R	54.2°C	5'-ACTCCCATCATTGCCTCTTCC-3'
AtMYB70-F	53.7°C	5'-GCTGGTGGAGTGGTGATTGA-3'
AtMYB70-R	54.7°C	5'-CGGTGGAGTTGTTGACTCATTG-3'



A. Young cells of pseudobulb at early vegetative stage

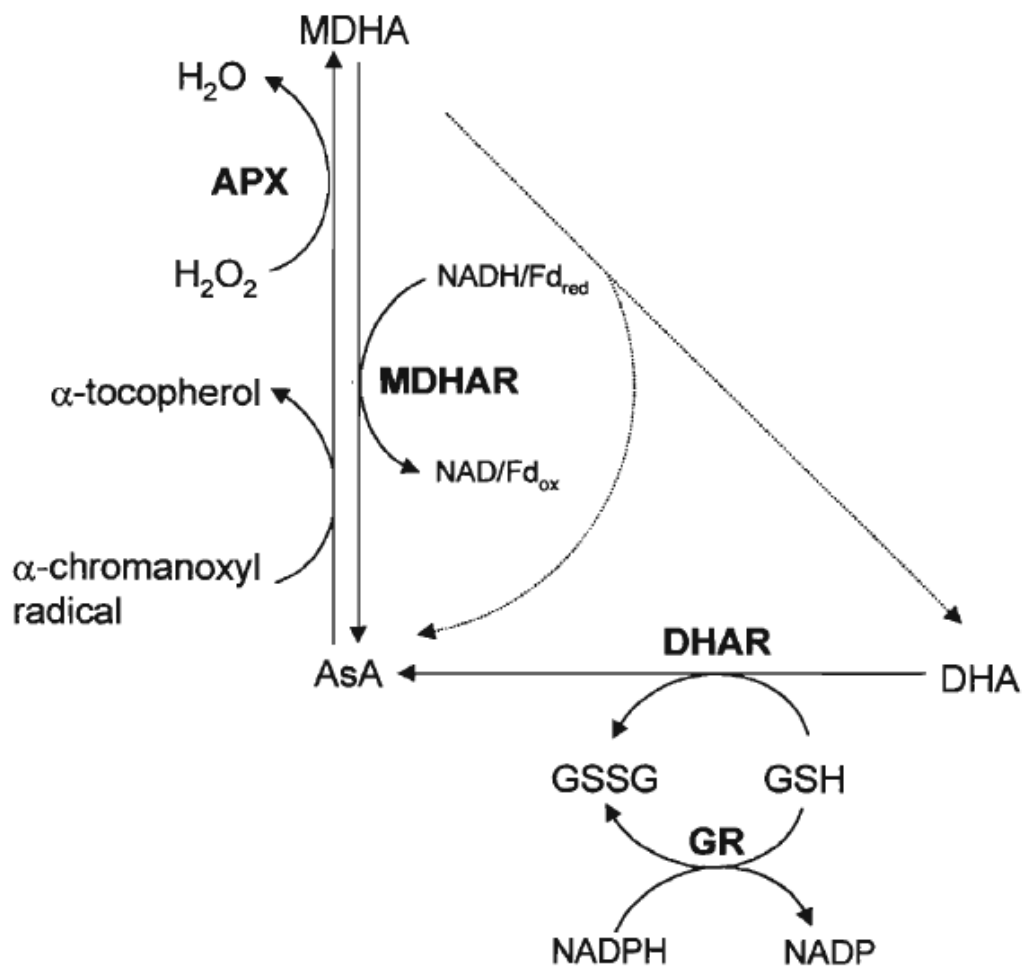
B. Mature cells of pseudobulb at late vegetative stage

C. Mature cells of pseudobulb at reproductive stage

Appendix 2. Schematic representation of ascorbate homeostasis in pseudobulb cell of *Oncidium* orchid in three developmental stages.

(Reproduced from Shen and Yeh, 2010)





Appendix 3. Ascorbate oxidation and regeneration from monodehydroascorbate (MDHA) and dehydroascorbate (DHA).

(Reproduced from Smirnoff and Wheeler, 2000)

Appendix 4. Abbreviation:

AsA	Ascorbate
AO	Ascorbate oxidase
<i>APRR9</i>	<i>PSEUDO-RESPONSE REGULATOR 9</i>
APX	Ascorbate peroxidase
<i>ATHAP2B</i>	<i>HEME ACTIVATOR PROTEIN 2B</i>
<i>CDF1</i>	<i>CYCLING DOF FACTOR 1</i>
<i>CO</i>	<i>CONSTANS</i>
<i>FKF1</i>	<i>FLAVIN-BINDING, KELCH REPEAT, F-BOX 1</i>
<i>FLC</i>	<i>FLOWERING LOCUS C</i>
<i>FLM</i>	<i>FLOWERING LOCUS M</i>
<i>FRI</i>	<i>FRIGIDA</i>
<i>FT</i>	<i>FLOWERING LOCUS T</i>
<i>GID</i>	<i>GIBBERELIC INSENSITIVE DWARF 1</i>
<i>GI</i>	<i>GIGANTEA</i>
LD	Long-day photoperiod
<i>LFY</i>	<i>LEAFY</i>
<i>LHY</i>	<i>LATE ELONGATED HYPOCOTYL</i>
MDHA	Monodehydroascorbate
PME	Pectin methylesterase
<i>QQS</i>	<i>QUA-QUINE STARCH</i>
ROS	Reactive oxygen species
SD	Short-day photoperiod
<i>SMZ</i>	<i>SCHLAFMUTZE</i>
<i>SNZ</i>	<i>SCHNARCHZAPFEN</i>
<i>SOC1</i>	<i>SUPPRESSOR OF OVEREXPRESSION OF CONSTANS 1</i>
<i>SPL3</i>	<i>SQUAMOSA PROMOTER BINDING PROTEINLIKE 3</i>
<i>SVP</i>	<i>SHORT VEGETATIVE PHASE</i>
<i>TOC1</i>	<i>TIMING OF CAB EXPRESSION</i>
<i>TOE1</i>	<i>TARGET OF EAT 1</i>
<i>VRN1</i>	<i>VERNALIZATION 1</i>
<i>VRN2</i>	<i>VERNALIZATION 2</i>
<i>VRN3</i>	<i>VERNALIZATION 3</i>